Investigating the role of right parietal cortex in multistable perception using non-invasive brain stimulation

Dissertation

Zur Erlangung des Grades eines
Doktors der Naturwissenschaften

der Mathematisch-Naturwissenschaftlichen Fakultät
und
der Medizinischen Fakultät
der Eberhard-Karls-Universität Tübingen

vorgelegt
von

Georg Schauer
aus Hoyerswerda, Deutschland

im November 2018

Tag der mündlichen Prüfung:	10. April 2019
Dekan der Math.-Nat. Fakultät:	Prof. Dr. W. Rosenstiel
Dekan der Medizinischen Fakultät:	Prof. Dr. I. B. Autenrieth
1. Berichterstatter:	Prof. Dr. Andreas Bartels
2. Berichterstatter:	Prof. Dr. Hong Yu Wong
Prüfungskommission:	Prof. Dr. Nikos Logothetis Prof. Dr. Andreas Bartels Dr. Hendrikje Nienborg PD Dr. Axel Lindner

Erklärung / Declaration:

Ich erkläre, dass ich die zur Promotion eingereichte Arbeit mit dem Titel:

"Investigating the causal role of right anterior IPS in multistable perception using non-invasive brain stimulation"

selbständig verfasst, nur die angegebenen Quellen und Hilfsmittel benutzt und wörtlich oder inhaltlich übernommene Stellen als solche gekennzeichnet habe. Ich versichere an Eides statt, dass diese Angaben wahr sind und dass ich nichts verschwiegen habe. Mir ist bekannt, dass die falsche Abgabe einer Versicherung an Eides statt mit Freiheitsstrafe bis zu drei Jahren oder mit Geldstrafe bestraft wird.

I hereby declare that I have produced the work entitled "Investigating the causal role of right anterior IPS in multistable perception using non-invasive brain stimulation", submitted for the award of a doctorate, on my own (without external help), have used only the sources and aids indicated and have marked passages included from other works, whether verbatim or in content, as such. I swear upon oath that these statements are true and that I have not concealed anything. I am aware that making a false declaration under oath is punishable by a term of imprisonment of up to three years or by a fine.

Tübingen, _____ _____

Date Signature

gewidmet meiner Mutter.
Unsere Wette läuft.

STATEMENT OF CONTRIBUTIONS

Chapter 1: Collection of the magnetic resonance imaging data as well as its initial preprocessing was carried out jointly with Oleksandra Shevtsova. Ms Shevtsova carried out a research internship at our lab. She was a student of the Faculty of Medicine, University of Tübingen.

Chapter 2: The visual stimuli were programmed jointly with Dr Jan Brascamp. In particular, Dr Brascamp provided some code from his own previous work. He is an assistant professor at the Department of Psychology, Michigan State University, East Lansing, Michigan, USA. The motor-evoked potential recordings were jointly collected with the help of Vladislav Royter based on a setup that he and Prof Alireza Gharabaghi provided. Prof Gharabaghi and Mr Royter are members of the division of Functional and Restorative Neurosurgery, University of Tübingen.

Chapter 3: One of the visual stimuli was based on a paradigm developed by Dr Naotsugu Tsuchiya. He was kind enough to provide some of his original code of that paradigm, which was subsequently used in the experiment. Dr Tsuchiya is an associate professor at the Department of Psychology, Monash University, Melbourne, Australia. The data collection was carried out jointly with Ms Carolina Ogawa, who completed a research internship at our lab. She is a student at the Instituto de Ciencias Biomédicas, Universidade de São Paulo, São Paulo, Brazil.

Chapter 4: One of the three visual stimuli was coded jointly with Dr Jan Brascamp.

ACKNOWLEDGEMENTS

My thanks go foremost to my supervisor Prof Andreas Bartels. He has been a delight to work with, supportive, constructive, inspiring and his door was (quite literally) always open. The past three years were well spent under his scientific tutelage. Supervision was also provided by the other two members of my advisory board, Prof Nikos Logothetis and Prof Hong Yu Wong, whose helpful criticisms I was glad to receive.

Further thanks deserve my collaborators in Tübingen and overseas. I am grateful to Prof Alireza Gharabaghi and Vladislav Royter, who were kind enough to allow usage of their equipment and to aid in doing so. I thank Prof Naotsugu Tsuchiya and Julian Rodney Matthews for their helpful comments, ideas and snippets of code that we shared at the ISSA workshop in Osaka 2017. I thank furthermore Dr Jan Brascamp for our correspondence and support in piloting and coding experimental paradigms.

During the past years, I had the privilege of supervising three students, Oleksandra Shevtsova, Carolina Ogawa and Mareike Brych. I thank them for bringing their ideas and hard work to the lab. Life in the office was enriched by their humour and good spirit. I also thank Pablo Grassi, Michael Bannert, Andreas Schindler, Fabienne Schlüsener, and all other members of the AG Bartels, for being my daily companions on this journey. I could not have asked for more pleasant and kind lab-mates.

Thanks also go to the Graduate Teaching Centre for Neuroscience, the Barbara-Wengeler Foundation, the German Research Council, the University Hospital Tübingen, the Psychological Institute of the University of Tübingen, as well as the Max-Planck-Institute for Biological Cybernetics.

Last, but certainly not least, I would like to thank a brave group of people who are often neglected in mentions of gratitude. The unnamed heroes of human cognitive neuroscience: participants. Taken together, just shy of a hundred volunteers walked through the lab door to provide the data presented in this thesis. It was a pleasure to welcome them, and I am immensely happy to now consider some of them my friends.

CONTENTS

FIGURES & TABLES

SUMMARY

Multistable perception describes the spontaneous fluctuation between two or more perceptual states when sensory input is ambiguous. An example hereof is bistability, which occurs when a stimulus has two competing interpretations that perceptually alternate over time. For instance, in structure-from-motion (SFM) bistable perception, the coherent movement of dots creates the illusion of a rotating sphere, where the direction of movement is uncertain. Another example is binocular rivalry (BR), which occurs when the two eyes are presented with dissimilar visual stimuli in the same retinal space, leading to an alternation of conscious awareness between the two stimuli. Multistable perception has been used to investigate the neural correlates of conscious experience, since an unchanging stimulus leads to a change in awareness, hence dissociating consciousness from sensory processing. Functional magnetic resonance imaging (fMRI) has consistently shown activity of the right intraparietal sulcus (IPS) and right superior parietal lobule (SPL) during perceptual transitions in multistable perception. Previously, transcranial magnetic stimulation (TMS) and in particular inhibitory theta burst stimulation (cTBS) has been used on the IPS to probe its causal role in multistable perception. That endeavour has produced inconsistent results on whether IPS inhibition shortens or lengthens multistable dominance durations. Problematically, the neural effects of cTBS over IPS during multistable perception are unknown, as is indeed the causal role of IPS in mediating perceptual reversals.

Chapter 1

cTBS was applied over IPS or over vertex control site, between two sessions of fMRI, to illuminate the changes in neural activity accompanied by IPS cTBS. During the fMRI sessions, participants viewed alternating blocks of a bistable SFM stimulus or a replay condition using depth-cue disambiguated SFM. Behaviourally, it was found that IPS cTBS lengthened dominance durations when comparing pre vs post cTBS as well as when comparing IPS with vertex stimulation. Neurally, IPS cTBS led to a decrease in blood-oxygen-level dependent (BOLD) response in thalamus, foveal V1, right superior parietal lobule and middle frontal gyrus compared to vertex cTBS. Moreover, a decrease of functional connectivity between activity in IPS and ipsilateral hippocampus was observed. The present results suggest that the combined effects of a reduction of sensory processing as well as decoupling between IPS and the memory site hippocampus allows inhibitory TMS over parietal cortex to stabilise the current perceptual content. Together, these results provide a hitherto unreported insight into the brain networks that subserve the resolution of bistable perception and how IPS stimulation modulates them to bring about a behavioural effect.

Chapter 2

Next to the IPS, also the more posterior SPL has been indicated as serving a causal role in multistable perception. TMS has been used to modulate bistable dominance durations for both sites, but in opposite directions. This led to the proposal that parietal cortex is fractionated, such that IPS and SPL serve opposing functions. However, neuroimaging evidence also suggests that higher cortical activity, including parietal cortex, is diminished when BR percept switches are either unreported or unreportable. This suggests that parietal regions have no causal role in multistable perception, but are active only as consequence thereof. To resolve this conflict, *chapter 2* investigates whether cTBS to the IPS as well as the SPL affects the temporal dynamics of BR using regular button press rivalry as well as no-report and invisible rivalry paradigms. Specifically, it was hypothesised that cTBS would lead to a change in BR dominance when it was visible or unreported, but not when invisible. However, contrary to expectation, not only was it not possible to replicate the previously observed functional fractionation of parietal cortex, but also no difference was found between any cTBS condition. To verify if cTBS had its desired inhibitory effect, also motor-evoked potentials (MEP) were recording prior and following cTBS to primary motor cortex. It was found that cTBS to M1 decreases MEP amplitude. However, this effect did not correlate with the main findings over parietal cortex, leading to the conclusion that cTBS is not an apt neurostimulation technique to answer the present research question.

Chapter 3

Relative intensities of steady-state responses (SSRs) over early visual cortex have been reported to correlate with conscious perception in paradigms like BR and have even be used to predict the content of consciousness. However, their causal role in perception remains uninvestigated despite their common use. Are modulations of SSRs mere epiphenomena of perception or do they aid in determining its content? To test this, it was enquired if interference with the SSR by means of transcranial alternating current stimulation (tACS) would affect conscious perception. Sham or real tACS across left and right parieto-occipital cortex was applied at either the same or a different frequency or in and out of phase with an SSR eliciting flicker stimulus, while participants viewed either BR or tried to detect stimuli masked by continuous flash suppression (CFS). It was found that tACS did not differentially affect conscious perception in the forms of BR predominance, CFS detection accuracy, reaction time, or metacognitive sensitivity. Importantly, the present null-findings are supported by Bayesian statistics. In conclusion, the application of tACS at frequencies and phases of stimulus-induced SSRs does not have perceptual effects. The relationship of tACS with SSRs and the possibility that SSRs are epiphenomenal to conscious perception is discussed.

Chapter 4

One reason for the difference between findings of studies, which attempted to modulate multistable dominance durations thought cTBS to the IPS, may be that different stimuli were used, dissimilar properties of which modulated the TMS effect direction. To test this, cTBS was applied to the IPS between two sessions of SFM bistable perception (*chapter 1*), random dot motion BR (*chapter 2*), as well as checkerboard BR (*chapter 3*). It was foremost hypothesised that the findings of the first two chapters would be replicated, and moreover that the TMS effect would correlate between stimuli. Contrary to this hypothesis, cTBS neither consistently affected dominance durations in any of the stimuli, nor were effect sizes correlated across participants. This is supported by Bayesian statistics. Baseline dominance durations prior to TMS correlated across the three stimuli, suggesting a common mechanism to resolve multistability. However, the lack of correlation pertaining to the cTBS effect points towards the absence of any cTBS effect. Considering the present results, the small samples and effect sizes of previous studies, as well as recent literature of variable cTBS effects on motor cortex, this chapter concludes that there is good reason to cast general doubt over the ability of parietal cTBS to modulate dominance durations in multistable perception.

Chapter 1 pointed towards the importance of multiple brain networks including the IPS in the resolution of multistability. *Chapters 2 & 4* by contrast presented with null results that do not allow inference as to the causal role of IPS. Similarly, the use of tACS to modulate SSRs in *chapter 3* was not able to demonstrate conclusively whether SSRs have a causal role in multistability. The search for the contribution of IPS by use of cTBS or tACS has been hindered by methodological concerns over whether these methods have an interpretable or even any effect on IPS activity. In summary, the causal role of IPS activity in multistable perception remains elusive.

INTRODUCTION

1. Multistable perception and consciousness

Bistable perception occurs when an stimulus has to competing percepts, awareness of which fluctuates over time. An example hereof is structure from motion (SFM), where coherently moving dots create the illusion of a rotating sphere, the direction of which is uncertain (Miles, 1931; Wallach & O'Connell, 1953). A special case of bistable perception is binocular rivalry (BR). Here, two images are presented to the same retinal space in both eyes. Instead of seeing a fusion of both images, perception switches back and forth between the two. BR is characterised by eye competition, especially just after perceptual reversals (Bartels & Logothetis, 2010). However, the temporal dynamics of BR are largely determined by competition of stimulus properties, similar to other bistable perception (Blake & Logothetis, 2002; Tong et al., 2006). Attention affects the temporal dynamics of BR (Paffen et al., 2006; Mitchell et al., 2004), and inattention even abolishes it altogether (Brascamp & Blake, 2012). Together, SFM bistability and BR are known under the umbrella term of multistable perception.

One of the primary reasons for studying the neural basis of multistability is its relevance in identifying the neural correlates of consciousness (NCC). Fleshing out how multistable perception can aid in the search for the NCC has been a multilayered task, both conceptually and empirically. The debate centres on two main questions: 1) How do states of consciousness, such as sleep or coma come about (Koch et al., 2016)? 2) What are the minimal neuronal mechanisms jointly sufficient for any one specific conscious percept (Crick & Koch, 1995)? The latter is relevant in the study of multistability, as we search for a content-specific NCC. The presumption is that every separable conscious content has a distinct NCC, such that seeing a blue flicker, hearing a high pitched sound, seeing a specific person or any other phenomenal experience will have its own neural substrate (Koch et al., 2016). Perturbation of this NCC must lead to the extinction of the conscious percept. Vice versa, inducing this specific NCC via transcranial magnetic stimulation (TMS), optogenetics, cell stimulation or other mean will necessarily lead to the phenomenal experience associated with that NCC (Tononi & Koch, 2015). A common strategy for investigating this content NCC is to hold a stimulus constant while there is a change in consciousness, for instance by use of a thresholded stimulus, which may be visible or invisible on separate trials (Aru et al., 2012, critically Lau, 2008). Alternatively, any paradigm in which the stimulus and resulting brain activity with its resulting percept diverge can be used, for instance in BR, SFM, masking through continuous flash suppression, motion-induced blindness, change blindness or the attentional blink (Tononi & Koch, 2008).

In the study of multistable stimuli, an unchanging stimulus leads to a fluctuating change in conscious perception (Hohwy et al., 2008; Clark, 2013: 183). This means that, presumably, neural

activity time locked to percept switches would not be attributable to new sensory input and processing, but primarily to conscious perception. This is because consciousness and sensory processing are not the same and dissociate. For instance, conscious mental imagery occurs in the absence of sensory stimulation, yet leads to activity in sensory areas (Amedi et al., 2005).

2. Importance of the IPS

Early work on the neural basis of multistable perception was carried out by Leopold & Logothetis (1995). They used electrophysiological recordings in macaques while viewing BR. They found only weak percept modulation in V1 neurones, which were more prone to be regulated by the stimulus corresponding to their visual field. At the same time, activity of neurones in the inferior temporal cortex corresponded closely to perceptual dominance (Sheinberg & Logothetis, 1997) This can be interpreted as signifying that the NCC cannot be localised to V1, but instead involves (but need not be exclusive to) inferior temporal cortex in the macaque (Tononi & Koch, 2008). Similarly, only 20 % of neurones on macaque V1 correlate with the content of consciousness in an SFM stimulus, compared to up to 90 % in V4 or V5/MT+ (Grunewald et al., 2002; Maier et al., 2007).

In humans, processing of multistable stimuli occurs at multiple states of the visual hierarchy. Previously, visual consciousness of BR dominance could be decoded from activity in V1 (Haynes & Rees, 2005; Polonsky et al., 2000; Tong & Engel, 2001), lateral geniculate nucleus (LGN; Haynes et al., 2005; Lee et al., 2005) and extra-striate areas (Tong et al., 1998; Moutoussi et al., 2005, Wunderlich et al., 2005), using BR (review in Rees et al., 2002; Blake & Logothetis, 2002).

While all these areas are linked to multistability, it is uncertain whether their activity alone is sufficient for conscious perception. Extrastriate lesions can lead to quadrantanopia, characterised by blindness in one quarter of the visual field (Horton & Hoyt, 1991), while patients with V1 lesions but intact extrastirate areas can still experience phosphenes following TMS to the IPS (Mazzi et al., 2014). Parietal lesions can lead to visual extinction (review in Rees et al., 2002). Also, large-scale lesions to the fronto-parietal network in monkeys lead to blindness, even if V1 and extra-striate areas are left intact (Nakamura & Mishkin, 1980). This indicates a role of higher cortical areas in bringing about conscious perception of multistability.

A multitude of functional magnetic resonance imaging (fMRI) studies have shown that conscious multistable percept switches elicit blood-oxygen-level-dependent (BOLD) activity in contrast to unambiguous replay conditions in various higher brain areas, especially the right-lateralised fronto-parietal network in BR (Lumer et al., 1998; Zaretskaya et al., 2010; Knapen et al., 2011; Weilnhammer et al., 2013; Frässle et al., 2014; Buckthought et al., 2015; Brascamp et al., 2015) and other bistable stimuli (Kleinschmidt et al., 1998; Sterzer & Kleinschmidt, 2005, 2007;

Sterzer et al., 2002; 2003; Brouwer & van Ee, 2007; Beer et al., 2009; Weilnhammer et al., 2013; Zaretskaya et al., 2013; Watanabe et al., 2014). This suggests a common high level neural substrate in areas associated with top-down control and executive function for all multistability, even though BR is much less prone to voluntary modulation compared to SFM (Meng & Tong, 2004).

More specifically, activity of the right anterior intraparietal sulcus (IPS) has been consistently replicated across laboratories and across different classes of bistable stimuli (Lumer et al. 1998; Kleinschmidt et al., 1998; Lumer & Rees, 1999; Zaretskaya et al., 2010, 2013; Weilnhammer et al., 2013, 2017; Grassi et al., 2017, 2018; review in Brascamp et al., 2018); marking it as prime candidate for a brain area that subserves a role in mediating perceptual switches in multistability (opposing fMRI evidence in Knapen et al., 2011; Brascamp et al. 2015). More recently, it was shown using dynamic causal modelling that coupling strength of IPS with the more posterior superior parietal lobule (SPL) and V5/MT+ could predict dominance of a bistable stimulus (Megumi et al., 2015), as could resting state connectivity between IPS and striatum (Baker et al., 2015), as well as the relative strength of IPS & SPL activity in an energy landscape analysis (Watanabe et al., 2014).

In an effort to further examine the causal role of parietal cortex, a number of studies employed TMS to the IPS. This is a more direct technique to probe the causal role of this brain region. TMS offers multiple protocols for interfering with brain regions, which can elucidate the involvement thereof (Schutter et al., 2004). Online repetitive TMS applied during perception is meant to inject noise into the system during its operation, whereas offline inhibitory repetitive TMS presupposes an inhibitory after-effect, during which perception can be measured (Fitzgerald et al., 2006; Casula et al., 2014). A special form of offline repetitive TMS is continuous theta-burst stimulation (cTBS), whereby for a matter of 40 seconds, six hundred TMS pulses are applied to produce inhibitory aftereffects of several minutes (Huang et al., 2005).

Carmel et al. (2010) first demonstrated that inhibitory 1 Hz offline repetitive TMS to IPS (at the maximal BOLD activation location of Lumer et al., 1998), applied prior to participants observing BR, could shorten BR dominance durations. This has later been replicated using inhibitory 2 Hz offline repetitive TMS (Wood et al., in prep), as well as cTBS (Kanai et al., 2011). Conversely, Zaretskaya et al. (2010) showed the exact opposite effect with house/face BR using inhibitory 2 Hz repetitive TMS in a region only 3 mm away, a finding that which could not be replicated (Wood et al., in prep), whilst Kanai et al. (2010) prolonged dominance of SFM using cTBS, stimulating the SPL. Similarly, Vernet et al. (2016) used single pulse TMS to the IPS to establish that TMS applied 70 ms prior to bistable stimulus presentation destabilised the percept. Interpretations of these findings vary from inferring that IPS is involved in percept maintenance

(Carmel et al., 2010), to percept destabilisation (Zaretskaya et al., 2010), to computation of error signals in a predictive coding framework (Kanai et al., 2010, 2011; Friston, 2005). Problematically, these interpretations are based solely on a TMS modulation of bistable dominance durations. It is however doubtful how a change in a single continuous variable could allow for meaningful inferences on the function of the parietal cortex. What is needed to make this inference is richer neural data that links the TMS effect on dominance to a TMS effect on neural activity. Providing this crucial linkage is the aim of *chapter 1*:

In *chapter 1*, a study is presented in which SFM was utilised. This stimulus is bistable, but can be disambiguated when depth-cues are provided. Participants reported SFM dominance while neural activity was recorded using fMRI. Blocks of bistable viewing alternated with blocks of disambiguated replay. During a break, cTBS to IPS or the vertex as control site was applied (counterbalanced across participants), followed by identical fMRI testing runs. The aim was to compare, both behaviourally and neurally, how IPS cTBS would affect bistable perception. The expectation was to replicate the shortening of SFM dominance found by Kanai et al. (2011). Moreover, it was hypothesised that IPS activity would be inhibited by cTBS, along with other functionally connected areas. Also, it was expected cTBS to modulate the functional connectivity between IPS and other regions that were previously indicated in bistable perception. At last, it was hypothesised that direction and size of the behavioural effect would correlate with neural effects, which would indicate a direct relationship between a change in a brain state and participants' perception.

3. No-report and invisible paradigms

In all the above studies on the neural basis of multistable perception, what remains questionable is whether the activity can be considered indicative of the NCC. Specifically, any observed brain activity could pertain to one of three things: Prerequisites of consciousness, neural substrates of consciousness, and neural consequences thereof (de Graaf et al., 2012). One consequence that is particularly troublesome is motor report. Participants are routinely asked to report their conscious percept using a button press. This means however that the neural signature of BR and SFM will be tainted with neural activity pertaining to motor planning and execution. Moreover, the very idea that perception leads to action can modulate the correlates of perception. One way to address this concern is with the introduction of no-report paradigms.

As previously outlined, right superior anterior IPS has been shown to become active time locked to perceptual reversals (Lumer et al., 1998; Zaretskaya et al., 2010, 2013; Knapen et al., 2011, Frässle et al., 2014; Brascamp et al., 2015; Sterzer et al., 2009). What remains unclear is the

causal role of this activation. Does it aid in bringing about perceptual reversals, or is it merely a consequence of conscious perception (Aru et al., 2012; De Graaf et al., 2012)? Parietal activity precedes percept switches under electroencephalography (EEG), suggesting an involvement in initialising them (Britz et al., 2010). Similarly, the previously discussed TMS evidence is indicative of a causal role of the IPS as well as the SPL in bringing about perceptual reversals, given that their inhibitory stimulation leads to changes in dominance durations. Relevantly, while inhibitory TMS of IPS prior to BR has consistently led to an increase in percept switch frequency (Carmel et al., 2010; Kanai et al., 2011; Wood et al., in preparation), stimulation of SPL has been shown to decrease switch frequency (Kanai et al., 2011). Interpretations of this fractionation of parietal cortex into two regions with opposing functional roles, range from IPS maintaining BR dominance, over SPL initiating percept switches, to IPS and SPL resolving predictions and error signals respectively in a predictive coding framework (Friston, 2005; Hohwy et al. 2008). The picture that emerges is that the parietal cortex is not just a substrate for visual consciousness of multistable perception, but also is causally involved in the perceptual processes that bring about percept switches.

This proposal on the functional relevance of IPS and SPL in BR has not remained unchallenged. For instance, Knapen et al. (2011) used fMRI to compare BR not to replay with instantaneous percept switches, but instead more gradual ones that reflect participants phenomenology. They found no increased fronto-parietal BOLD activation in that contrast, suggesting that fronto-parietal activity is not rivalry specific, but instead indicative of conscious perception thereof. Frässle et al. (2014) furthermore showed that when BR is not reported through button presses, but percept dominance passively inferred using eye-tracking, BOLD signal strength in the fronto-parietal network time-locked to percept switches decreased substantially. This suggests that some of the fronto-parietal activity may in fact only be a neural correlate of motor percept switch report.

Zou et al. (2016) elegantly demonstrated that BR can occur also in the absence of conscious perception. They employed incongruous flickering gratings that were seen as uniform, but could be used to infer the temporal dynamics of BR since they induced aftereffects and orientation-specific adaptation. They found consistent V1 activity in visible as well as invisible BR, but no fronto-parietal activity in the latter, suggesting that V1 resolves BR, while parietal regions serve as substrates for conscious awareness thereof (Klink & Roelfsema, 2016). Essentially, invisible stimuli can induce BR, which casts general doubt on the link between rivalry and consciousness (Giles et al., 2016).

More drastically, Brascamp et al. (2015) were able to demonstrate that BR occurs even in the absence of any statistically significant fronto-parietal activity when rendered invisible. They developed a novel BR paradigm, where percept switches became unreportable due to the similarity of the rivalling stimuli, but where the occurrence of BR percept switches could still be demonstrated. This was achieved by indexing percept dominance in time intervals independent of percept switches, and later calculating the temporal dynamics of BR from these dominance 'snapshots' in the absence of percept switch report or reportability. This allowed for the study of the neural correlates of BR independent of visual consciousness thereof. They interpret the absence of substantial fronto-parietal BOLD responses as indicating no causal relevance of that network in the resolution of BR, but rather that its activity is a consequence of percept switches and their conscious perception.

This presents a problem: If fronto-parietal BOLD activity is merely a consequence of the resolution of BR, specifically conscious perception and motor report, then why would TMS stimulation of IPS and SPL have led to changes in the frequency of percept switches, suggesting their causal involvement? Moreover, if parietal BOLD signal strength is diminished when BR percept switches are unreported or unreportable, does that entail that TMS stimulation would have a differential effect on BR contingent on whether it is perceived?

Finding an answer to this problem is the aim of *chapter 2*. To test this proposition, a psychophysical paradigm was used that included reported, unreported and unreportable BR percept switches akin to Brascamp et al. (2015). The effect of cTBS to both IPS, SPL and vertex control on the frequency of these switches was measured. It was hypothesised that if the causal role of the parietal cortex lies with the conscious perception of BR, then cTBS inhibition should show an effect in reported and unreported, but not unreportable percept switches. This result would be philosophically relevant since it suggests a causal efficacy of consciousness on perceptual processes and that certain modulation of interpreting incoming sensory signals is contingent on the presence of perceptual awareness. If the causal role of the parietal cortex network lies with percept report and motor planning, then reported, but not unreported and unreportable percept switches should be affected by cTBS. If on the other hand, TMS shows an effect in all three, this would suggest that there is a causal role for the parietal cortex network independent of the transient BOLD signal accompanying percept switches. For any cTBS effect, it was hypothesised consistency with the previously observed fractionation of parietal function where effect direction of IPS stimulation on BR is opposite to that of SPL (Kanai et al., 2010, 2011).

That cTBS has an inhibitory effect on parietal cortex is a primary presumption of *chapters 1, 2 & 4*. This notion is driven by observations that cTBS to primary motor cortex (M1) significantly

lowers motor-evoked potential (MEP) amplitude (Huang et al., 2005). Unlike M1 through MEPs, the parietal cortex offers no independent way of confirming that activity in stimulated tissue has been inhibited. Moreover, not all participants react similarly to M1 cTBS stimulation, where a substantial subsample are non-responders (Hamada et al., 2012). In a separate experiment of *chapter 2*, electromyography (EMG) of TMS induced muscle potentials pre and post cTBS to M1 was measured. It was hoped this would aid in classifying participants into cTBS responders and help interpret the main results. It was hypothesised that MEP amplitude would be significantly decreased in this sample, and moreover expected to see a correlation between cTBS effects over M1 and parietal cortex. Such a correlation would confirm the hitherto unsupported assumption that the effects of cTBS are transposable across to superior parietal regions. On the other hand, the failure to replicate a change in MEP amplitude would lessen faith in the main result. Finally, a reduction of MEP amplitude coupled with a failure to see a correlation with the cTBS effect over SPL would cast serious doubt on the usability of cTBS protocol outside M1 and on the parietal cortex in particular.

4. Causal role of the steady-state response

When participants are presented with a flickering visual stimulus, the firing rate of neurons in the early visual cortex synchronises to the frequency of the stimulus flicker and its harmonics (Regan, 1989; Herrmann, 2001; Pastor et al., 2003; Norcia et al., 2015). These oscillatory brain responses can be recorded non-invasively by electroencephalography (EEG) or magnetoencephalography (MEG) and are known as steady-state response (SSR). Amplitude and phase of the SSR are highly contingent on driving stimulus properties. However, they are also influenced by cognitive factors. EEG-recorded SSR Power has previously increased as attention was directed towards the location of the flicker, independent of task relevance (Morgan et al., 1996; Kim et al., 2007). SSRs have been used for researching spatial attention (Morgan et al., 1996; Itthipuripat et al., 2013; Toffanin et al., 2009) stimulus-feature attention (Andersen et al., 2013; 2015), and BR (Srinivasan et al., 1999; 2006).

SSRs are especially useful for tracing the conscious perception of flickering stimuli by use of frequency tagging, where the presence of the stimulus' frequency in the neural recording may indicate perceptual processing and even conscious perception of that stimulus (Tononi et al., 1998; Andersen et al., 2011), making it another candidate for unlocking the NCC. To date, the neurophysiological nature of SSRs remains controversial (Keitel et al., 2014). While some argue that SSRs are an intrinsic neural oscillation externally entrained by the flickering stimulus (Mathewson et al., 2012; Spaak et al., 2014), others suggest that visual evoked potentials phase locked to the

stimulus are added to ongoing electrophysiological signal, comprising the SSR (Shah et al., 2004; Vialatte et al., 2010; Capilla et al., 2014).

One issue that remains unclear is the causal role of SSRs. While they can correlate with visual stimulus presentation, perception and consciousness, and have been used to decode these (Tononi et al., 1998), it is unknown if they are involved in determining the content of perception, or are merely epiphenomenal. If they are epiphenomenal, they behave like a shadow does in relation to the object that cast it: while any change to the object leads to a change in the shadow, this relationship is purely unidirectional. Conversely, for neural oscillations not to be epiphenomenal to a process, then the process should be altered by interference with the oscillation (Sejnowski & Paulsen, 2006). Hence, if interfering with SSRs leads to a behavioural effect, then that activity can be said to be causally involved in bringing about that behaviour. The question is hence: can conscious perception be modulated by interfering with SSRs?

As Ruhnau et al. (2016) reported, SSRs can be modulated by use of transcranial alternating current stimulation (tACS), a non-invasive brain stimulation technique. tACS interferes with neural oscillations through the application of a weak sinusoidal electric current on the head through two electrodes (Antal & Paulus, 2013; Herrmann et al., 2013).

tACS has been shown to affect conscious perception (Kanai et al., 2008; Laczó et al., 2012; Neuling et al., 2012a; Strüber et al., 2014) and behaviour (Pogosyan et al., 2009). For instance, tACS stimulation of V1 lowers its phosphene threshold (Kanai et al., 2010b) and aids in the detection of weak stimuli (Neuling et al., 2012a). Also, tACS lowered the contrast discrimination threshold while contrast sensitivity remained unaltered in a four-alternate-forced-choice paradigm (Laczó et al. 2012). Conversely, tACS at 6 and 10 Hz can also impair visual detection (Brignani et al., 2013). Even though it is not completely understood how tACS interacts with neural oscillations, entrainment of neural oscillations is the prime candidate for explaining the mechanism behind the effect on neural oscillations during tACS stimulation (Neuling et al., 2012a; Witkowski et al., 2016; for opposing views see Battleday et al., 2014; Keitel et al., 2014). Entrainment here is the temporal phase alignment of neural oscillations with an external driving source (Thut et al., 2011; Vossen et al., 2015). Not only does tACS entrain alpha oscillations during stimulation, but this effect is still evident even 10 min after stimulation offset (Zaehle et al., 2010).

Ruhnau et al. (2016) argue that SSRs and tACS might be a natural fit, since the stationary sinusoidal structure of SSRs lends itself to the similarly stationary sinusoidal tACS modulation. They hypothesised that since alpha power increases with tACS, so should the SSR. Indeed, they showed that the amplitude of higher order harmonics of the SSRs can be increased when tACS at the same frequency as the SSRs is applied. They also demonstrated that a different frequency tACS

had no discernible effect on the SSRs. They did not however aim to demonstrate that a modulation of the SSRs translates into a modulation of conscious perception. This is what was attempted in *chapter 3*. Two psychophysical paradigms lend themselves for testing this proposition, BR and continuous flash suppression (CFS):

When SSR eliciting stimuli are used in BR, the power of the SSRs in part reflects conscious perception. The amplitude of a visually evoked potential is larger when the stimulus eliciting it is consciously perceived (Brown & Norcia, 1997). Similarly, EEG modulation of the SSR is dependent on whether a rivalry stimulus is being suppressed or perceived (Lawwill & Biersdorf, 1968). Tononi et al. (1998) used MEG frequency tagging and measured the SSRs for both of the stimuli's frequencies. They found that frequency power was modulated contingent on perceptual dominance. Specifically, when an image entered consciousness, its power amplitude increased at the expense of power of the other image by as much as 85%.

CFS is a variant of BR, in which one eye is presented with the target stimulus and the other is presented with flashing dynamic high-contrast pattern masks (Tsuchiya & Koch, 2005). The dynamic Mondrian masks in one eye suppress perception of the target in the other eye, which remains invisible for dozens of seconds depending on the target contrast until it overcomes suppression and breaks into consciousness (Yang et al., 2014). Unlike normal BR, where the potency of both images is equal, here, detection of the masked stimulus registers its capacity to overcome suppression and break into consciousness. This can serve as indicator of unconscious processing of the target stimulus (Rabovsky et al., 2016). Crucially, CFS masks have been reported changing at frequencies usually associated with the SSR (Tsuchiya & Koch, 2005).

In essence, both of these paradigms allow for the use of flickering stimuli that elicit SSRs. In BR, both stimuli can be tagged with different SSR frequencies. Under CFS, the mask and target can be made to evolve at SSR eliciting frequencies. Here tACS was applied to participants either while they viewed BR or during a perceptual discrimination task under continuous flash suppression (CFS) in three separate experiments. The main objective of *chapter 3* was to find evidence for a causal role of SSRs on flickering perception by means of tACS. In other words, it was intended to elucidate whether interference with SSRs can modulate conscious visual perception.

Specifically, all stimuli flickered at either 7.2 Hz (slow) or 9 Hz (fast). In BR, each eye's stimulus had one speed. For CFS, the mask was fast, while the target was slow. tACS parameters were applied in a three-by-two design: There were three tACS frequencies: slow, fast or sham. tACS could also be either in-phase with the stimulus, where SSRs and tACS waveforms were in synchrony (0° phase lag), or out-of-phase, in which there was a 90° phase lag between the two waveforms. Since there is a lag between flickering stimulus presentation and the SSR onset, an EEG pre-

experiment was performed, which allowed the estimation of SSR latency in order to consequently control the tACS phase to either 0 or 90 degrees.

In the BR experiment, it was aimed to test if tACS frequency and tACS phase influenced percept dominance durations. Regarding the tACS frequency condition, it was hypothesised that when tACS was set at the slow frequency, the stimulus flickering slowly would be perceived longer than the one flickering at the fast frequency, i.e. concurrent tACS should increase the SSR amplitude of the corresponding stimulus, making it more likely to enter consciousness. This is because the two SSR frequencies fluctuate according to the conscious perception of the participant. Increasing the SSR amplitude of the slow stimulus over the fast should lead to SSRs that are more characteristic of when the slow stimulus is consciously perceived. The same holds for the fast stimulus, while an effect for the sham tACS condition was not expected. Regarding the tACS phase, it was hypothesised that in-phase tACS (0° phase lag between SSR and tACS waveform) would increase predominance of the stimulus corresponding to the stimulation frequency, while the out-of-phase (90° phase lag) would not. This hypothesis was derived from previous findings of the effect of tACS phase on behaviour: it has been demonstrated that stimuli presented in-phase to endogenous neural oscillations are perceived better compared to stimuli presented counter-phase (Sherman et al., 2016; Montemurro et al., 2008; Busch et al., 2009; VanRullen et al., 2011; Spaak et al., 2014). In fact, while in-phase stimulation enhanced performance in a letter discrimination task, out-of-phase stimulation had an opposing effect (Polania et al., 2012).

In a first CFS experiment it was aimed to test if tACS frequency and phase influenced the ability to detect targets breaking through CFS. Participants were asked to indicate the position of a target as soon as they saw it, allowing me to compute accuracy and reaction time (RT). In a second CFS experiment the effect of tACS on metacognition was tested. To this end, participants were presented with a CFS masked target for a period of time too short for the target to break into awareness. Participants were then asked to make a judgement on the position of the target paired with a confidence judgement. This allowed me to compute metacognitive sensitivity, i.e. how interospectively aware of the quality of their visual information processing participants were (Persaud et al., 2007; Rounis et al., 2010). While TMS over frontal cortex has already been used to impair metacognitive sensitivity (Rounis et al., 2010), it was the aim of *chapter 3* to uncover if tACS impaired or even improved metacognitive sensitivity based on its parameters.

Regarding the tACS frequency, since the mask flickered fast while the target stimulus slowly, it was hypothesised that the target would be detected faster when the tACS was set at the slow frequency, i.e. when tACS and target frequencies matched. Conversely, it was expected that when tACS frequency matched the mask frequency (9 Hz), mask perception would be favoured and thus

target detection would be hindered. Moreover, it was proposed that in-phase tACS would have a favourable effect on task performance, while out-of-phase tACS would not.

5. Resolving contradictory TMS findings

As outlined above, inhibitory TMS studies on the IPS have found conflicting results on whether TMS has had an shortening or lengthening effect on dominance durations. While *prima facie* the difference between these results maybe due to dissimilar TMS protocols, new results shed a more opaque light on the situation: Wood et al. (in prep) used both online 2Hz repetitive TMS and offline 2Hz repetitive TMS to the IPS and were able to replicate the shortening of Carmel et al. (2010), but the lengthening of Zaretskaya et al. (2010). Using global-local bistable perception, Zaretskaya et al. (2013) also found a shortening of dominance after cTBS. Kanai et al. (2011) also showed a shortening of SFM using cTBS over the IPS, yet the results of *chapter 1* showed lengthened dominance in a replication attempt. Also it was not possible to find an effect of cTBS to either IPS or SPL in random dot-motion BR (see *chapter 2*; stimulus akin to Brascamp et al., 2015). In essence, parietal stimulation during or prior to SFM and BR has led to inconclusive results at best.

In *chapter 4*, to clear up this fog, it was tested what effect IPS cTBS has on the dominance durations of three stimuli: SFM (*chapter 1*), random dot motion BR (*chapter 2*) and checkerboard BR (*chapter 3*). This was aimed to find out to what degree we would be able to replicate previous TMS effects: Would one find that cTBS affects dominance differentially in a stimulus-contingent manner, indicating an importance of stimulus properties on the TMS effect? Alternatively, would the cTBS effect be consistent across stimuli within each participant, demonstrating the relevance of inter-subject variability? At last, *chapter 4* engages with the possibility of not finding any TMS effect, which would cast doubt on the validity of those studies that were failed to replicate.

CHAPTER 1

Effects of cTBS over parietal cortex during bistable viewing on fMRI BOLD activity

1. Material and methods

1.1 Participants

40 healthy volunteers with normal or corrected to normal vision were recruited for the study (mean age 24.6 yrs ± 3.9 S.D.; 27 female, 34 right handed). Following health screening of all participants to ensure the safety of TMS application, written informed consent was acquired from all participants prior to the experiment, which was approved by the institute's ethics committee. Participants were then screened in a pre-experiment for psychophysical benchmarks appropriate for the fMRI experiment (see section 2.5.1). 20 participants were subsequently invited for the TMS-fMRI experiment (mean age 23.5 yrs ± 2.9 S.D.; 14 female, 17 right handed).

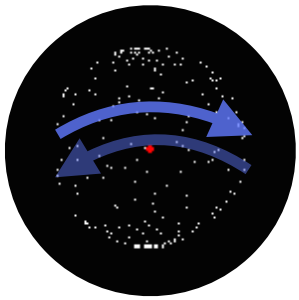

Figure 1 — SFM sphere stimulus
200 white dots on a black background moving coherently left and right within the boundaries of an invisible circle to create the illusion of a rotating sphere, a red fixation dot at the centre. The SFM sphere can be perceived as either rotating left or right. Blue arrows indicate possible directions of perceived movement.

1.2 Visual stimuli and apparatus

The stimulus used to create bistability was a SFM rotating sphere (*figure* 1). 200 white dots on a black background (minimum screen illumination) moved horizontally left and right within the invisible outline of a circle. All dots took the same amount of time to complete one journey, hence they moved at different speeds, creating the illusion of a moving sphere, that can be perceived as rotating left or right. Dots moved once back and forth, corresponding to a single complete rotation of the sphere, in 3 seconds. The sphere was 1.25 degrees visual angle (dva) in diameter. The display included a central red fixation dot (0.075 dva).

As control, I also used a replay SFM sphere, which was identical to the above, except for an added depth percept. To create this 3D illusion, participants were presented with two SFM spheres in the same retinal space for each eye separately via a 3D shutter and polarisation glasses. One sphere was presented as having moved slightly farther along than the other, mimicking the slight binocular disparity experienced when viewing three-dimensional objects. As a result, the SFM display was disambiguated and the rotation direction could be manipulated by adjusting which eye received the lagged image. The durations for how long the SFM replay sphere would turn in either

direction were sampled from a gamma distribution of participants' ambiguous SFM dominance durations recoded during the pre-experiment (see section 2.5.1).

For the pre-experiment, stimuli were presented on a 27 inch monitor (width = 602 mm, ASUS, Taiwan) operating at 120 Hz. There was no natural light contamination nor room lighting. Every participants' head position was fixated by a head and chin-rest. The distance between monitor and participant was 70 cm. All stimuli were created and controlled by a stimulus computer (Ubuntu 17.10) running Psychtoolbox 3 for Matlab R2014a (Mathworks, USA). Participants´ button press responses were collected with an adapted numeric keypad with eight buttons (two columns, one row).

For the main experiment, stimuli were presented through the MRI on visual display screen that was 29 by 16.5 dva in size. The screen was illuminated by a linearised projector operating at 120 Hz. There was no natural light contamination nor lighting. Every participants' head position was fixed by padding inside the MR receiver coil. Participants lay down and looked at the display through a mirror. The distance between monitor and participant was 900 mm.

1.3 MRI scan acquisition

All MRI scans were acquired using a 3T Siemens Prisma using a 64-channel head coil at the Max Planck Institute for Biological Cybernetics, Tübingen. For each participant, a T1-weighted ADNI sequence (Repetition time (TR) = 2000 ms, echo time (TE) = 3.06 ms, field of view (FOV) = 232 x 256 x 192 mm, voxel size = 1 x 1 x 1 mm, matrix 232 x 256, Flip angle 9°, 192 sagittal plane slices, acquisition time 7 min 46 s) was used to obtain structural MR images.

Functional images were acquired using an accelerated multi-band (factor 2) gradient-echo echo planar imaging (EPI) sequence using T2* weighted BOLD contrast (TR = 1200 ms, TE = 30 ms, FOV = 192 x 192 x 108 mm for whole brain coverage with 36 slices, isotropic voxel size =3 x 3 x 3 mm, Flip angle = 68°).

1.4 TMS protocol and neuronavigation

TMS pulses were delivered using a figure-of-eight coil (MC-B70) connected to a MagPro X100 stimulator (MagVenture). To account for individual differences in TMS magnetic field strength necessary to bring forth a detectable response following a single TMS pulse, I determined the resting motor threshold (RMT) for each participant as follows. Participants lay their right hand relaxed on an armrest. At initially 25 % maximum stimulator output, I applied single TMS pulses at a frequency less than 0.3 Hz to 2 cm anterior to the left hemispheric midline above the ear at a 45° coil angle relative to the ground (posterior-anterior coil position). We moved the coil between single

TMS pulses until a visible contralateral motor response could be elicited. Now, only at this location, I applied TMS pulses at various decreasing intensities, until TMS was able to just about produce a reliable motor response in 6 out of 10 pulses. The mean RMT was 32.88 % maximum stimulator output (± 3.19 S.D.). Participants reported muscle twitches and tingling during single pulse TMS stimulation, consistent with previous reports from TMS studies.

For the main experiment, TMS stimulation was a continuous theta burst protocol (Huang et al., 2005), consisting of bursts of three 50Hz TMS pulses, applied every 200 ms for 40 seconds (600 pulses in total). Intensity of the stimulation was set to 80% of individual RMT. Participants did not consume alcohol in the 24 hrs prior to each session and were well rested (both to avoid risk of lowered seizure threshold, see Rossi et al., 2009).

On separate days, cTBS was applied either to IPS (see section 2.6.2 and *figure* 4), or to the control site vertex. IPS was localised using individual BOLD activations from participant's first fMRI scanning session (see section 2.5.2). The standard MNI coordinates of the individual peak IPS cluster of that activation was entered into the neuronavigation system LOCALITE along with each participant's structural T1 scan. Using a Polaris infra-red camera (Northern Digital, Waterloo, Canada) and head-surface markers attached to participants, I tracked participants' head movements and co-registered them to their individual MR images. This allowed me to infer the stimulation location of TMS. We manually held the TMS coil to minimise the discrepancy between TMS stimulation direction and location of the IPS coordinates. The TMS coil shaft pointed posterior-inferior at a 45° angle and I maintained a maximum distance between actual and ideal coil location of 1.5 mm at all times. The vertex location was localised based on externally visible anatomical landmarks. It lay at the intersection between the the midpoint of the medial line on the scalp between nasion and inion and the midpoint of the lateral midline between the earlobes. For vertex stimulation, the coil was also held manually with its shaft pointed directly posterior, parallel to the floor.

1.5 Experimental design

1.5.1 Pre-experiment and participant screening

Participants were first screened for suitability for TMS using the criteria outlined by Rossi et al. (2009) and subsequently the RMT was measured.

In a screening experiment, carried out in a psychophysics lab, participants completed 10 trials of 120 seconds (20 minutes total) of viewing the SFM sphere. During this time, participants were instructed to fixate on the red fixation dot and not follow individual SFM dots with their eyes. Participants were instructed to press and hold one of two buttons to indicate their current percept:

during perceived left-wards rotation (front of the sphere moved left) the left button, during perceived right-wards rotation the right button. Both buttons were pressed using the right hand's index and middle fingers, respectively. Participants were instructed to press no button when percepts were unclear or mixed (which is rare for SFM stimuli). Bistable percept durations follow a gamma distribution (Levelt, 1967). We therefore extracted the median as measure of central tendency for each rotation direction and for all percepts. We also calculated their predominance of seeing a leftward rotation as the the proportion of the sum of left percept times divided by the sum of all percept times. Participants were excluded from further testing if their median dominance duration was shorter than 4 seconds, longer than 8, or if predominance was either greater than 0.7 or smaller than 0.3. Based on these criteria, half the sample was excluded (see section 2.1).

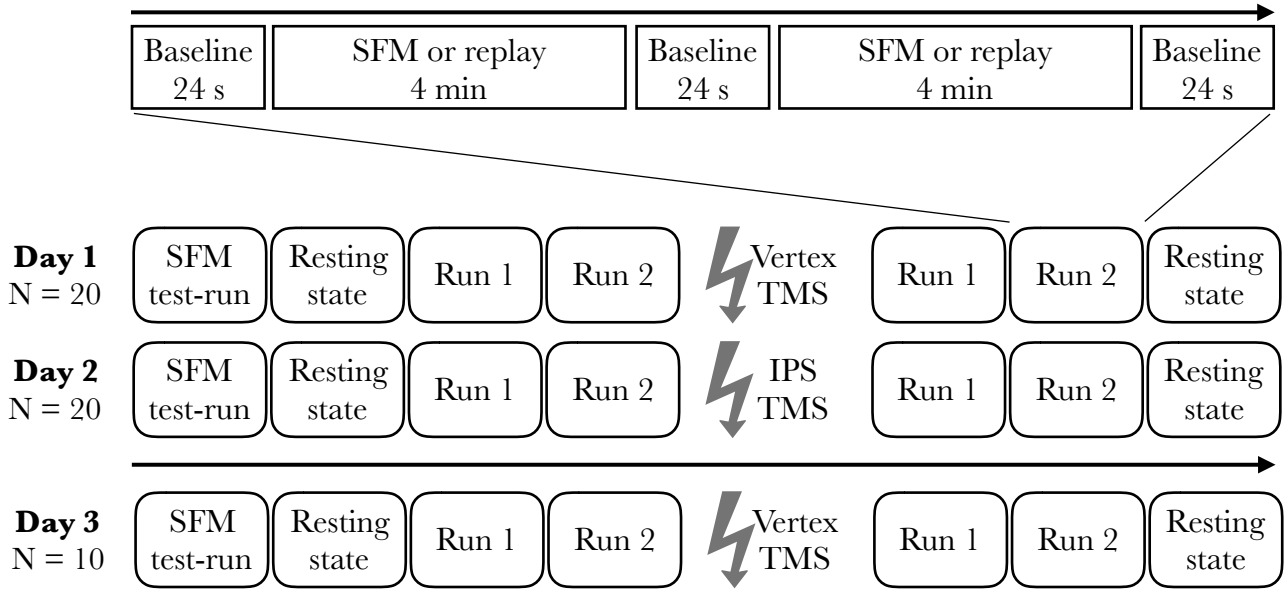

Figure 2 — Experimental design
Participants came to the MR lab on three separate days. They entered the MR scanner twice each time, once pre and once post cTBS application outside the scanner. Prior to TMS, they completed 5 min of SFM to reacquaint them with the stimulus, followed by resting state and two main experimental runs. After TMS came another two runs and resting state.

1.5.2 Main Experiment

For the main experiment, participants took part in either two or three fMRI sessions, at least 24 hours apart to prevent TMS carry over effects. Each fMRI session consisted of a total of 7 fMRI runs, four prior to TMS and three following TMS (see *figure* 2), as follows: Participants first completed 5 min (248 MR images) of viewing SFM inside the MR Scanner. This was to reacquaint participants with the stimulus, allow their percepts to stabilise and get them used to the scanner noise and surroundings. Afterwards I recorded 8 min (400 MR images) of resting state data, during which participants were instructed to fixate on a sole red fixation dot and allow their mind to turn blank. Next, participants completed two runs of the main test battery, each lasting 9.2 min (460 MR

images). Each main test run consisted of 24 s of baseline, during which participants merely focused on a fixation dot, 4 min of either SFM or replay, 24 s baseline, 4 min of SFM or replay, whichever they had not completed before, followed by another 24 s of baseline. The order of SFM and replay was kept constant within each participant, but was counterbalanced across participants. Next, participants came out of the scanner, went into the MR preparation room, where they received 40 s of cTBS. Immediately afterwards, they reentered the MR scanner and completed two runs of the main test battery, followed by another 8 min of resting state measurement (*figure* 2).

The reason that the test runs were kept to a mere 26.4 min (2 runs of 9.2 min plus 8 min resting state) was practical: The cortical inhibition following cTBS has been shown to last for up to 50 min (Huang et al., 2005; Schindler et al., 2008). However, there is also evidence for a much sooner dispersion of the stimulation effect between 16 and 30 minutes (Nyffeler et al., 2006; Zafar et al., 2008; Zapallow et al., 2011). The choice of paradigm aimed to ensure that the entirety of the MR recordings post cTBS would fall within this window of opportunity.

In the first fMRI session of each participant I stimulated the vertex site with cTBS. This allowed me to use the pre-TMS MR scans to localise the IPS in each participant for later cTBS. On the second appointment, IPS was then stimulated. Because of this, I could not exclude order and training effects that may explain the results. To circumvent this, I invited half the sample in for a third appointment, during which I stimulated vertex again. Of the 10 participants in question, half had each SFM and replay order, making the design fully counterbalanced. For the later analysis, I only considered the second vertex appointment for these participants, such that across all 20 participants also the order of stimulation site was fully counterbalanced.

1.6 Data analysis

1.6.1 Behavioural data

Our main measure of interest was the IPS-specific modulation of percept durations by cTBS. This was calculated using the formula: $(\text{pre - post})_{\text{IPS}} - (\text{pre - post})_{\text{vertex}}$, with pre and post referring to pre-TMS and post-TMS runs. Our reasoning and detailed procedure is described in the following: We first extracted the median percept duration from the pool of all percepts pre or post cTBS and for each session (i.e. stimulation site) separately. SFM bistable perception is associated with very short to non-existent mixed percept durations. We therefore excluded the time when participants pressed two or no buttons from the analysis. The reason I recorded a new SFM baseline for each session was to account for changes in arousal and attention day-to-day. Any pre-post difference in behavioural performance for cTBS to the vertex was assumed to reflect cTBS site-unspecific effects on the brain and was subtracted from the pre-post difference in performance found for the IPS cTBS site to find

the site-specific effect of parietal cTBS on behavioural performance. We used a one-sample t-test to determine statistical significance.

1.6.2 fMRI preprocessing and first-level analysis

All fMRI data was analysed using the SPM12 package for Matlab (Welcome Trust Centre, Department for Neuroimaging, London, UK). EPI volumes were first slice-time corrected, then realigned for motion correction, co-registered with each participant's structural T1 scan and normalised to the standard MNI brain template. Next, I applied a Gaussian smoothing filter to the images (12 mm full-width half-maximum). For the individual first level analysis, I separately examined each testing appointment and also pre and post TMS scans. For each of these, I modelled, in a standard general-linear model (GLM) approach, participants button presses for SFM (i.e. onset times for both buttons combined into one regressor to model percept-switches), the button presses during replay runs, as well as one block regressor for the entire SFM period and one for the replay period to account for the presence of the stimulus. We also included six movement regressors (three movement axes and three rotation directions) as regressors of no interest to model head movement from the realignment parameters. We also included an orthogonalised regressor modelling the mean signal intensity of each MR image. We used the parameter estimates of the button presses and stimulus blocks for further analysis.

1.6.3 ROI definition

Regions of Interest (ROI) were defined on a group-level using data that underwent the above preprocessing and first-level pipeline. To ensure independence between the ROI analysis and definition, I chose ROIs using the replay data, as it was not used for the main analysis. At a group-level, I examined all replay scans taken prior to TMS irrespective of TMS test site. We looked at regions activated during replay presses ($p < 0.05$ family-wise-error (FWE) corrected). ROIs were defined by selecting the peak voxel of each activated region in the left and right hemisphere separately and drawing a sphere around the peak voxel ($r = 12$ mm) including only significant voxels. Based on prior literature, I defined the following ROIs:

Inferior frontal gyrus (IFG). We primarily wanted to examine regions that in previous literature have shown activity modulation in bistable perception compared to a replay condition. Based on a meta-analysis of the past fMRI literature on bistability, Brascamp et al. (2018) concluded that inferior frontal cortex is consistently activated during bistability (analysis including contrasts from Lumer et al., 1998; Lumer & Rees, 1999; Kleinschmidt et al.,1998; Sterzer & Kleinschmidt, 2007; Zaretskaya et al., 2010; Knapen et al., 2011; Megumi et al., 2015; Frässle et al., 2014;

Brascamp et al. 2015). Our IFG regions were at MNI coordinates x = -44, y = 0, z = 6 cluster size (CS) 880 voxels (IFG-l) as well as x = 50, y = 14, z = 0, CS 846 voxels (IFG-r) (*figure* 3, rows 1 & 2).

Early visual cortex (V1). Early visual areas have been shown to display modulated activity based on stimulus interpretation (Fang et al., 2008; Grassi et al., 2017). Also, TMS to V1 has been shown to modulate bistable dominance durations (Pearson et al., 2007). We therefore included left and right V1 as ROIs. Our occipital regions lay at MNI coordinates x = -26, y = -88, z = -10 CS 621 voxels (V1-l) as well as x = 28, y = -86, z = -8, CS 764 voxels (V1-r) (*figure* 3, rows 3 & 4).

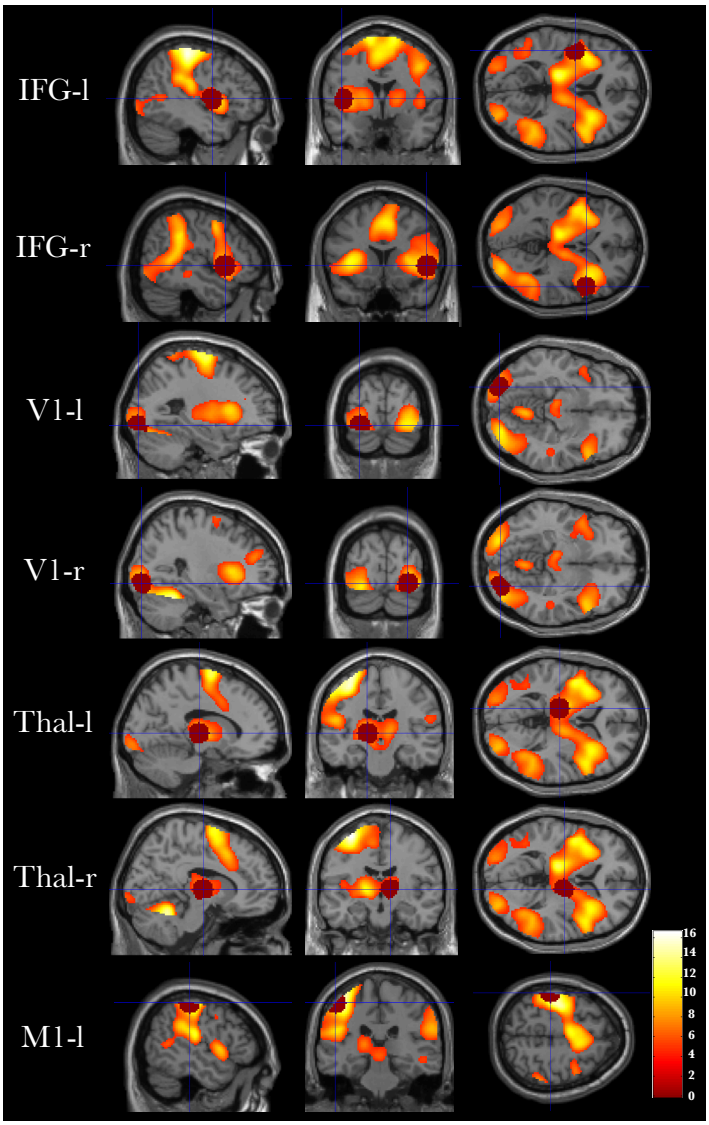

Figure 3 — ROIs localised using replay button presses
Group whole-brain result showing activity during replay button presses for all fMRI recordings prior to TMS irrespective of TMS site ($p < 0.05$ FWE corrected). Crosshairs indicate peak voxels of the selected ROIs. Around the peak, a sphere was drawn (r = 12 mm) including only significant voxels, shown for each ROI in burgundy.

Thalamus. The role of the thalamus and in particular the LGN in the resolution of has been demonstrated and its activity used to decode the content of bistable awareness (Haynes et al., 2005; Wunderlich et al. 2005). Also, cortical inputs to thalamus may be generally required to resolve bistability (Sillito et al., 2006). We therefore reasoned that TMS-induced modulation of bistability

may at least in part involve thalamic nuclei and included them as ROI. Our thalamic regions lay at MNI coordinates x = -14, y = -18, z = 4, CS 900 voxels (Thal-l) as well as x = 12, y = -12, z = 4, CS 736 voxels (Thal-r) (*figure* 3, rows 5 & 6).

Left primary motor cortex (M1-l). Neuroimaging studies investigating the neural signature of bistability have consistently found the involvement of left precentral gyrus or central sulcus (Lumer et al., 1998; Sterzer et al., 2002; Zaretskaya et al., 2010; 2013; Knapen et al., 2011, Roy et al., 2017). This is not surprising, since participants are normally asked to make button presses using the contralateral hand. However, the left motor cortex also dominantly shows activation in bistability compared to replay, even as the largest and most significant cluster in the present data (see Zaretskaya et al., 2010). While M1-l activity is usually shrug off as cognitively irrelevant for the resolution of perceptual ambiguity, I decided to investigate it for a conceptual reason: it is possible that previous TMS studies on bistability did not affect so much cognitive processes underlying awareness or attention, as much as participants ability to motor-express their percepts with button presses. If this were the case, then I would expect TMS modulation of left precentral activity. Our M1-l region lay at MNI coordinates x = -50, y = 28, z = 56, CS 505 voxels (*figure* 3, row 7).

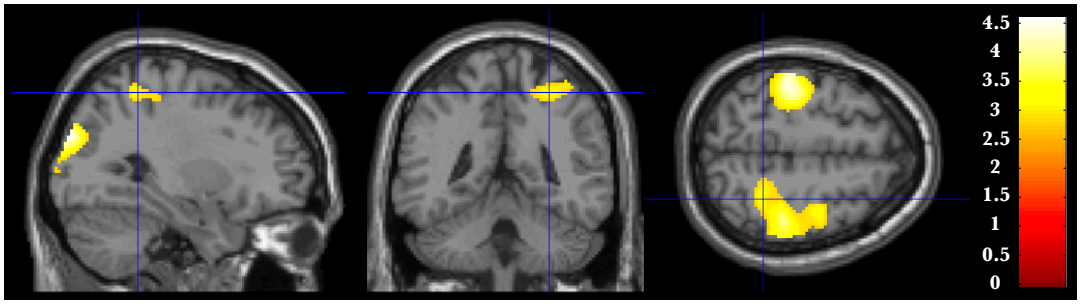

Figure 4 — IPS functional localisation
Group whole-brain result showing the contrast "SFM block > replay block" for all fMRI recordings prior to TMS irrespective of TMS site. Crosshairs denote the peak voxel of the anterior intraparietal sulcus at MNI x = 30, y = -44, z = 56, threshold $p < 0.005$ (uncorrected). Euclidian distance to a previously reported IPS region (Lumer et al., 1998) is 7.8 mm.

IPS. Since it was stimulated by TMS, I naturally wanted to examine the IPS as ROI. For the fMRI analysis I chose a group-level contrast to localise the IPS. Specifically, I examined all pre TMS scans irrespective of TMS site. We looked at right posterior parietal regions activated during the "SFM block > replay block" contrast ($p < 0.005$ uncorrected, *figure* 4). We now selected the peak voxel in the approximate ROI in the right hemisphere and drew a sphere around the peak voxel (r = 12 mm) including only significant voxels. This was done in order to safeguard consistency with the previous literature. Moreover, I wanted the ROI to capture where I actually stimulated with cTBS, hence decided against using a group-level defined IPS ROI. The peak voxel lay at a euclidian distance of 7.8 mm (Lumer et al., 1998), 6.6 mm (Zaretskaya et al., 2010) and 6.9 mm (Zaretskaya et al., 2013) from the peak IPS voxel reported by previous literature. To extract the ROI in the left

hemisphere, I flipped the right mask along the x axis. Our IPS regions lay at MNI coordinates x = ±30, y = -44, z = 56.

SPL & V5/MT. One prominent study investigating the causal interactions of right posterior brain regions found a network of three sites causally interacting during bistable perception of a SFM rotating sphere using dynamic causal modelling (Megumi et al., 2015), namely the IPS-r (10 mm sphere around the peak coordinates of Lumer et al., 1998); SPL-r (10 mm sphere around the peak coordinates of Kanai et al. 2010) and V5/MT-r (10 mm sphere around the peak coordinates of Dumoulin et al., 2000 and Mars et al., 2011). This model could successfully predict rivalry dominance durations based on the coupling strength between these three ROIs. We therefore chose to include SPL and V5/MT in this study as well. We used the method of Megumi et al. (2015) to localise them and used their flipped image to extract the ROIs also in the left hemisphere. Our SPL regions lay at MNI coordinates x = ±38, y = -64, z = 32, while I extracted V5/MT from x = ±44, y = -67, z = 0.

1.6.4 fMRI group-level analysis

ROI ANOVA. First, I conducted a ROI analysis. We extracted beta estimates for the regressor of interest (SFM button presses) for voxels within each of the ROIs. We next averaged the estimates across voxels and runs for each participant. Beta estimates were normalised by calculating percent signal change using each ROIs mean signal as normalisation reference. First, I tested whether the hemisphere impacted the TMS signal modulation by constructing a repeated measures ANOVA using percent signal change as dependent variable with the following factors: TMS site; whether the recording was taken pre or post TMS, ROI, and hemisphere. This analysis did not include M1-l, since this was a unihemispheric ROI. Based on the outcome that hemisphere or its interaction with ROI or TMS was not significant (see section 3.3.1), I averaged beta estimates across hemispheres for each ROI in each participant. Now, I conducted another repeated measures ANOVA using percent signal change as dependent variable with the factors TMS site, whether the recording was taken pre or post TMS, and ROI.

ROI TMS effect. We calculated for each ROI the IPS specific TMS effect by using the same formula applied to the behavioural data: $(pre - post)_{IPS} - (pre - post)_{vertex}$, with pre and post referring to pre-TMS and post-TMS runs. We tested for significance using Bonferroni corrected one-sample t-tests on the resulting TMS modulation of percent signal change for each ROI. We also investigated the relationship between the modulation of beta estimates through TMS with the modulation of behavioural data by correlating them with SFM percept duration modulation.

Whole brain. Next, I performed a whole-brain analysis. To identify voxels modulated by IPS-TMS, I used a second-level GLM comprised of a two-way ANOVA akin to the one used in the ROI analysis. It included four images per participant from the first-level analysis for SFM-button presses: vertex-pre, vertex-post, IPS-pre, IPS-post, and tested for a directed interaction contrast given as [1 -1 -1 1] at a liberal threshold of $p < 0.001$ uncorrected.

1.6.5 Seed-based connectivity

In order to examine whether cTBS altered functional connectivity of the stimulated IPS site I conducted a seed-based correlation analysis using the right IPS ROI as seed region. The mean time course of the IPS was extracted for each testing run as well as separately for the resting state data and entered into two general linear models (one for task, one for resting state). Both GLMs included also global mean signal and movement parameters as regressors of no interest. Resulting correlation maps were transformed to Fisher's z-scores prior to group analysis. At the second-level I used the same procedure as in the task-based analysis above. Results were corrected for multiple comparisons using family-wise error (FWE) correction.

2. Results

2.1 Pre-experiment

Participants' median dominance duration was 7.58 s (± 6.20 s.d.). The mean TMS resting motor threshold was 32.7 % maximum stimulator output (± 4.9 s.d.). Out of the 40 screened participants, 20 met the requirements for the main experiment (median dominance 6.03 s ± 2.16 s.d.).

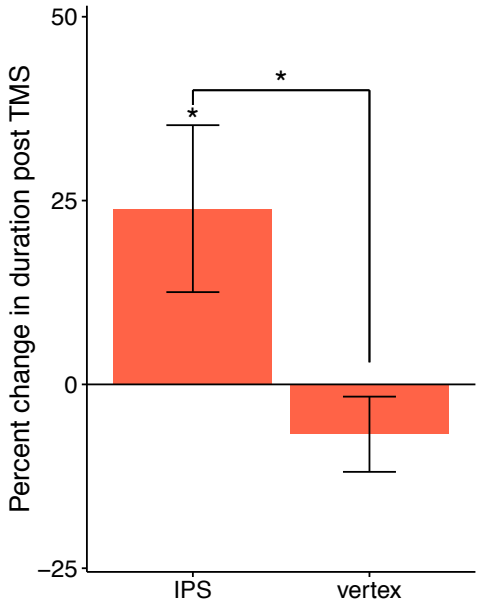

Figure 5 — TMS effect on dominance durations
Percentage change in dominance durations after TMS for the test sites vertex and IPS. * t-test significance $p < 0.05$. Error bars are ± 1 s.e.m.

2.2 Behavioural data

As expected, control site vertex cTBS had no effect on rivalry dominance durations when comparing post to pre cTBS median dominance ($t(19) = -0{,}32$, $p = 0.20$). However, cTBS to the IPS led to a significant lengthening of SFM percept durations of 23.9 % ($t(19) = 2.11$, $p = 0.049$). A comparison between the cTBS effect on IPS with vertex showed that this lengthening remained significant after subtracting the site-unspecific vertex cTBS effect ($t(19) = -2.35$, $p = 0.03$; *figure* 5).

Descriptive and inferential statistics

Site	TMS	duration (s)	s.e.m.	% diff.	s.e.m.	one sample t(19)	p	paired t(19)	p
IPS	pre	5.59	0.42	23.9	11.35	2.11	0.049*		
	post	6.84	0.84					-2.35	0.03*
vertex	pre	6.19	0.53	-6.78	5.12	-0.32	0.20		
	post	5.47	0.41						

Table 1 — Descriptive and inferential statistics
Median dominance duration in seconds ± 1 s.e.m for each test site and for pre and post TMS recordings. Given is also the percent difference pre vs post TMS for vertex and IPS ± 1 s.e.m, and one sample t-test on the percentage differences as well as a paired t-test between the percent differences. * t-test significance $p < 0.05$.

2.3 TMS-induced BOLD modulation

2.3.1 ROIs

The main question of this study was whether the change in percept dominance durations due to parietal cTBS was accompanied by a modulation in BOLD signal. We analysed activity related to perceptual switches (i.e. beta-estimates obtained for the button-response regressor during viewing of SFM stimuli), for pre- and post-TMS runs for the IPS and the vertex site. First, I tested if the ROI activity was significantly lateralised between hemispheres by modelling a repeated measures ANOVA on normalised beta estimates using the factors TMS site, whether the data is pre or post TMS, and hemisphere. This model did not include M1-l, since this region was only extracted unilaterally. We found a significant interaction between TMS site and pre-post ($F(1,19) = 7.18$, $p < 0.002$), but no main effect of hemisphere or interaction term including hemisphere ($F(1,19) < 1$, *ns*). We therefore averaged normalised beta estimates across hemispheres in bilateral ROIs in every participant and henceforth analysed ROIs irrespective of hemisphere.

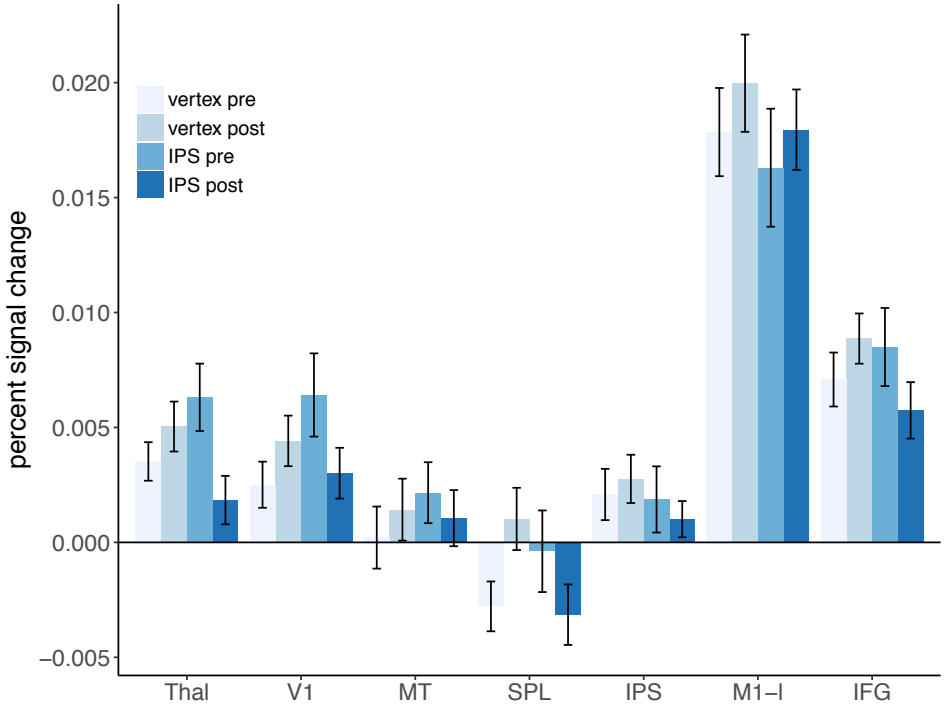

Figure 6 — Percent signal change per ROI and TMS condition during percept switches
Percent signal change for each previously defined ROI across the different TMS sites as well as pre or post TMS. Consistent with whole-brain results, the strongest activity was observed in primary motor cortex. Consistently, post IPS signal was weaker than pre IPS, while this effect was reversed for vertex. Error bars are ± 1 s.e.m.

Next, I performed the main repeated measures ANOVA on normalised beta estimates using the factors TMS site, pre-post, and ROI. Mauchly´s test indicated that the assumption of sphericity had been violated, hence degrees of freedom were corrected using Greenhouse-Geisser estimates of sphericity for the main effect of ROI ($\chi^2(5) = 55.60$, $p > 0.0001$, $\varepsilon = 0.52$) as well as the three-way

interaction term ($\chi^2(5) = 37.28$, $p = 0.002$, $\varepsilon = 0.60$). We found a significant main effect of ROI ($F(6,114) = 57.32$, $p < 0.0001$), as well as a significant three-way interaction between all factors ($F(6,114) =$, $p = 0.019$) (*figure* 6). Interestingly, IPS cTBS in all ROIs except M1 tended to decrease activity, while vertex cTBS led to the opposite.

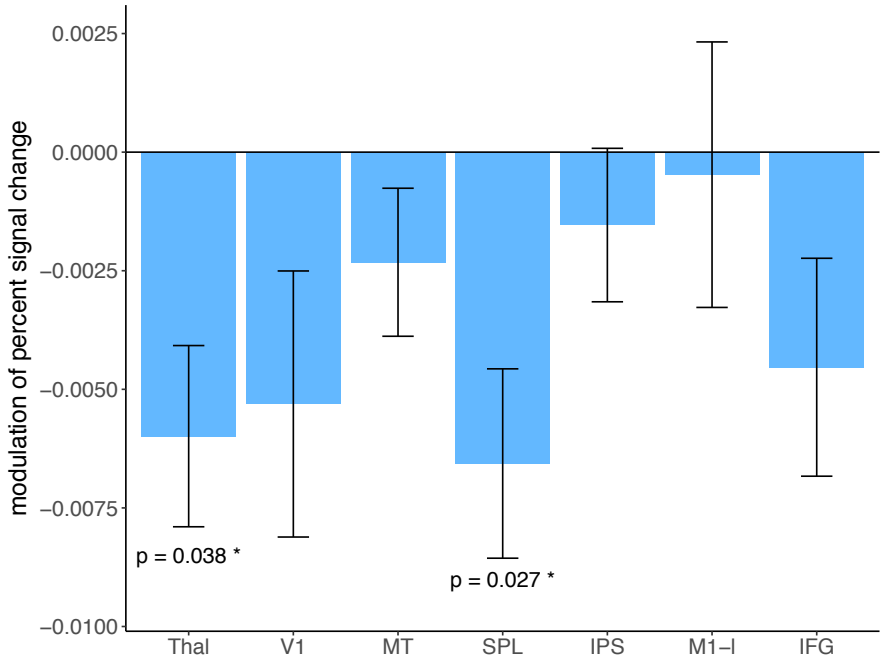

Figure 7 — TMS modulation of percent signal change across ROIs
Modulation of percent signal chance for each ROI calculated as directed interaction contrast between vertex-pre, vertex-post, IPS-pre, IPS-post [1 -1 -1 1]. * t-test significance $p < 0.05$ Bonferroni corrected. Error bars are ± 1 s.e.m.

ROI one sample t-tests (df = 19)

ROI	t-statistic	p-value (uncorrected)	p-value (Bonferroni)	significance
Thalamus	-3.13	0.0054	0.038	*
V1	-1.89	0.073	0.52	
V5/MT-r	-1.49	0.15	1	
SPL	-3.29	0.0038	0.027	*
IPS	-0.95	0.35	1	
M1-l	-0.17	0.87	1	
IFG	-1.97	0.06	0.44	

Table 2 — t-tests on TMS modulation across ROIs
One-sample t-tests for each ROI on the modulation of percent signal change, i.e. the difference pre-post vertex TMS subtracted from the difference pre-post IPS TMS. * t-test significance $p < 0.05$ (Bonferroni corrected). Error bars are ± 1 s.e.m.

In what followed, I examined not the normalised beta-estimates, but rather their TMS modulation, i.e. the difference pre-post vertex cTBS subtracted from the difference pre-post IPS cTBS. We entered this modulated estimate into a one-way ANOVA using ROI as factor. Mauchly´s test indicated that the assumption of sphericity had been violated, hence degrees of freedom were corrected using Greenhouse-Geisser estimates of sphericity ($\chi^2(20) = 35.20$, $p > 0.02$, $\varepsilon = 0.60$). We

found a significant main effect of ROI ($F(6,114) = 3.31$, $p = 0.019$). We hence proceeded with post hoc Bonferroni corrected one-sample t-tests to find ROIs for which the TMS modulation was significantly different from zero (*figure* 7, *table* 2).

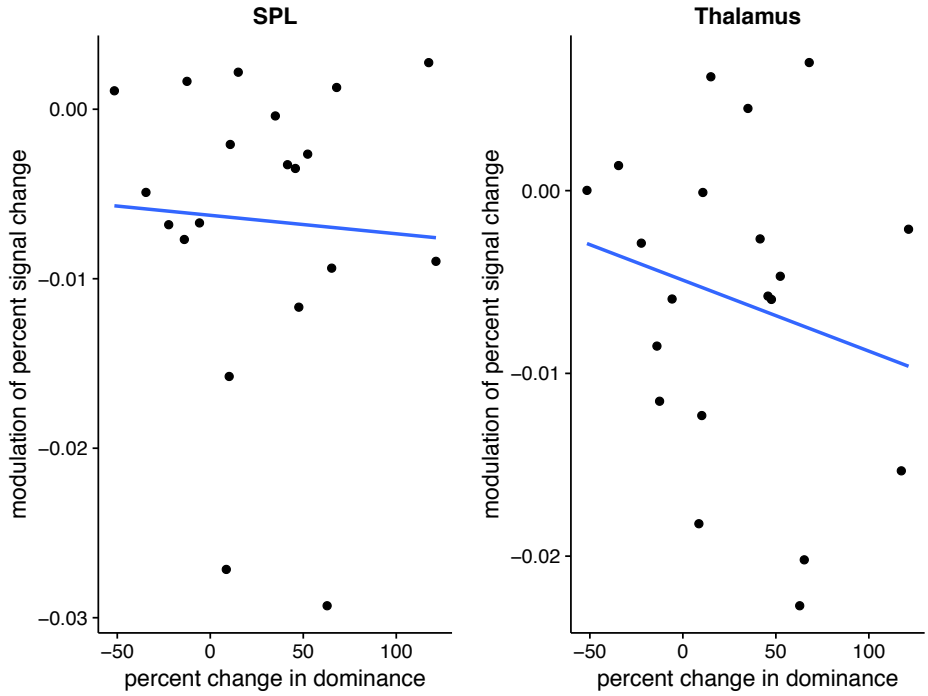

Figure 8 — Correlation of TMS modulation of percent signal change and SFM percepts
Modulation of percent signal chance for SPL (left) and thalamus (right), given as directed interaction contrast between vertex-pre, vertex-post, IPS-pre, IPS-post [1 -1 -1 1], are correlated against modulation of SFM bistable dominance durations. Neither was statistically significant ($|r| < 0.25$, *ns*).

At last, I attempted to correlate the cTBS modulation of percent signal change with the cTBS modulation of SFM percept durations using Pearson's r. The presence of such a correlation would substantially strengthen confidence in the result, since it would entail that participants who respond favourably to TMS in the behavioural domain also show a larger TMS modulation of their BOLD signal. Alas, I found no such correlation for the two significant ROIs (SPL: $r = -0.06$, $p = 0.81$; Thalamus: $r = -0.21$, $p = 0.37$) (*figure* 8).

2.3.2 Whole-brain

In order to discern any brain areas whose BOLD signal may have been modulated by cTBS, but that did not appear in the ROI analysis, I also performed a whole-brain survey. As a first step, I charted how the signal associated with SFM button presses was affected by vertex cTBS. We found no suprathreshold voxels deactivated by cTBS, but several small clusters that showed increased activity post TMS (*figure* 9, I., *table* 3, I.). Given their spread, the liberal alpha threshold of 0.001 uncorrected, as well as the result that none of the clusters are statistically significant following cluster-correction, I interpret these as noise. In contrast, when examining IPS stimulation, I found

no activation, but instead inhibition of BOLD activity in the bilateral thalamus, left V1 as well as right posterior medial frontal cortex (*figure* 9, II., *table* 3, II.). Finally, I turned to the main contrast, namely BOLD modulation following IPS stimulation, with the vertex (TMS site unspecific) effect subtracted (I. > II.). This revealed that IPS cTBS inhibited BOLD signal in the thalamus, left V1, left middle frontal gyrus and right posterior medial frontal cortex (*figure* 9, III., *table* 3, III.).

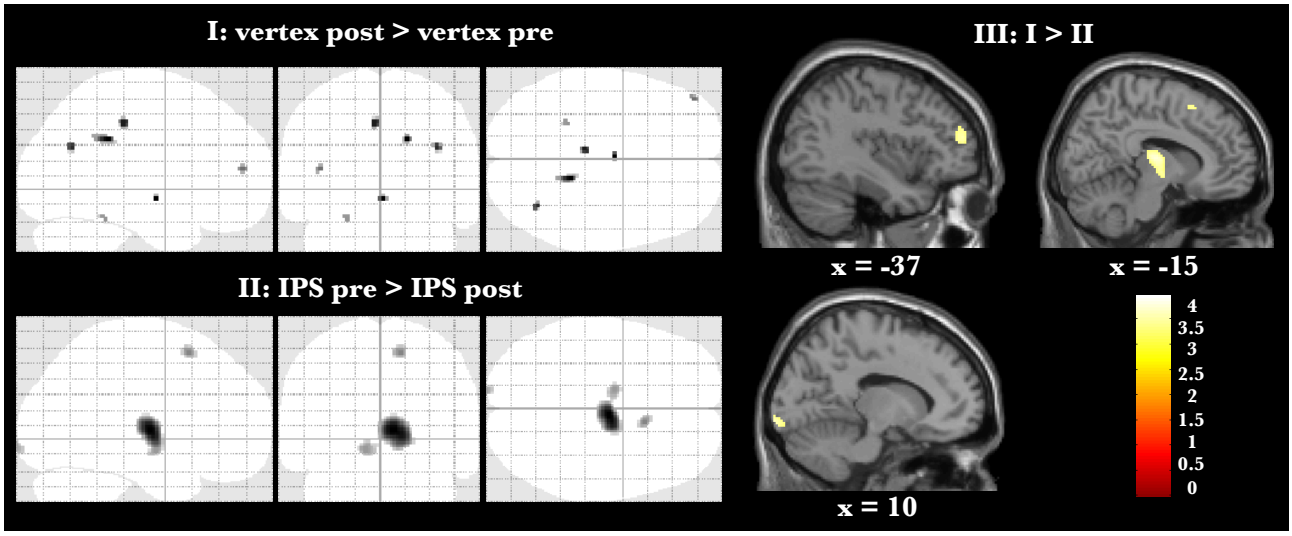

Figure 9 — Whole-brain fMRI results
Brain areas showing differential activation post vs pre TMS when vertex was stimulated (top left) and when IPS was stimulated (button left). Decrease in BOLD activity when IPS is stimulated with the vertex effect subtracted, when on sagittal slices of the MNI T1-template (right), directed interaction contrast between vertex-pre, vertex-post, IPS-pre, IPS-post [1 -1 -1 1]. Threshold $p < 0.001$ uncorrected.

2.4 TMS-induced connectivity changes

There was a highly significant decrease in connectivity between the right IPS and ipsilateral hippocampus following IPS TMS, vertex TMS effect subtracted (III. according to the design in section 3.3.). This was the only significant cluster at (x = 34, y = -22, z = -16, cluster size 51 voxels, z (peak) = 4.53, $p < 0.05$, FWE corrected). There was no significant increase or decrease in connectivity for the resting state data (*figure* 10).

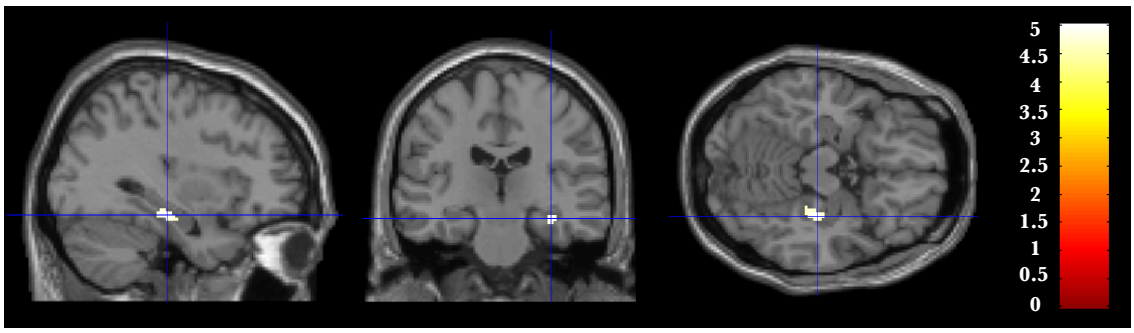

Figure 10 — Whole-brain connectivity results
Brain areas showing a decrease in functional connectivity when IPS is stimulated with the vertex effect subtracted on the MNI T1-template. Directed interaction contrast between vertex-pre, vertex-post, IPS-pre, IPS-post [1 -1 -1 1]. Threshold $p < 0.05$ FWE corrected. Only significant cluster in right hippocampus.

Whole-brain analysis results

brain region	x, y, z (mm)	Cluster size (voxels)	*z* (peak)	*p* (uncorrected)
I: vertex post > vertex pre				
R. thalamus	0 -8 -8	4	3.23	0.001
R. area 45	16 -40 32	23	3.23	0.001
L. MCC	-6 -30 42	15	3.21	0.001
R. area 45	36 -64 26	10	3.20	0.001
L. middle frontal	-42 50 12	5	3.16	0.001
L. lobule V	-24 -42 -22	4	3.14	0.001
II: IPS pre > IPS post				
R. thalamus	6 -12 4	483	3.71	< 0.001
R. posterior medial frontal	12 14 56	38	3.34	< 0.001
L. thalamus	-12 -8 -8	44	3.28	0.001
L. hOc1 (V1)	-12 -102 -8	18	3.26	0.001
III: I > II				
R. thalamus	-2 -10 -8	504	3.69	< 0.001
L. middle frontal gyrus	-42 50 14	59	3.39	< 0.001
L. hOc1 (V1)	-12 -102 -8	51	3.35	< 0.001
R. ventricular noise	14 -32 30	5	3.25	0.001
R. posterior medial frontal	10 16 56	25	3.25	0.001

Table 3 — Results of whole-brain fMRI analysis
Areas showing increased activity post vertex cTBS (I.), increased activity post IPS stimulation (II.), as well as their difference, i.e. areas that were preferentially deactivated by IPS stimulation (III.). Areas accompanied by MNI coordinates, cluster size, z-scores p-values. Voxels thresholded at $p < 0.001$ uncorrected. Anatomical designations derived from the SPM anatomy toolbox at a threshold of $p < 0.01$ uncorrected (Eickhoff et al., 2005). No statically signifiant clusters following cluster-correction, $p > 0.05$ in all cases. L. is left, R. is right.

3. Discussion

The nature of the effect of IPS cTBS on bistable perception remains elusive. We therefore recorded fMRI before and after IPS cTBS to generate rich data to elucidate it. We found that SFM dominance durations lengthened following IPS cTBS compared to vertex control. This lengthening was accompanied by a modulation of BOLD signal, specifically a reduction of activity in the thalamus, visual cortex, SPL as well as middle frontal gyrus. At the same time, correlation of activity between the IPS and ipsilateral middle hippocampus was reduced.

3.1 Behavioural TMS effect

The here observed lengthening of dominance stands in direct opposition to Kanai et al. (2011) who, using an identical stimulus and TMS protocol and found a shortening of dominance. Also, such a shortening of dominance durations has been reported following cTBS to IPS for another bistable stimulus, and also using offline repetitive TMS on BR, both of which were regarded as impairment of attention allocation (Carmel et al., 2010; Wood et al., in prep). However, the present result is compatible with the interpretation of Zaretskaya et al. (2010), who found a lengthening of dominance following rTMS that was applied during stimulus viewing. Their interpretation was that TMS had a stabilising effect by injecting neural noise into IPS activity. IPS in turn was hypothesised to be involved in causing perceptual reversals in context of stimulus selection, a widely accepted function attributed to IPS. Similarly to Kanai et al., 2010, they reason that this modulation may be related to a removal of attentional resources, akin to the psychophysical result that diverting attention from bistable stimuli prolongs them (Paffen et al., 2006). Also, Zaretskaya et al. (2013) observed a selective shortening of dominance of the Gestalt as opposed to the components percepts in a special case of bistable perception, where the two percepts are asymmetric in terms of their complexity following IPS cTBS. This effect was attributed to the hypothesised role of IPS in visual scene segmentation. The differences between these results can in part be explained by discrepancies between high and low level stimuli as well as TMS protocols (Wood et al., in prep), despite many reasons speaking for a common neural mechanism of BR and bistability (Petruk et al., 2018). Another difference could lie in the use of individual fMRI-based localisation of IPS in the present study (as well as in Zaretskaya et al., 2010; 2013), but not in Kanai et al. (2010, 2011) or Carmel et al. (2010) who used average coordinates based on Lumer et al. (1998). This could have led to systematic differences in stimulation strength between studies. Apart from the above-mentioned differences, one cannot exclude the possibility that either the cTBS effect is variable based on sample, or that the effect itself is unstable. Unlike previous studies however, I

have the luxury of concurrently recorded fMRI data, that allows me to directly interpret neural cTBS effects that accompanied the behavioural effects.

3.2 TMS modulation of ROI activity

Most generally, I found across all ROIs but left primary motor cortex, that vertex cTBS led to a numeric increase in BOLD signal, whereas IPS cTBS brought about the opposite. This interaction is the primary drive behind the IPS-specific results.

3.2.1 IPS

Given the inhibitory nature of cTBS (Huang et al., 2005), I expected a reduction of BOLD signal in IPS. We did not observe this, but there are possible explanations for the absence of such an effect: Foremost, it may be that the cortical inhibition observed by Huang et al. (2005) following cTBS to M1 may be specific to M1. There, the direction and efficacy of the effect is contingent on TMS coil orientation as well as the specific cortico-spinal tracts stimulated by cTBS (Hamada et al., 2012). It is unclear whether these mechanisms can be transposed to the parietal cortex, especially since there is no active measure like motor-evoked potential (MEP) amplitude available to directly test the success of cortical inhibition over IPS.

Wang et al. (2013), using a searchlight multivariate pattern analysis (MVPA), showed that bistability was associated with both bottom-up and top-down interactions between visual and higher-level cortical areas. Critically, unlike their BOLD analysis, MVPA did not highlight the IPS, suggesting that this region itself does not code for visual content. The same may be true here: if IPS activity during bistable perception is more indicative of a central processing hub rather than content encoding, and if cTBS affects remotely areas that do encode such information, then I would expect modulation of frontal, visual and thalamic regions, while leaving activity in IPS intact. Against this notion speaks that IPS activity has been successfully used to decode SFM percepts (Brouwer & van Ee, 2008).

Still, it is important to stress the relevance of whole brain networks in the resolution of bistability: it need not take place in IPS alone simply because the region was indicated using fMRI or TMS. Rather, it could be that cTBS affects several connected brain areas in the visual hierarchy merely *through* IPS. In this vein, Schauer et al. (2016a) showed how EEG potentials of single pulse TMS to IPS during SFM viewing travel to a variety of cortical areas. Also, using diffusion tensor imaging, Wilcke et al. (2009) found that large portions of the fronto-parietal network reported in Lumer et al. (1998) are structurally connected. This has also been elegantly demonstrated by Ruff et al. (2006), who applied TMS to the frontal-eye fields (FEF) while recording fMRI and found a

decrease of V1 activation immediately following the stimulation. This effect was not present when they stimulated vertex control. In other words, a higher level stimulation fed backwards as top-down modulation of V1 activity, showing that TMS can mitigate activity in distant brain regions.

3.2.2 SPL

One region of particular interest to me was the SPL, since cTBS to it has previously also led to a lengthening of SFM dominance (Kanai et al., 2010). Indeed, I found that IPS cTBS significantly reduced SPL activity, which *prima facie* suits the result of Kanai et al. (2010) if there is a unified parietal function for bistability. However, it is more likely that there is a fractionation between IPS and SPL with distinct roles, not routed in a fractionation of sustained and spatial attention (Schauer et al., 2016b). Kanai et al. (2011) interpreted this functional fractionation between IPS and SPL in terms of predictive coding (Rao & Ballard, 1999; Friton, 2005; Hohwy et al., 2005): According to this framework, perception is dynamic Bayesian process of inference, where higher level predictions about the content of perception is compared to actual sensory input, yielding an error, which is then sent upward the predictive hierarchy to correct the prediction. Hence, I perceive ever more accurate predictions of the world, which are constantly corrected for error signals. Applied to SFM, one perceives one's current rotation direction interpretation of the stimulus, while error signals pertaining to the suppressed direction build up until a critical point where the percept switches. IPS and SPL are then meant to play opposing roles in calculating predictions and errors. According to Kanai et al. (2011), IPS processes predictions, hence cTBS induced shortening of bistable dominance is interpreted as weaker predictions, hence a faster build up of error signals and bistable switching (Kanai et al., 2010, 2011). SPL is meant to calculate error signals. cTBS inhibition then leads to a lengthening of dominance since error signals need longer to build up and force a perceptual reversal. Specially for SFM, exposure to prior expectation can bias perceived motion direction, suggesting a role of prediction in SFM perceptual selection (Dogge et al., 2018). This view is not without critique. The fractionation of IPS and SPL could not be replicated using TMS-EEG (Schauer et al., 2016a). Moreover, Kanai et al. (2011) fall victim to the fallacy of affiliating a brain area with single function based only the TMS modulation of dominance durations. Still, the modulation of SPL activity is consistent with this view, in that mitigation of SPL activity via IPS could have led to a weakening of error signal processing in SPL, which in turn lengthens bistable dominance.

3.2.3 V5/MT+

Another ROI where I would have expected an effect was right V5/MT+. A correlation between perceived motion direction and V5/MT+ activity has previously been reported (Bradley et al., 1998; Dodd et al., 2001). Using support-vector machines, Brouwer & van Ee (2008) could also decode SFM motion direction from V5/MT+ as well as extra-striate fMRI activity. Also, Megumi et al. (2015) showed with dynamic causal modelling how bi-directional coupling strength between right IPS, right SPL and right V5/MT+ can predict SFM dominance durations. It therefore stands to reason that V5/MT+ is part of the functional network subserving the resolution of SFM bistability. Critically, stimulating the IPS using short burst TMS while recording occipital fMRI, Ruff et al. (2008a; 2008b) found that V5/MT+ activity was attenuated by IPS TMS when a moving stimulus was presented. They interpreted this as signifying a disruption of neural activity that encodes moving stimuli. It also fits with the proposal that movement information is represented between V5/MT+ and posterior parietal cortex (Huk & Shadlen, 2005). That I do not replicate the exact findings of Ruff et al. (2008a; 2008b) is inconsequential, since their online short burst TMS is believed to have different cortical effects from (offline) cTBS (Huang et al., 2005). We are however agnostic as to why I found no activity modulation, especially since I argue above how the lack of modulation in IPS is not indicative of a lack of TMS effect.

3.2.4 Visual cortex

We did however observe a reduction of V1 activity, which I am cautious to interpret since it appeared only in the whole-brain analysis with an uncorrected tendency ($p=0.073$) in the ROI analysis. Given the size of the ROI compared to the more concise whole-brain result in the occipital pole, it may be that the ROI was too broadly defined to pick up mostly foveal modulation. Still, top-down modulation of striate activity via high-level attention modulation originating from the fronto-parietal network has been robustly observed (Kastner & Ungerleider, 2000; Corbetta & Shulman, 2002; Ruff & Driver, 2006; Driver et al., 2004; Serences & Yantis, 2006; Blankenburg et al., 2008; 2010; Ruff et al., 2008a, 2008b; 2010), as has suppression of V1 activity accompanied by high IPS activity during bistable perception (Grassi et al., 2016, 2018; Zaretskaya et al., 2013). One group stimulated IPS using bursts of TMS while simultaneously recording fMRI activity using an occipital surface coil (Ruff et al. 2008a; 2008b; Blankenburg et al. 2010). In three separate studies they found a distinct influence of IPS stimulation on BOLD signal in visual cortex areas V1-V4 as well as V5/MT+. This effect was specific to right rather than left IPS and while V1-V4 activity was increased when no visual stimulus was presented, it was left untouched and instead V5/MT+ activity decreased in the presence of a moving stimulus (Ruff et al., 2008a; 2008b). They believe that during

visual stimulation, bottom-up signals from V1-V4 overpower TMS-induced top-down effects. Critically, this influence of IPS TMS on V1-V4 activity could be modulated by the participant's attentional state (Blankenburg et al., 2010). This increases confidence in the finding that IPS cTBS leads to V1 modulation. Within the predictive coding framework, Zaretskaya et al. (2013) suggested that V1 is involved in prediction-error calculation, because of its reduced activity during periods of stability during bistable perception, indicating that V1 error signals are cancelled by temporarily accurate IPS predictions. Those results have later been shown to be associated to a detailed map of distinct stimulus features (inducers, fore- and background) associated to distinct modulations in V1 and V2 compatible with the predictive coding framework (Grassi et al. 2018). Our results are consistent with this theory: If V1 calculates error signals, then the observed IPS top-down attenuation of its activity should lead to weaker error and the observed lengthening of dominance.

3.2.5 Thalamus

Further downward the visual hierarchy, I found a strong modulation in the thalamus for both whole-brain and ROI analyses. In BR, the thalamic LGN has received much attention, since rivalry correlated strongly with LGN BOLD signal (Wunderlich et al., 2005; Haynes et al., 2005). Our observed reduction in thalamus activity cannot be reduced to LGN modulation however, since both the ROI and the whole-brain cluster encompass multiple thalamic nuclei, which have been shown to play unique functions in perception: while LGN neurones show spiking modulation exclusively to information on the retina, pulvinar neurones changed their activity equally based on stimulus visibility (Wilke et al., 2009). This is sensible since the pulvinar receives inputs from cerebral cortex (Sherman & Guillery, 2002; Shipp, 2003), and visual areas in particular (Kaas & Lyon, 2007). Pulvinar damage has moreover been implicated in shifting spatial attention (Petersen et al., 1987), as well as hemispatial neglect (Karnath et al., 2002). In reverse, LGN and pulvinar neurones are also modulated by top-down attention (O'Connor et al., 2002; Kastner et al., 2004; Casagrande et al., 2005; McAlonan et al., 2008). While the fMRI results are not fine-grained enough to localise a TMS effect to any specific nucleus, I did observe a reduction in signal in more middle to posterior aspects of the thalamus, indicating the pulvinar. A modulation of pulvinar neurones by IPS cTBS would also be sensible: connections between frontal and posterior regions do not only run directly via cortico-cortical monosynaptic connections, but indirectly via the pulvinar in macaques (Gutierrez et al., 2000; Contini et al., 2010). This feeds into the idea that perceptual awareness of bistable figures can only arise from functional connectivity dynamics between fronto-parietal areas and the pulvinar (Panagiotaropoulos et al., 2014). Sillito et al. (2006) similarly argue that thalamic activity, while possibly causal for the resolution of bistable perception, still requires cortical inputs

from V1 and V5/MT+ to modulate its activity based on higher level attention. They believe it is this interplay of V1, V5/MT+ and thalamic activity that enables at least motion perception. Crucially, also Kanai et al. (2015) have posited that the pulvinar and LGN are separate sites at which error-prediction and precision calculations take place. These strong connections to the pulvinar make it a prime candidate for IPS cTBS cortical modulation, which I consequently observed. Within the predictive coding framework, I hence theorise that cTBS to the IPS attenuates thalamic activity, thereby disrupting early error signals, which in turn lead to fewer SFM perceptual reversals. Also outside the predictive coding framework a reduction of pulvinar function is compatible with the idea of attenuated resources for attention and hence perceptual selection, as argued by Zaretskaya et al. (2010) and Paffen et al. (2006) to account for dominance lengthening. If thalamic activity is as relevant as I posit, the question arises why the above mentioned studies stimulating IPS while recording fMRI (Ruff et al., 2008a, 2008b; Blankenburg et al., 2010) did not pick up any thalamic modulation. However, they used an occipital surface coil for recording fMRI signal, which is severely limited in its brain coverage, hence it is possible that their TMS bursts had thalamic effects that lay beyond their local recording capabilities.

3.2.6 Frontal cortex

More precarious is the interpretation of the activity reduction in middle frontal gyrus (MFG). The neighbouring IFG has been been most strongly indicated in a meta-analysis of previous fMRI work on bistable perception (Brascamp et al., 2018). Also, an fMRI model based approach showed that a prediction-error model faired well in explaining neural bistability data, especially in inferior frontal gyri (Weilnhammer et al., 2017). In contrast, I observed no signal modulation in IFG, but only an uncorrected reduction in MFG over the whole-brain. Given the weak effect size, I am cautious to interpret this effect but concede that within a predictive coding framework, a lengthening of SFM dominance should have been associated with stronger predictions, hence either an increase in frontal regions or at least no change if error signals are instead weakened. This is contrary to what I have observed.

3.3 Bistability and attention

Another crucial factor to consider is the interaction between bistable perception and attention, which is so strong as to have revitalised Helmholtz' idea of all perception as inference (exemplary Paffen et al., 2006; Mitchell et al., 2004; van Ee et al., 2005; Schenkluhn et al., 2008). Inattention even abolishes bistable perception altogether (Brascamp & Blake, 2012). Moreover, parietal cortex is strongly associated with shifting attention (Corbetta et al., 1995; Hilgetag et al.,

2001; Yantis et al., 2002) and IPS is part of the dorsal attention network (Corbetta & Shulman, 2002, review Bor & Seth, 2012). Hence, interpretations of the TMS effects on IPS in bistable perception in terms of impairment of attention allocation (Carmel et al., 2010) or directing attention (Zaretskaya et al., 2010) were never far. Our results can similarly be interpreted within this framework: cTBS to IPS leads to an impairment of spatial attention shifting, which manifests as a lengthening of bistable dominance durations. Neurally, this is realised via cortico-thalamic feedback projections from IPS and SPL to the pulvinar, which has been shown to be attention modulated (Kanai et al., 2015) and even proposed as central hub for processing spatial attention (Shipp, 2004). This modulation feeds back upward the visual hierarchy via V1, whose activity is hence also attenuated by the impairment of spatial attention shifting.

3.4 Connectivity decrease between IPS and hippocampus

Another main find of this study is the decrease of functional connectivity between IPS and ipsilateral hippocampus. This may indicate the involvement of memory circuits in the resolution of bistable perception. Indeed, IPS BOLD signal strength during bistable perception linearly depends on working memory load (Intaitė et al., 2016). In addition, recent memory studies highlight a close interaction between parietal cortex and hippocampus, that is particularly strong during the initial encoding of stimuli (Brodt et al., 2016). Our TMS stimulation is likely to have influenced this highly connected system. Despite a direct causal influence through cTBS, I did not measure effective connectivity, as the measures of statistically-dependent activity between regions within each fMRI testing run does not permit the implication of causality. Also, without more investigation focussed on network connectivity changes via independent component analysis rather than presently used seed-based approaches, the data does not lend itself to interpretation.

3.5 Limitations

This study faced some limitations in its execution. Foremost, through technical failure, I could not produce a reliable SFM replay condition, but instead likely recorded bistability as well. For this reason, I am unable to replicate the rivalry-replay contrast of previous studies (Lumer et al., 1998; Zaretskaya et al., 2010, 2013; Weilnhammer et al., 2013, 2017; Grassi et al., 2017, 2018; review in Brascamp et al., 2018). However, given the robustness of this effect, this did not impede the other results and moreover gave me the chance to define ROIs on bistable data that was independent from those data used in the main analysis to avoid double-dipping.

Another point of caution are the weak effect sizes I report throughout. The whole brain-results for instance did not survive FWE or false-discovery-rate correction at the voxel or cluster-

level. Also, the inconsistent nature of behavioural TMS effects across the literature raises questions with regard to the validity or context-dependence of offline parietal TMS effects on bistable percepts in general. One way to test for this is to correlate behavioural with neural effects. For instance, Zaretskaya et al. (2010) could support their TMS finding by demonstrating that participants with higher IPS BOLD signal lateralisation showed greater lateralisation of TMS modulation of dominance durations. We were unable to do so, as cTBS BOLD percent signal change modulation in thalamus and SPL did not correlate with the change in dominance duration. However, I should also note that in an analysis that corresponds more closely to ours, namely a correlation between unilateral behavioural TMS effects and BOLD signal change, Zaretskaya et al. (2010), also did not find an effect.

CHAPTER 2

Failure to replicate functional fractionation of parietal cortex in visible and invisible binocular rivalry using theta burst TMS

1. Material and methods

1.1 Participants

34 healthy volunteers with normal or corrected to normal vision were recruited for the study (mean age 24.4 yrs ± 3.6 S.D.; 25 female, 28 right handed). Following a health screening to ensure the safety of TMS application, written informed consent was acquired from all participants prior to the experiment, which was approved by the institute's ethics committee. Following screening of participants during the pre-experiment (see section 2.3.3), 24 participants were invited for a structural MRI scan (mean age 24.3 yrs ± 3.8 S.D.; 18 female, 20 right handed). Out of these participants, 12 took part in the main TMS experiment (mean age 23.9 yrs ± 2.7 S.D.; 10 female, 10 right handed). The study was approved by the local ethics committee.

1.2 Visual stimuli and apparatus

Visual stimuli were identical to the ones used in the main fMRI experiment of Brascamp et al. (2015). BR occurred between stereoscopically presented apertures (inner radius = 0.15 degrees of visual angle (dva), outer radius = 1.25 dva) filled with moving dots (radius = 0.08 dva; density = 165 dots per dva2; speed = 5.7 dva per second). To aid fusion, the apertures were surrounded by a white ring (radius 2.9 dva) and a pattern of random white and black pixels within a square outline (side length 7 dva). In the centre of each eye's aperture was a white fixation mark (circular plateau, radius = 0.025 dva, surrounded by a Gaussian radial falloff to background luminance, σ = 0.03 dva). The background was grey at 30% gamma corrected screen luminance. Both eyes' stimuli were identical, except for the moving dots, which differed in motion direction and in some experimental conditions also colour (*figure* 11).

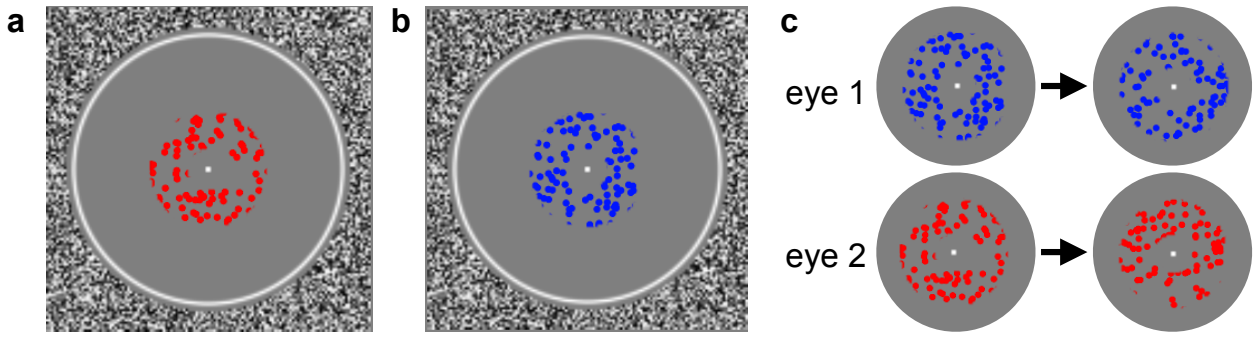

Figure 11 — Random dot motion stimulus
100 red or blue dots moving at random within a black and white patch of fixation aid with a single white fixation dot at the centre. Either colour was presented to the right and left eye respectively (**a,b**), leading to alternating percepts of the two (**c**).

Apart from motion pulse intervals (see below), each aperture's dots had a within-eye coherence of 0.4, i.e. 40% of dots moved in a single direction (signal dots), while the rest moved randomly (noise dots). Dot direction was reset in 300 ms intervals, where identity and movement direction all dots were randomly assigned, subject to signal dots in one eye moving at a direction ± 90° (randomly chosen) removed from the direction of the other eye's signal dots.

All dots in a given eye were either red-tinted or blue-tinted. The luminance of both colour tints were approximately identical. The luminance of the maximum screen output of blue (1.393 cd/m2, through the mirror stereoscope) was used to obtain equivalent luminance levels for red and white by use of heterochromatic flicker photometry (Kaiser & Comerford, 1975). The colour tint was created by blending portions of either this red or blue with the equalised white.

There were two types of stimuli used in separate trials: In same colour stimulus trials, the presented colour was chosen at random for each trial. This entailed that participants were not able to distinguish which stimulus was currently dominant. In different colour stimulus trials, the the side on which each colour was presented was chosen at random for each trial.

Motion pulses lasted 600 ms and and coincided with two of the above mentioned 300-ms intervals. During motion pulses, all dot's motion direction angle was randomly drawn from a uniform distribution (width 135°) centred on due leftward in one eye and on due rightward in the other (randomly assigned for each pulse). In addition, a black dot inside the fixation mark (radius = 0.013 dva) signalled the presence of a motion pulse throughout the 600 ms interval. Since there is constant BR between the two dot motion apertures, on the assumption that a motion pulse occurs during perceptual dominance of one aperture over the other, participants perceived motion pulses as sudden increase in dot coherence where dots move in a similar direction either left or right. This offered 'snapshots' of rivalry dominance. Motion pulses occurred every 1.525 s ± 250 ms. Motion pulses were always present in the experiment, even when they were task irrelevant in order to minimise the difference between the stimuli used for the various experimental conditions (see Main experiment).

Stimuli were presented through a mirror stereoscope at a distance of 50 cm from the participant. The total path travelled by light between stimulus presentation and eye was 70 cm. A black separating board in the middle of the setup as well as around the space between monitor and stereoscope prevented participants from seeing anything apart from the intended image. All stimuli were displayed on a 27 inch Eizo monitor (60 Hz refreshing rate at 1600 x 1200 pixel resolution) controlled by a HP computer running Windows 7 using the Psychtoolbox package for MATLAB R2014b. There was no natural light contamination nor room lighting. A chin rest was used to minimise head movements.

1.3 Experimental design

1.3.1 Visual task

During stimulus presentation, participants indicated BR percepts in one of two ways:

"Button hold report" involved participants continuously pressing one of two buttons to indicate their current percept. For different colour trials this entailed holding the right button for as long as the blue-tinted dots were perceived and the left button for the red-tinted dot percept. During periods of mixed percept dominance, no button was pressed. All participants used their right hand for button presses. Bistable dominance durations were calculated from the length of these presses and their median derived. In this task, participants were asked to ignore motion pulses.

"Motion pulse report" coincided with the previously described motion pulses. Depending on eye dominance during the motion pulse, participants perceived coherent motion either to the left or right. Participants then indicated this direction with a single press of one of the two keys. When participants were unsure of the motion direction, no button was pressed.

1.3.2 Pre-experiment and participant screening

First, I performed heterochromatic flicker photometry to equalise the luminance of red and blue stimuli (see Visual stimuli and apparatus).

Second, participants completed 10 trials of 120 seconds (20 minutes total) of reported BR (different colour stimulus - button hold report). During these trials, motion pulses were presented every 1.525 s ± 250 ms, but participants were told to ignore these and instead respond using button hold report. We nonetheless indexed button presses for motion-pulse analysis based on button-press report. We then calculated median dominance of participant's BR percepts using both report methods (see below). BR follows distinct stochastic properties (Levelt, 1967; Brascamp & Blake, 2012), with dominance durations being drawn from a stationary gamma distribution. A previous psychophysical simulation of the motion-pulse analysis data revealed that some BR distributions are unsuitable for this kind of analysis (Schauer et al., in prep a). Based on this result, participants were excluded from further testing if 1) their median dominance duration was shorter than 4 seconds, 2) the shape, scale, mean and variance of the gamma distribution describing their button-press dominance durations does not fall under one of the acceptable combinations, 3) eye dominance of either eye was greater than 0.7, and 4) the difference between the median dominance yielded by button press analysis is no more than 20% greater or shorter than that of the motion pulse analysis to ensure that any TMS effect would not be masked by error arising from choice of analysis method.

Third, I controlled for whether percept switches in the same-colour trials were actually unreportable. To this end, participants completed 6 trials of 60 seconds (6 minutes total) of either 1) Chance press BR (same colour stimulus - button hold report), or 2) Fusion (Both eye's stimuli identical - button hold report), where there is no rivalry at all. If the same-colour-stimulus leads to unreportable percept switches, then participants button press behaviour in 1) and 2) should be identical, i.e. at chance level and different from what was observed during the second pre-experiment. Participants for whom this was not the case were excluded from subsequent testing.

Fourth, participants were trained in using the motion pulse report by completing 120 second trials of unreported BR (different colour stimulus - motion pulse report), and later unreportable BR (same colour stimulus - motion pulse report) until they comfortably were able to respond. In both cases, I analysed motion pulses to ascertain whether the resulting autocorrelations were sensible based on the result of the second screening step.

Last, I measured participants resting motor threshold (RMT), to ensure that cortical excitability for each participant was high enough to administer TMS, but without exceeding 50 % maximum stimulator output. RMT was determined individually for each participant, by varying stimulation intensity over the left motor cortex until stimulation elicited a visible contralateral finger muscle twitch in 5 out of 10 pulses.

1.3.3 Main TMS experiment

There were 3 experimental conditions: 1) BR with reported percept switches (different colour stimulus - button hold report), 2) BR with unreported percept switches (different colour stimulus - motion pulse report), 3) BR with unreportable percept switches (same colour stimulus - motion pulse report). There were 9 trials in an experimental session. Each experimental condition appeared in 3 trials. Each trial lasted for 120 seconds. The order of trials was randomised for each participant, but not across experimental sessions. An experimental session lasted 18 minutes.

While cortical inhibition following cTBS has been observed in time windows ranging up to 50 minutes post stimulation (Huang et al., 2005; Schindler et al., 2008), evidence also suggests that its effect might disperse much sooner in the range of 16-30 minutes (Nyffeler et al., 2006; Zafar et al., 2008; Zapallow et al., 2012). To ensure that the entirety of the post-TMS recording lay within this window of opportunity, I chose a conservative session length of 18 minutes. Also, the results of a data simulation using motion pulses to estimate dominance durations suggested BR recordings longer than 6 minutes will not yield substantially more accurate results (Schauer et al., in prep a).

For the main experiment, participants came to the lab on three separate occasions, at least 24 hours apart to prevent TMS carry over effects. During each occasion, participants first

completed an experimental session, followed by application of theta burst TMS to either IPS, SPL or vertex (*figure* 12). The order of TMS sites was fully counterbalanced. Immediately after TMS application, participants completed another experimental session.

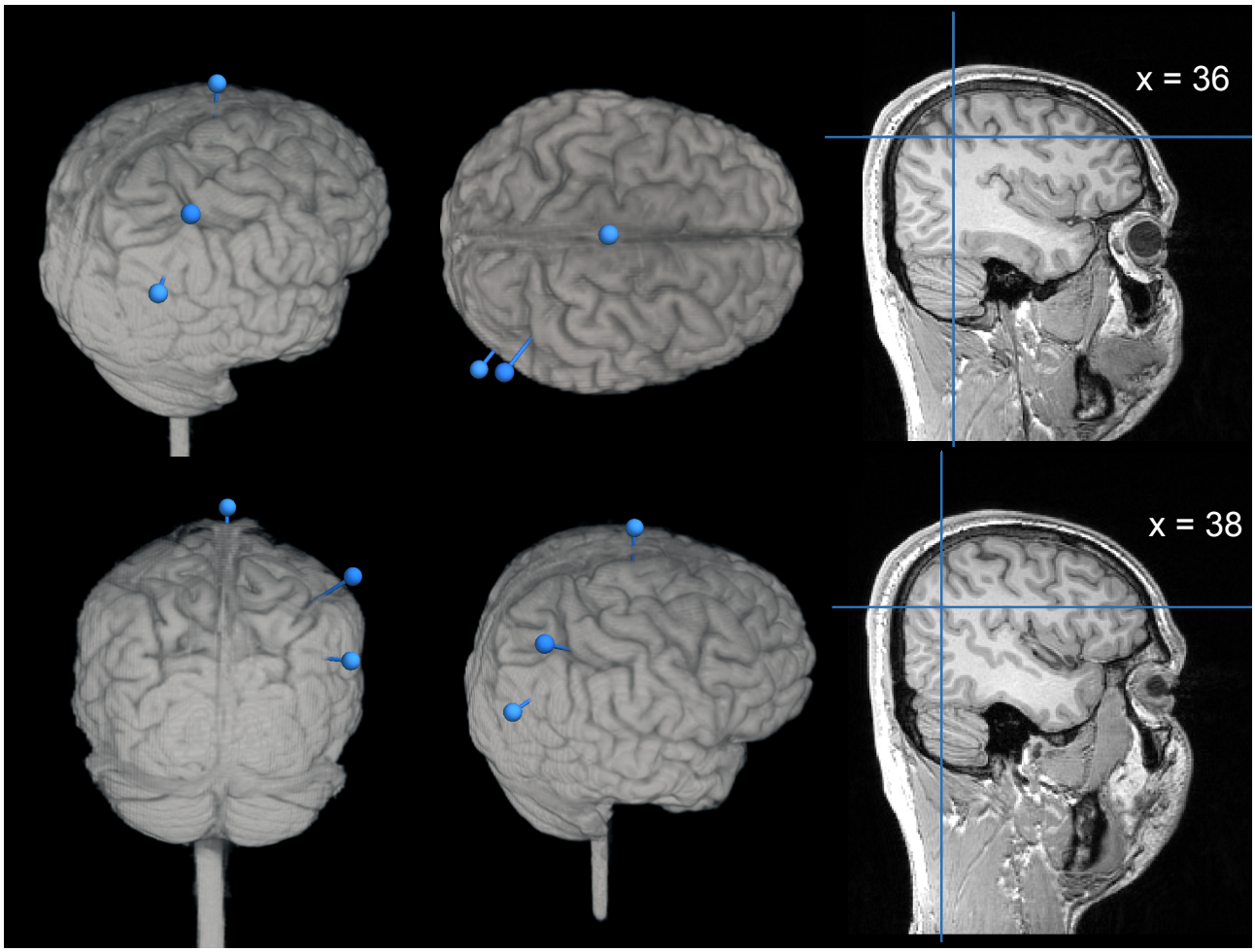

Figure 12 — TMS locations
Ant-SPLr and SPL on the T1 MRI scan of a representative participant. Left, surface markers for neuronavigation of both SPL sites and vertex, located at the most superior point of the cortex. Approximate coordinates for visualisation purposes.

1.3.4 MEP experiment

This component of this study was performed in a different laboratory with a different TMS stimulator from the main experiment, which is why I remeasured the RMT. First, participants were seated in a reclining chair and systematically stimulated above and around the primary motor cortex of the participant using single TMS pulses (< 0.3 Hz) at initially 40% of maximum stimulator output. If this intensity proved insufficient, it was increased in 5% steps, until a motor evoked potential (MEP) was visible in the online analysed electrode output. A hotspot was chosen at coordinates in the neuronavigation system where MEP amplitude was greatest and all stimulation from this point occurred at that hotspot (*figure* 13). To determine the RMT, I varied stimulation intensity until MEP peak-to-peak amplitude reliably reached 50 mV in about 5 out of 10

consecutive pulses (Groppa et al., 2012). Lastly I determined the intensity that evoked a stable MEP with a peak-to-peak amplitude of about 100 uV. This stimulus intensity was now used in the main EMG recording.

Following these preparations, I commenced measurement of motor cortex excitability by recording 30 MEPs with an inter stimulus interval between 4.5 to 5.5 s at stimulus intensity with the participant at rest. Next, I applied the same cTBS protocol described in section 2.5 to the hotspot area at 90% of the RMT measured in this session. Then came a rest period of 10 minutes, during which participants were instructed not to move or talk. Lastly, another 30 MEPs were recorded same as before cTBS. Analysis involved an intra-participant comparison between the MEPs prior to cTBS and those 10 minutes after.

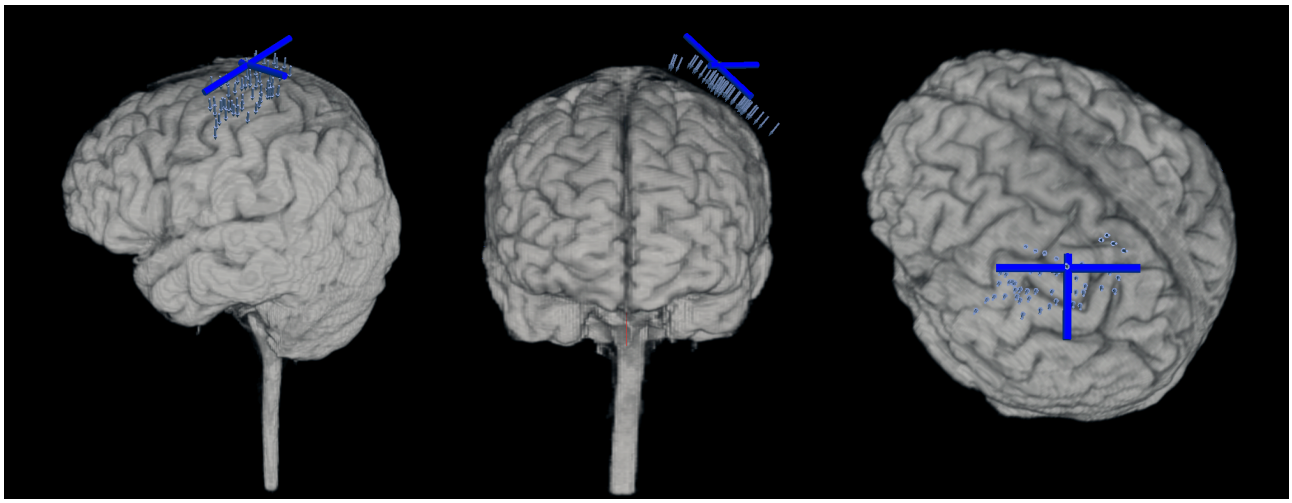

Figure 13 — MEP test site selection
TMS locations in the T1 MRI scan of a representative participant. Single pulses of TMS were applied to various locations in the left primary motor cortex in a grid (blue arrows), from which the site was chosen that yielded the largest peak to peak MEP amplitude. This site and TMS coil position was then used as benchmark for all further stimulation (dark blue T-maker).

1.4 MRI scan acquisition

MRI scans acquired using a 3T Siemens Prisma at the Max Planck Institute for Biological Cybernetics, Tübingen. For each participant, a T1-weighted ADNI sequence (TR = 2000ms, TE = 3.06ms, FOV = 232 x 256 x 192 mm, voxel size = 1 x 1 x 1 mm, matrix 232 x 256, Flip angle 9°, 192 sagittal plane slices, acquisition time 7 min 46 s) was used to obtain structural MR images.

1.5 Inhibitory TMS protocol and neuronavigation

For the main experiment, TMS stimulation was a continuous theta burst protocol (Huang et al., 2005), consisting of bursts of three 50Hz TMS pulses, applied every 200 ms for 40 seconds (600 pulses in total). TMS pulses were delivered using a figure-of-eight coil (MC-B70) connected to a

MagPro X100 stimulator (MagVenture). Intensity of the stimulation was set to 80% of individual RMT, resulting in a mean stimulation intensity of 31.5 % ± 4.2 S.D. maximum stimulator output. Participants did not consume alcohol in the 24 hrs prior to each session and were well rested (both to avoid risk of lowered seizure threshold, see Rossi et al., 2009). On separate days, these pulses were applied either to the SPL (MNI: x = 38, y = -64, z = 32), to the IPS (MNI: x = 36, y = -45, z = 51), or to the control site vertex (see *figure* 12).

The two parietal locations were localised using standard MNI brain coordinates on the basis of each participant's anatomical MRI scan using the neuronavigation system LOCALITE with an tracking system using a Polaris infra-red camera (Northern Digital, Waterloo, Canada), by co-registering individual MR images with the participant's head to which surface markers were attached. The coil was held manually by the experimenter with its shaft pointed posterior inferior at an angle of 45° from the floor (posterior-anterior position according to Hamada et al., 2012). The distance between actual coil location and its optimal positioning was kept at less than 1.5 mm at all times during stimulation. The vertex was localised using externally visible anatomical landmarks. Using flexible measuring tape, the midpoint of the medial line on the scalp between nasion and inion was marked on the swim cap, which is directly superior to the vertex. For vertex stimulation the coil was held against the participant's scalp with its handle pointing straight behind the participant, with the experimenter standing behind the participant and holding the coil parallel to the floor.

1.6. EMG Recordings

For the EMG recording I used two Ag/AgCI AmbuNeuroline 720 wet gel surface electrodes (Ambu GmbH, Germany), which were fixated on the right extensor digitorum communis muscle belly at a distance of 2 cm. A third ground electrode was fixed to the elbow. The signal was filtered online between 0.16 Hz and 5 kHz. EMG was recorded at 5 kHz through a BrainAmp ExG Amplifier and transferred to MATLAB 2014a (Mathworks) for online analysis and visualisation as well as offline storage. TMS pulses were delivered using a figure-of-eight coil (MCF-B70) connected to a MagPro-R30+MagOption stimulator (MagVenture). Application was neuronavigated in the same manner as the main experiment (see section 2.5).

1.7. Main experiment data processing

All data was analysed using MATLAB 2014a (Mathworks). First, BR dominance durations were extracted from psychophysical recordings that used button-hold report. Button presses that were held at the end of a trial were excluded. Periods in which either no button was pressed or both

simultaneously were treated as mixed percepts. Given that dominance durations follow a gamma distribution (Levelt, 1967), I pooled all dominances from each experimental condition in each recording and extracted the median as measure of central tendency. For trials that utilised the motion-pulse report I similarly extracted medians using the method described by Brascamp et al. (2015): Based on pre-experiment, I used inter-motion pulse intervals based on percept switch rate for each participant to minimise intervals with more than one switch, such that for each interval, either a one or zero switch was most likely. For all intervals between motion pulses I calculated whether a change in percept had occurred, which allowed me in turn to derive an autocorrelation curve describing the likelihood of a change in percept having occurred as a function of time. To convert this autocorrelation to its corresponding percept duration distribution, I first created a bank of over 8000 theoretical autocorrelations corresponding to distinct gamma shape and scale parameters describing possible dominance duration distributions, by randomly sampling durations from these distributions and calculating autocorrelations of those percept sequences. This is possible since BR has stochastic properties that are expressible as autocorrelation curves (Brascamp & Blake, 2012). We then searched the bank for the theoretical autocorrelation that best fit the empirical autocorrelation. Lastly, I calculated the median of the gamma distribution from which this theoretical autocorrelation was derived. Finally, also for the button-hold trials I calculated a median based on the motion-pulse technique, presupposing that the motion direction of the patch corresponding to whichever button participants held at the time of motion pulses would have been selected. This allowed me to test whether motion pulse and button-press extracted medians were correlated within the same data.

For the main TMS experiment, I analysed the change in BR dominance as a result of parietal cTBS. To this end, I compared dominance pre vs post TMS for each test site separately using a series of repeated measures ANOVAs. Each TMS testing day, I recorded a new baseline to control for within-subject differences in arousal and attention. We then subtracted the TMS effect of vertex stimulation, which is assumed to be site-unspecific, from the parietal results. In an identical fashion, I also examined TMS-induced change in the proportion of responses that participants marked “unsure” in the motion-pulse task.

2. Results

2.1 Pre-experiment

Participants' median dominance duration was 3.60 s ± 1.62 s.d., where the distribution of their dominance durations was described by a mean gamma shape parameter of 2.92 ± 2.03 s.d. and a mean gamma scale parameter of 2.26 ± 2.50 s.d., and the average gamma mean was 4.20 ± 2.04 s.d. at a variance of 21.70 ± 22.65 s.d.. Heterochromatic flicker photometry yielded an average result of 103.61 ± 28.99 s.d., on a scale from 0 to 200, where 0 represents all blue and 200 all red. The mean TMS resting motor threshold was 39.7% ± 5.24 s.d. of maximum stimulator output.

Only 12 participants out of 34 passed the screening criteria and were subsequently tested. To ensure the validity of the motion pulse analysis, I first examined the autocorrelation curves for those 12 participants (*figure* 14). Specifically, I examined if there was a good fit between the empirically drawn curve and the autocorrelation that was proposed by algorithm. We aimed to exclude cases where the autocorrelation analysis yielded sensible results, even though the comprising data was nonsensical. Visual examination of all autocorrelation curves successfully eliminated this possibility.

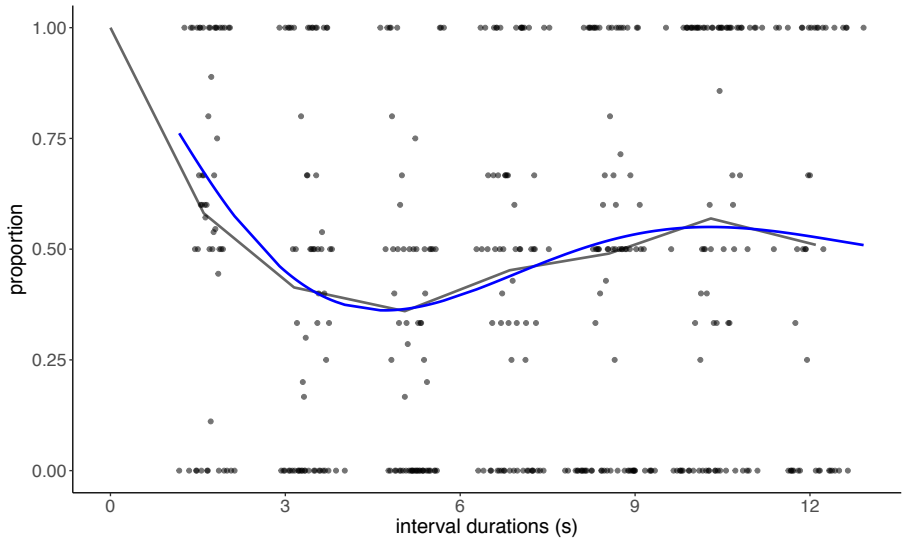

Figure 14 — Autocorrelation curve of a representative participant
Each black dot represents the mean of percept change occurrences (1 = yes) for each interval duration between two motion pulses (N = 450). For visualisation, an empirical autocorrelation curve was drawn by averaging the value of these dots for seven discrete time bins (black line). These average values were used to fit one autocorrelation curve from the bank of 8000 hypothetical curves. The best fitting one is drawn, which corresponded to the behavioural parameters: gamma shape = 4.4, gamma scale = 1.1, median percept duration = 4.48.

2.2 Main TMS experiment

2.2.1 Data validation

To begin, I aimed to rule out differences in the baseline rivalry recordings between TMS sessions that could later account for any differences between experimental conditions. To this end, I entered baseline rivalry median dominance as dependent variable into a repeated-measures ANOVA using TMS site as factor. This I did three times, once for each stimulus condition. All ANOVAs were non-significant ($F < 1$, *ns*), indicating that there were no systematic differences in baseline arousal and stimulus viewing between the three days that participants came to the lab.

Next, I wanted to ensure that the motion pulse analysis worked correctly. To test this, I performed a motion pulse analysis on the button report data, where I used the button-hold press at the time the motion pulses would have had occurred to simulated what participants would have pressed if motion-pulse report had been their task. We then analysed the rivalry dominance durations using the normal button presses as well as the inferred motion pulses. If the motion pulse analysis is successful, it should yield a median dominance that is similar to that of the button-hold analysis. We therefore correlated their median dominance durations durations from the button-hold and the motion-pulse analysis, separately for each test site, and separately prior and post TMS (*figure* 15). We found consistently strong correlations between these analysis techniques, which strengthens confidence in their respective success.

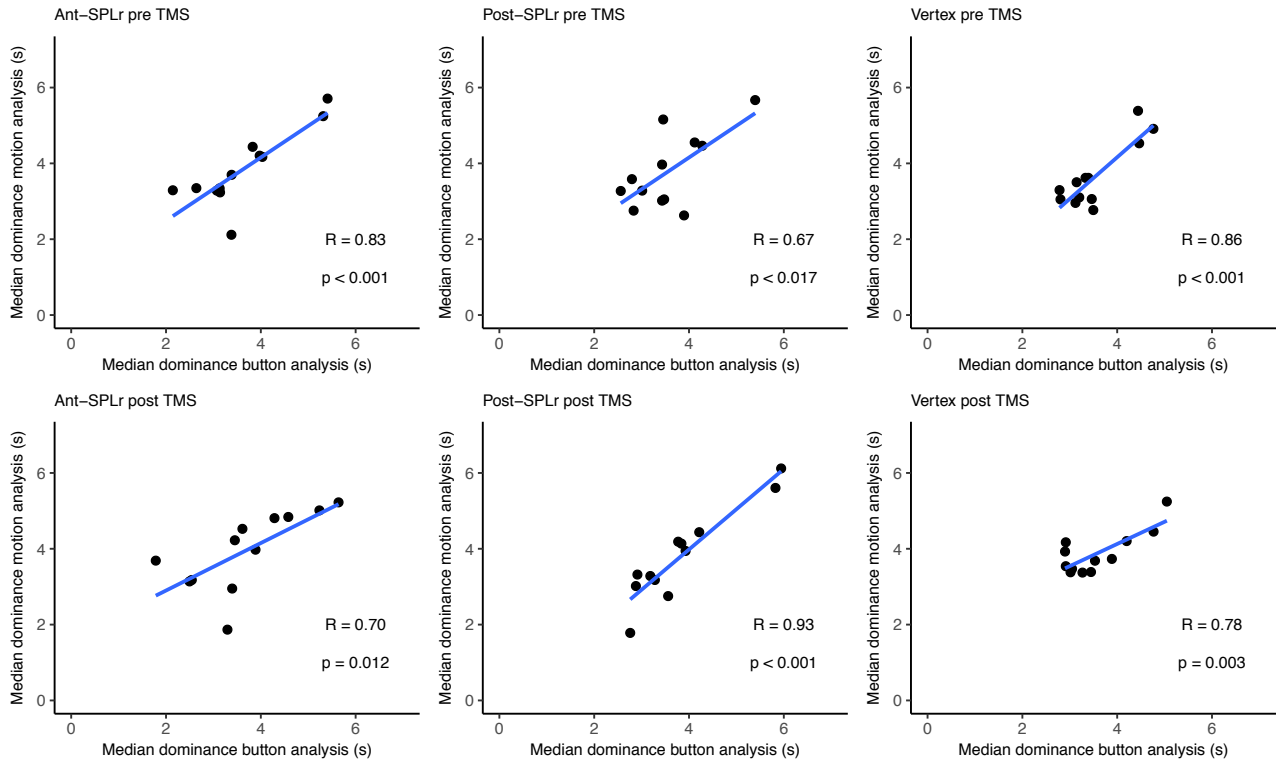

Figure 15 — Correlation between analysis methods
Pearson's correlations between median dominance durations obtained through traditional button-hold analysis of the experimental data and those obtained from using motion pulse analysis on the same data. Once for each TMS site pre and post

Next, I wanted to verify if this success of analysis also expanded to unreported and unreportable rivalry. If those are perceived correctly and if (as I assume), dominance durations within participants correlate across stimuli, then I also would expect correlations between unreported and unreportable rivalry. We did this again separately for each testing day / TMS site as well as separately prior and post TMS (*figure* 16). We were able to find the expected correlations in four of the six analyses, while the other two showed a visible trend. If there were no BR in the unreportable condition, then the inferred dominance durations should be different and uncorrelated to the ones from the reportable rivalry conditions. This again increased confidence the invisible rivalry stimulus was perceived by participants in manner consistent to that reported by Brascamp et al. (2015).

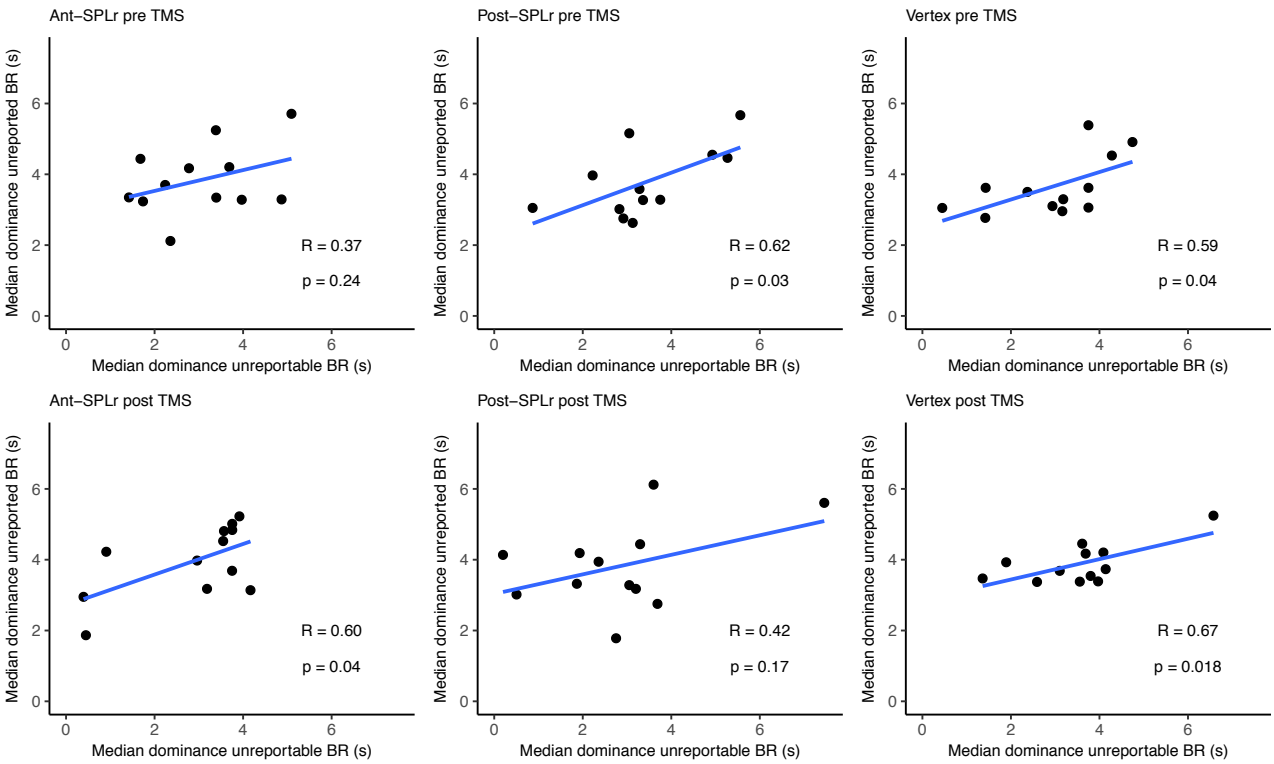

Figure 16 — Correlations between unreported and unreportable rivalry
Pearson's correlations between median dominance durations obtained through motion pulse analysis in the unreported BR condition with dominance durations in the unreportable BR condition.

2.2.2 TMS induced behavioural changes

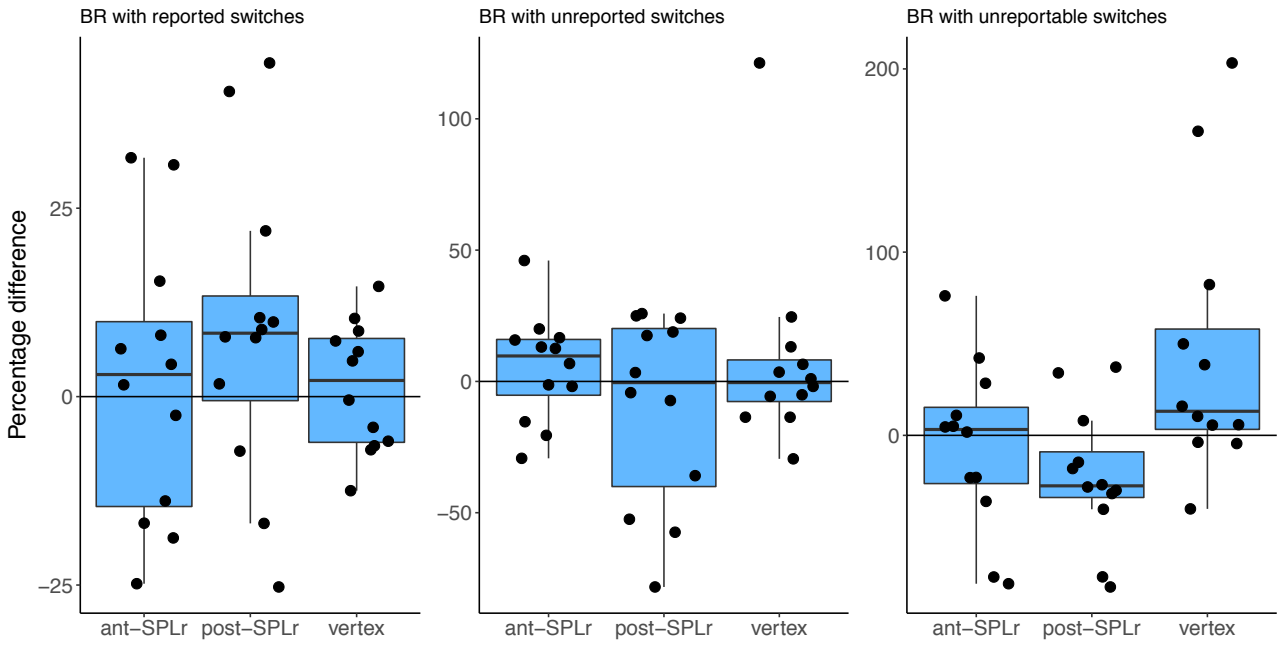

Figure 17 — Main TMS result
Percentage difference in median rivalry dominance durations across TMS conditions, separately for the three task conditions. Each dot is a data point from one recording of one participant.

We began the main analysis by examining the button report data (*figure* 17 left). We entered the percent change in rivalry dominance into a repeated-measures ANOVA using TMS site as factor. Mauchly´s test indicated that the assumption of sphericity had been violated ($\chi^2(2) = 30.18$, $p < 0.001$), therefore degrees of freedom were corrected using Greenhouse-Geisser estimates of sphericity ($\varepsilon = 0.58$). This was driven by the much smaller variance of dominance duration change in the vertex condition. The ANOVA revealed no significant main effect ($F(2,22) < 1$, *ns*). In essence, TMS did not differentially affect dominance durations contingent on test site. Since frequentist statistics do not allow any positive inference in favour of null results, I repeated this analysis using the BayesFactor package (0.9.2) for R64, by modelling a Bayesian ANOVA using the theoretical background of Rouder et al. (2012). We computed a Bayes Factor (BF) for the main effect of TMS site against the null hypothesis that all effects are 0. This yielded a BF of 0.3 in favour of a TMS result, which is considered borderline substantial evidence in favour of the null (Kass & Raftery, 1995). A series of frequentist t-tests as well as Bayesian comparisons between the TMS sites found similar results. We were therefore, in a first step, unable to replicate the previous cTBS results on bistable perception and BR of Carmel et al. (2010), Kanai et al. (2010, 2011), as well as Zaretskaya et al. (2010, 2013).

		pre (s)	s.d.	post (s)	s.d.	% change	s.d.
reported	IPS	3.62	0.97	3.68	1.13	1.79	18.39
	SPL	3.56	0.78	3.84	1.06	8.68	20.37
	vertex	3.53	0.66	3.58	0.74	1.27	8.47
unreported	IPS	3.84	1.13	3.93	1.12	5.21	20.48
	SPL	3.94	1.21	3.53	1.59	-10.08	36.75
	vertex	3.63	1.41	3.62	1.09	8.39	38.13
unreportable	IPS	3.05	1.22	2.86	1.41	5.94	45.75
	SPL	3.43	1.32	2.82	1.84	-22.55	36.83
	vertex	2.93	1.29	3.53	1.30	44.11	72.81

Table 4 — Main TMS result
Median dominance durations across participants for each task and TMS condition, both pre and post TMS as well as the respective percentage difference with corresponding standard deviations.

Next, I examined results from the unreported BR task condition (*figure* 17 middle). Once more, I entered the percent change in rivalry dominance into a repeated-measures ANOVA using TMS site as factor, which revealed no significant main effect ($F(2,22) = 1.11$, *ns*). In essence, TMS did not differentially affect dominance durations contingent on test site. A Bayesian ANOVA yielded a BF of 0.39 in favour of a TMS result, which is considered inconclusive evidence. A series of Bayesian comparisons between the TMS sites found also consistently inconclusive results. Therefore, I am unable to show a TMS effect on unreported BR, but at the same time cannot claim that there is no effect either.

Last, I turned to unreportable BR (*figure* 17 right). Entering the percent change in rivalry dominance into a repeated-measures ANOVA using TMS site as factor, I found a significant main effect ($F(2,22) = 5.61$, $p = 0.01$). This was corroborated by a Bayesian ANOVA (BF = 4.39, strong evidence in favour of an effect). Post hoc t-tests revealed that this effect is driven by a near significant shortening of rivalry dominance in the SPL condition ($t(11) = -2.12$, $p = 0.057$, BF = 1.49 (inconclusive)), a near-significant lengthening of dominance in the vertex condition ($t(11) = 2.10$, $p = 0.06$, BF = 1.45 (inconclusive)), as well as the comparison between these two ($t(11) = -3.78$, $p = 0.003$, BF = 15.80 (strong evidence)). It appears then that SPL stimulation leads to a significant shortening of rivalry dominance compared to vertex control. This result stands in direct contradiction of Kanai et al. (2010). However, I am hesitant to infer any strong conclusion from this analysis for two reasons: First, the variance in the unreportable BR condition is substantially larger than in the normal reported BR case, yielding percent changes in dominance pre and post TMS of up to over 200 %. Given the results of the reported BR condition, this seems hardly credible and speaks more likely to a lack of precision in the motion pulse analysis for the unreportable BR, which

in turn could account for this effect. Secondly, since I failed to replicate a TMS effect in the reported BR condition, I am especially cautious about this more indirect rivalry.

As a further step, I examined the unsure responses that participants gave in the motion pulse analysis for the unreported and unreportable BR. Here I hypothesised that a TMS effect could be evident not only in a change in dominance, but also participant's confidence in having seen the motion pulses. Since in this task there is no correct answer, I am unable to perform any signal detection analysis on the data, however, I analysed the proportion of unsure responses across experimental conditions. In the case of unreported BR, a repeated-measures ANOVA, with TMS site as factor, showed that this proportion was not significantly different across sites ($F(2,22) < 1$, *ns*). This was corroborated by a Bayesian ANOVA (BF = 0.28, substantial evidence in favour of the null). For the unreportable BR, I also entered the unsure proportion into a repeated-measures ANOVA using TMS site as factor. Mauchly´s test indicated that the assumption of sphericity had been violated ($\chi^2(2) = 26.46$, $p < 0.001$), therefore degrees of freedom were corrected using Greenhouse-Geisser estimates of sphericity ($\varepsilon = 0.57$). The resulting ANOVA revealed no significant main effect ($F(2,22) < 1$, *ns*). This was again supported by Bayesian analysis (BF = 0.22, substantial evidence in favour of the null). In summary, TMS did not differentially affect people's ability to discriminate motion pulses.

2.3 Voxel-based morphometry

Based on the previous finding of a significant correlation between percept dominance durations and grey matter density using small volume correction over both the SPL (Kanai et al., 2010) as well as IPS (Kanai et al., 2011), I conducted an identical voxel-based morphometry analysis over these sites using the T1-weighted structural MRI images of this study's participants (N = 24). First, grey and white matter were segmented using the automated segmentation algorithms of the Matlab package SPM12 (http://www.fil.ion.ucl.ac.uk/spm), which was followed by inter-subject registration of only the grey matter images using the 'diffeomorphic anatomical registration through exponentiated lie algebra' (DARTEL) function. The resulting images were smoothed with a Gaussian kernel of FWHM = 8 mm and then mapped onto the Montreal Neurological Institute (MNI) template. Given the strong theoretical support for correlations at specific regions of interest (ROIs), specifically the IPS and SPL, a regression analysis was carried out predicting dominance durations from grey matter density over these two parietal sites, using small volume correction with a sphere radius of 15 mm, centred on IPS (x = 36, y = -45, z = 51) and SPL (x = 38, y = -64, z = 32) MNI co-ordinates.

We found a significant positive correlation between grey matter density and individual median percept duration in the IPS (peak level: $z = 3.16$, $p < 0.001$ uncorrected, $p = 0.066$ family-

wise error corrected, MNI peak location: x = 45, y = -36, z = 45). This is consistent with the finding in Kanai et al. (2011). However, I did not find a negative or positive correlation in the SPL even with a liberal statistical threshold ($p > 0.05$, uncorrected), which entails a failure to replicate the result of Kanai et al. (2010). Voxel-based morphometry usually requires substantially larger samples to yield significant results, which makes the null finding over SPL non-problematic. In contrast, the replication of the positive correlation between IPS grey matter volume and dominance durations at this sample size increase confidence in the finding of Kanai et al. (2011).

2.4 MEP experiment

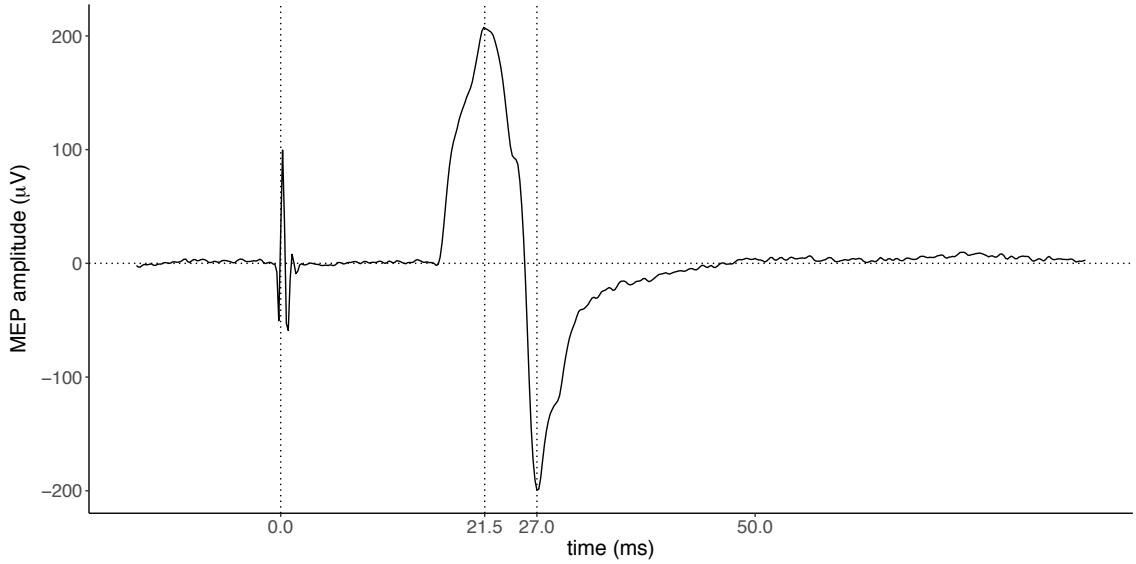

Figure 18 — TMS artefact and resulting MEP
Time-course of recorded electrical activity of a representative trial in a representative participant. Zero on the x-axis signifies the onset of the TMS pulse, around which the TMS artefact resulting from the direct exposure of the recording electrodes to the magnetic field, followed by the MEP, with a peak-to-peak amplitude of 406.8 μV (+ 207.4 μV to - 199.4 μV) between 21.5 ms and 27 ms post TMS.

Visual examination of individual muscle recordings showed that single pulse TMS produced reliable motor evoked potentials, comprised of TMS artefact resulting from the direct exposure of the recording electrodes to the magnetic field, followed by the MEP (*figure* 18). As a first step, I analysed the effect of cTBS on the MEPs of each participant separately. We compared the peak-to-peak MEP amplitude of the 30 trials post and pre cTBS using a Wilcoxon signed-rank test. We found that for 10 of the 12 participants, mean MEP amplitude was reduced, significantly so in five (*figure* 19). Two participants showed an increase of MEP amplitude, which was significant in one.

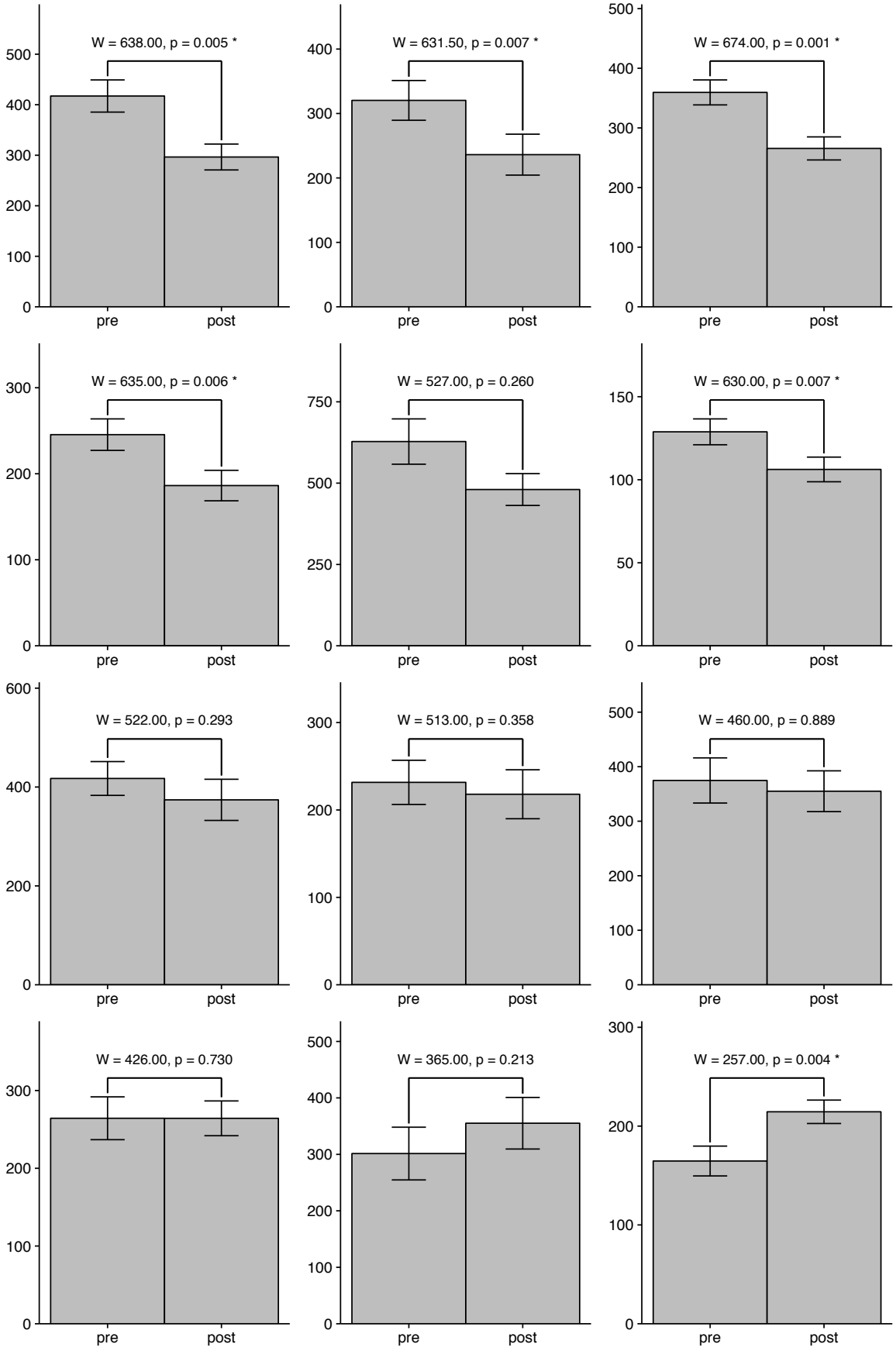

Figure 19 — Individual MEP amplitude change
For each participant, MEP amplitude in μV on the y-axis is shown pre and post cTBS. Error bars are ± 1 s.e.m. Comparisons are unpaired Wilcoxon signed-rank tests. * indicates statistical significance.

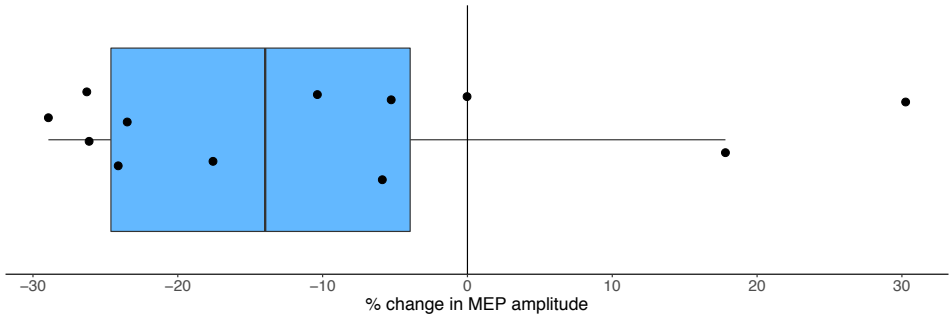

Figure 20 — cTBS induced decrease in MEP amplitude
Group-level analysis of change in MEP amplitude pre vs post cTBS. Each dot is a data point from a single participant.

Next, I examined the group-level effect of cTBS on MEP aptitude. Consistent with previous findings, cTBS led to a decrease in MEP amplitude (*figure* 20; $t(11) = 2.31$, $p = 0.04$). Even though the normality assumption of this test was not violated (Shapiro test: $V = 0.87$, $p = 0.07$), I chose to also confirm this analysis via a non-parametric statistic (Wilcoxon signed rank test: $W = 65$, $p = 0.04$). Bayesian analysis turned out to be more agnostic at a BF of 1.92, indicating inconclusive evidence, which is however not entirely surprising given the relatively small N of 12.

Finally, I examined correlations between the change in MEP amplitude with the percent change in dominance durations pre vs post cTBS respectively. We did this separately for the three test sites, vertex, IPS and SPL, using Pearson's correlations. We found no relationship whatsoever (*figure* 21). Similarly, the latency of the MEP did not correspond to whether participants were cTBS responders or not as was predicted by Hamada et al. (2012). However, while I used a TMS coil orientation that is associated with eliciting I-waves, the participants' hand muscles were at rest, which substantially deviates the procedure used in that study.

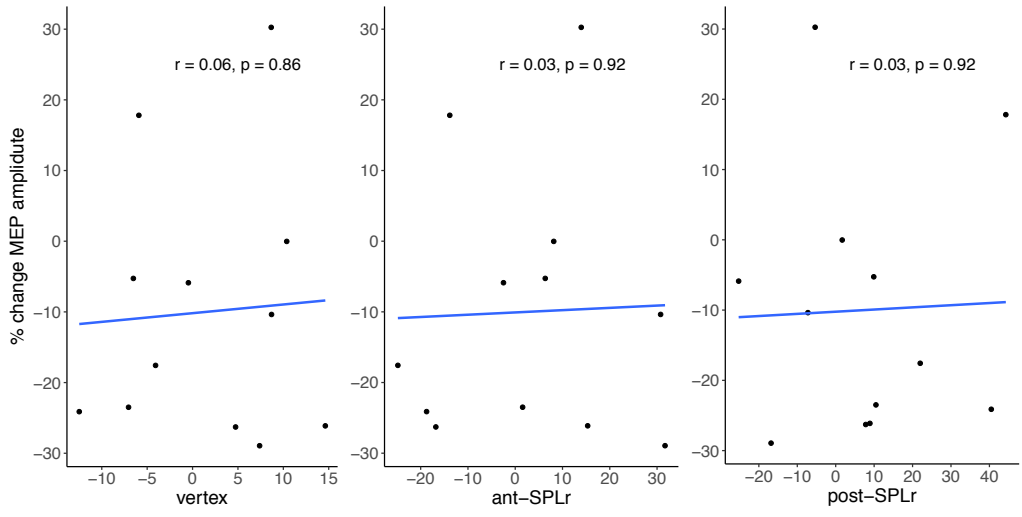

Figure 21 — Correlation between cTBS effect on MEP and BR
For each test site (vertex, IPS, SPL), x-axis displays percent change in BR dominance duration pre vs post cTBS, correlated with the percent change in MEP amplitude yielded by M1 cTBS. Numeric results are Pearson correlations.

3. Discussion

Our results confirm the viability of the psychophysical method employed by Brascamp et al. (2015) to render BR unreportable. Moreover, I could observe BR in a visible, but no-report condition. This further strengthens the hypothesis that BR does not require report or even conscious awareness to occur. In other words, the neural mechanisms that subserve BR remain operational independent of consciousness. We could also replicate the finding of Kanai et al. (2011), who found a positive correlation between grey matter volume and bistable dominance durations, making this the third independent replication of that result (Sandberg et al., 2016; Wood et al., in prep). However, the main experiment failed to replicate the previously observed modulation of dominance durations by parietal cTBS stimulation (Kanai et al., 2010; 2011; Zaretskaya et al., 2013; Schauer et al., in prep b). This held true irrespective of stimulus condition or TMS test site. We replicated the finding that cTBS to M1 significantly reduced MEP aptitude (Huang et al., 2005). However, this effect did not correlate with the cTBS modulation of dominance durations.

3.1 Unreported and unreportable BR

Our use of unreported and unreportable BR challenges some of the common notions employed by BR research. One reason that makes BR particularly interesting to consciousness researchers, is the assumption that unchanging stimulus gives rise to changes in consciousness allowing this paradigm to unravel the neural correlates of consciousness (NCC; Clark, 2013). Within this framework, bold activation of the fronto-parietal network time-locked to percept switches is assumed to reflect the neutral substrate of changes in awareness. One danger in this venture is the overestimation of the NCC by confounding changes in consciousness with those of attention, expectation and working memory (Tsuchiya et al., 2015). One way to circumvent this problem is to utilise no-report paradigms, where fluctuations in consciousness can be inferred from physiological markers, rendering the necessity of perceptual description by the participant unnecessary. For instance, Frässle et al. (2014) could demonstrate that when BR percepts are inferred from eye-tracked optokinetic nystagmus and pupil dilation rather than motor report, much fronto-parietal activity is diminished. The use of unreported BR is not without critique though: It becomes difficult to disentangle if such a setup measures consciousness or something else, resulting in just another overestimation of the NCC with different confounds, such as introspection, attention direction and metacognitive reflection (Overgaard & Fazekas, 2016).

Based on recent studies, I have gone a step further in rendering BR unreportable. The first psychophysical evidence that conscious awareness is not necessary for BR to occur comes from a study that used random dot motion rivalry at participants' luminance threshold (Platonov &

Goossens, 2014). They found typical temporal dynamics of BR to emerge even when participants reported no awareness of any dot motion. Unreportable BR could also be observed via V1 recordings in anaesthetised monkeys, where ocular dominance columns in V1 were alternatingly activated akin to conscious BR perception, a feature which could also be modulated by varying stimulus features, strongly indicating the presence of rivalry in the absence of consciousness (Xu et al., 2016). Most recently, Zou et al. (2016) used incongruous flickering gratings that appeared uniform to participants, but induced tilt aftereffects and orientation-specific adaptation that allowed tracking the temporal dynamics of BR between them. They could investigate this invisible BR to find that while visual cortical activity was indicative of BR, higher fronto-parietal activity became negligible. They aptly conclude that visual cortex resolves BR in the absence of consciousness, which in turn would have been subserved by parietal cortex (Klink & Roelfsema, 2016).

Taken together, these results challenge the idea that BR is a "window into consciousness" (Logothetis, 1999), as it is most prevalently thought to comprise of stimuli vanishing from conscious awareness (Blake & Logothetis, 2002). It hence stands to question whether BR is a good consciousness paradigm, if it occurs in the absence thereof (Giles et al., 2016). This ties back to the original question of what the causal role of parietal cortex in BR, specifically whether its activity is a neural prerequisite, substrate or consequence of conscious perception of BR (de Graaf et al., 2012). Would inhibitory TMS to either parietal region replicate the functional fractionation previously observed; and would that effect be contingent on whether BR is consciously perceived or reported?

3.2 Viability of cTBS

Alas, I were unable to answer this question, due to the failure of the chosen TMS stimulation technique to adequately inhibit function in the parietal cortex. We chose cTBS for two reasons: It is fast and easy to apply, as well as congruous with previous studies, allowing replication. However, the use of neurostimulation techniques is not without hazard. There are large individual differences in the reaction of participants to rTMS contingent on age, sex, arousal and attention (review Ridding & Ziemann, 2010). Also, I rely on the assumption that the cortical inhibition observed in M1 transposes to the parietal cortex. However, there is poor correlation of TMS-measured excitability across cortical areas (Stewart et al., 2001; Kähkönen et al., 2005), and the fashion in which cTBS inhibits neural activity is not well understood. Di Lazzaro et al. (2005) could demonstrate that spiral spinal recordings of M1 single pulse TMS induced signal transmission, that cTBS reduces early indirect waves (I-wave). Moreover, people with more easy late I-wave recruitment, indicated by a faster MEP onset latency when TMS was applied at a 315° angle (shaft

pointing anterior-superior), were more likely to show the expected inhibitory effect of cTBS on MEP amplitude (Hamada et al., 2012). Crucially, this effect only held true for participants who at the same time had late MEP onset when TMS was applied with the coil shaft pointing downwards at 90°. In fact, the larger the temporal difference between the two latencies, the more pronounced was the expected cTBS effect. We were not able to replicate the correlation between MEP latency and cTBS effect, which is however due to a difference in methodology, since the participants' hand muscles were at rest. What further complicates this matter is that whether direct (D-weaves) or I-waves are preferentially evoked by TMS to M1 depends greatly on TMS coil orientation (Day et al., 1989; Sakai et al., 1997; Hamada et al., 2012). Hamada et al. (2012) concluded that cTBS has an inhibitory effect not on M1 in general, but specifically on cortical circuits activated by I-waves.

Based on the present results, I concur with this conclusion. In fact, I found direct evidence against a generalisation to the parietal cortex. Our failure to correlate cTBS induced changes in MEP amplitude with modulation of dominance duration entails that cTBS plasticity responses are contingent on specific neural networks in M1 and cannot be generalised across the cortex. This raises the question of why previous studies that used cTBS over parietal cortex observed modulations in dominance durations. There is large inconsistency of results, where some studies found lengthenings (Kanai et al., 2010; Schauer et al., in prep b), or shortenings (Kanai et al., 2011; Zaretskaya et al., 2013) of dominance durations following parietal cTBS together with one other null finding (Schauer & Bartels, in prep). Given the current results, it seems more likely that there is in fact no consistent effect of cTBS and that the afore-mentioned studies are false positives due to low statistical power.

3.3 Fractionation of parietal cortex

In the same breath I must question the fractionation of parietal cortex on which I based this study. Originally, it was proposed by Kanai et al. (2011) based on differential cTBS results. As I now argue, these are likely fallacious. Also, probing both IPS and SPL with single pulse TMS while concurrently recording EEG revealed no systemics differences between these sites in the TMS-evoked EEG signal (Schauer et al., 2016a). However, since its inception this fractionation has served as basis for further results, such that SPL and IPS are part of opposing energy landscapes, the respective strength of which under fMRI predicts dominance durations (Watanabe et al., 2014). The fractionation holds also with respect to opposing correlations between dominance durations and grey matter density over SPL and IPS (Kanai et al., 2010; 2011), in dynamic-causal-modelling (Megumi et al., 2015), as well as with functional connectivity (Baker et al., 2015).

Kanai et al. (2011) interpreted this in terms of the Bayesian hierarchical model of predictive coding (Friston, 2005; Hohwy et al., 2008). Higher-level cortical regions produce perceptual predictions, that are fed downwards the visual hierarchy and are compared to incoming sensory signals. Divergences are coded as prediction error, which is sent up the hierarchy to periodically update the top-down predictions in an effort to minimise prediction error. They posit an involvement of IPS in generating predictions (inhibition leads to weaker predictions, hence faster build-up of error signals and hence shorter dominance durations), whereas SPL codes prediction error (inhibition weakens error signals, top-down predictions dominate longer leading to fewer perpetual reversals). This image is questionable for two reasons. First off, the idea that these predictive processes are separated into distinct cortical areas is counterintuitive, given the close computational links between prediction and error, making it more likely that both are computed within the same neural populations (Kanai et al., 2015). Second, the account is overly simplistic in regard to attentional processes as well as the previously reported dissociation between subconscious resolution of BR outside SPL and parietal involvement in conscious awareness thereof (Brascamp et al., 2015; Zou et al. 2016).

Next to predictive coding, there is yet another parsimonious explanation for this fractionation of parietal function: Schauer et al. (2016b) posited that perhaps the fractionation is due to different attentional functions being subserved by these subregions. That hypothesis is not unreasonable since there are strong links between attention and BR: One affects the temporal dynamics of the other (Paffen et al., 2006; Mitchell et al., 2004; Paffen & Van der Stigchel, 2010) and inattention even abolishes rivalry altogether (Brascamp & Blake, 2012). There are also successful computational models that explain BR by positing that rivalry arises from attentional modulation and mutual inhibition, and hence requires attention (Li et al., 2017). It was also shown that the strength of posterior parietal BOLD in BR is directly modulated by attentional load in a dual-task design (Intaitė et al., 2016). In fact, the links between consciousness and attention so strong that it was questioned whether they are just identical (Koch & Tsuchiya, 2007). To address this, based on TMS work that found modulation of spatial attention shifting when stimulating a region close to IPS (Hilgetag et al., 2001) as well as lesion results that indicated SPL in sustained attention (Malhotra et al., 2009), Schauer et al. (2016b) used cTBS to both parietal loci between measures of attention. They found that while cTBS had a trend to impair spatial attention, there was no evidence for a fractionation of parietal cortex. In light of current evidence, this is likely due to cTBS also not modulating parietal cortex function in an inhibitory way.

Based on Bayes factors speaking in favour of a null effect in the main experiment, coupled with this lack of correlation between MEP amplitude suppression and BR dominance modulation, I

am forced to conclude that cTBS to parietal cortex does not affect BR. Despite my failure to generate data that elucidates differential causal roles of SPL and IPS in normal and unreportable BR, there is evidence to support such a role. Brascamp et al. (2018) conducted a meta-analysis of the fMRI difference maps between multistable perception and replay of 10 neuroimaging studies (Lumer et al., 1998; Kleinschmidt et al., 1998; Lumer & Rees, 1999; Sterzer & Kleinschmidt, 2007; Zaretskaya et al., 2010; Knapen et al., 2011; Weilnhammer et al., 2013; Frässle et al., 2014; Megumi et al., 2015; Brascamp et al., 2015). They confirmed the involvement of predominantly right-lateralised fronto-parietal regions, most consistently over inferior frontal gyrus, temporoparietal junction and IPS. Parietal cortex may hence be involved in "checks and balances" which influence the dynamics of multistability (Leopold & Logothetis, 1999), or alternatively only represent the conscious noticing of perceptual reversals without any causal role.

CHAPTER 3

Flicker perception in binocular rivalry and continuous flash suppression is not affected by tACS induced SSR modulation

1. Materials and method

1.1 Participants

24 healthy volunteers with normal or corrected to normal vision took part in the tACS experiments (mean age = 26.58 yrs ± 10.1 s.d., 12 female, 12 male, 2 left-handed). Out of this sample, 10 participants took part in the EEG pre-experiment (mean age = 26.60 yrs ± 2.99 s.d., 3 female, 1 left-handed). All participants were screened to meet health guidelines for neurostimulation and gave written consent. The study was approved by the local ethics committee.

1.2 Visual stimuli and apparatus

All stimuli were presented on a 27 inch monitor (width = 602 mm, ASUS, Taiwan) operating at 144 Hz, on a grey background (half of maximum illumination). There was no natural light contamination nor room lighting. Participants' head position was fixed by a head and chin-rest. Binocular rivalry between two stimuli was created with a mirror stereoscope: The two stimuli were presented on the two sides of the screen separated by a board. The stereoscope then projected the images into the same retinal space of the participant. The mirrors were carefully adjusted for each participant to achieve fusion of the fixation cross and lines. The distance between monitor and participant through the stereoscope was 700 mm. All stimuli were created and controlled by a stimulus computer (Ubuntu 17.10) running Psychtoolbox 3 for Matlab R2014a (Mathworks, USA). Participants´ button press responses were collected with an adapted numeric keypad with eight buttons (two columns, four rows).

1.2.1 Binocular rivalry stimuli

Two circular flickering checkerboards (both 3.5 dva in diameter) were presented to the same retinal space in both eyes through the mirror stereoscope: one was black and green while the other was black and red (*figure* 22a). The checkerboard flickered at a preassigned frequency (see session 2.3), where the flickering was created through alternating presentation of the circular checkerboard and its inverted image. This method has been used successfully to elicit SSRs (Regan, 1966). Moreover, the checkerboards rotated clockwise (36 degrees/s). Around each checkerboard there was a fusion aid to assist in keeping the two stimuli overlapping, which was a black and white checkerboard frame with a width of 7 dva. The initial screen presented before the trial was comprised of the fusion aid in addition to a red fixation cross at its centre. The presentation eye of the checkerboards (i.e. which eye was presented with which checkerboard) was determined randomly.

1.2.2 CFS stimuli

Two images were presented to the same retinal space in both eyes, a CFS mask and a grey target canvas (half of maximum illumination), both delimited by a square black and white fusion aid (12 dva in width). The 200 CFS masks were composed of a set of colourful overlaid circles of various sizes. The target canvas included a single target (0.7 dva in diameter), which was a low-contrast black and white checkerboard, which could either be 1.5 dva to the right or left side of a fixation cross (*figure* 23). The target flickered at a preassigned frequency (see session 2.3), where the flickering was created through alternating presentation of the circular checkerboard and its inverted image. The CFS masks changed at a frequency of 9 Hz. The initial screen presented before the trial start was comprised of a fusion aid and the red fixation cross. To begin each trial, participants pressed either the lower left or right button on the numeric keypad. The presentation position of the stimuli (i.e. which eye was presented with the target canvas and which eye with the CFS mask) as well as the presentation position of the target (i.e. whether the target would appear to the left or right of the fixation cross) was determined randomly, with equal frequency over all trials.

1.3 Experimental design

Participants came to the laboratory on two separate days: once for an EEG-pre-experiment and once for three tACS experiments.

1.3.1 EEG pre-experiment

An important issue when applying tACS concurrent with SSRs is the difference in time needed for both to have a neural effect. The signature of both follows a sinusoidal curve, however, their onset is not concurrent: SSRs occur after a given latency relative to stimulus presentation due to neural signal conduction delays from the eyes to the visual cortex. To ensure that the neural signatures of both overlap, tACS must be initiated at this latency. To do that, I attempted to estimate this latency in an EEG pre-experiment.

Participants were seated in a dark room, asked to put their chin onto the chin rest and instructed to fixate on the red fixation cross that was stereoscopically presented. The stereoscope was adjusted until a binocular match was achieved and participants reported only perceiving one single cross. Following a button press, participants viewed *Binocular rivalry stimuli* for 300 runs. In each run, after an initial jitter period of 0.8-1.2 s from the start trial button press, both circular checkerboards appeared for 2 s and were then succeeded again by the initial screen. The next run began when the participant pressed a button. Both binocular rivalry stimuli flickered in synchrony at the same frequency. In half the trials this frequency was 7.2 Hz, in the other 9 Hz. The task was to passively

fixate at the fixation cross from pressing the trial start button until the stimulus disappeared. Participants were encouraged to take a longer break every hundred trials. The experiment lasted about 30 min. EEG was recorded continuously during this time (see section 2.4).

1.3.2 tACS experiment 1: binocular rivalry

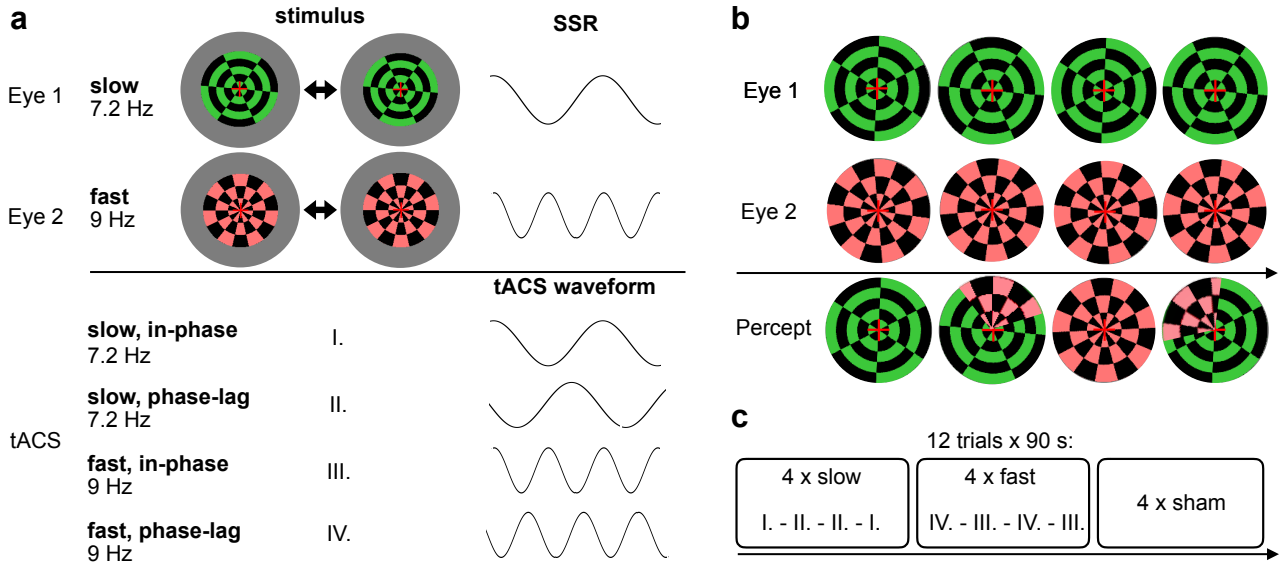

Figure 22 — tACS experiment 1: binocular rivalry
(a) Each eye was presented with a different circular checkerboard (green and red, respectively) in the the same retinal location, with a red fixation cross in the center. Flickering emerged through alternating presentation of the circular checkerboard and its inverted image (see left and right). One eye receives a fast (9 Hz) the other a slow (7.2 Hz) flicker. tACS could be slow (I. & II.) or fast (III. & IV.) also. Within each, tACS can be applied in-phase (I. & III.) or out-of-phase with a lag (II. & IV.) **(b)** Illustration of binocular rivalry stimuli and percept evolution over time. Both eyes were presented with either of the two checkerboards (upper two rows), which led to a percept that fluctuated between the two eyes (bottom row). Participants reported percept types by pressing and holding one of two buttons throughout 90 s of viewing time per trial. **(c)** Design overview: There were 12 trials of 90 s. tACS fast, slow and sham appeared four times each in consecutive blocks, counterbalanced. Within these, tACS was applied twice in-phase, twice counterphase, counterbalanced.

The first tACS experiment utilised binocular rivalry. Participants were instructed to fixate on the red fixation cross. Following a button press, participants viewed the *binocular rivalry stimuli* for 12 trials of 90 s each (*figure* 22b). During this time, the red checkerboard flickered at 7.2 Hz (slow frequency), while the green checkerboard flickered at 9 Hz (fast frequency). These frequencies were chosen as they have been associated with eliciting SSRs (Norcia et al., 2015), and also do not have matching harmonics below 35 Hz. Note that the precise choice of flicker frequency was constrained by the refresh rate of the monitor of 144 Hz (for a remedy see Andersen & Müller, 2015). Participants were instructed to report their perception by pressing and holding one of two buttons using their right hand: the left button while the red checkerboard was dominant, and the right button for green. Moreover, participants were asked to press no button during perceptual mixtures.

tACS was used continually throughout the 90 s trials. tACS intensity was linearly ramped up (0 to 1000 mA) during 10 s towards the beginning of the trial, and ramped down after it ended.

There were six experimental conditions in a three-by-two design: three tACS frequency conditions: 1) 7.2 Hz for the slow condition, 2) 9 Hz for the fast condition and 3) sham; and two phase conditions: 1) In-phase, where tACS onset was the SSR onset minus the ramp-up time. 2) Out-of-phase, where tACS onset was the SSR plus 1/2 the period of the tACS frequency minus the ramp-up time. In the sham condition there was no electrical stimulation during the trial, although the current fade-in and out were present at 8.1 Hz (midpoint between the slow and fast frequencies) so that participants were not able to know that the simulation was off, since most of sensation of having tACS applied occurs during the fade-in and fade-out periods. Each of the three tACS frequency conditions (fast, slow, sham) appeared for four consecutive trials. Each of these four trials was randomly assigned to one of two tACS phase conditions (in-phase or out-of-phase with the stimulus). The order of conditions was randomised.

1.3.3 tACS experiment 2: CFS & RT

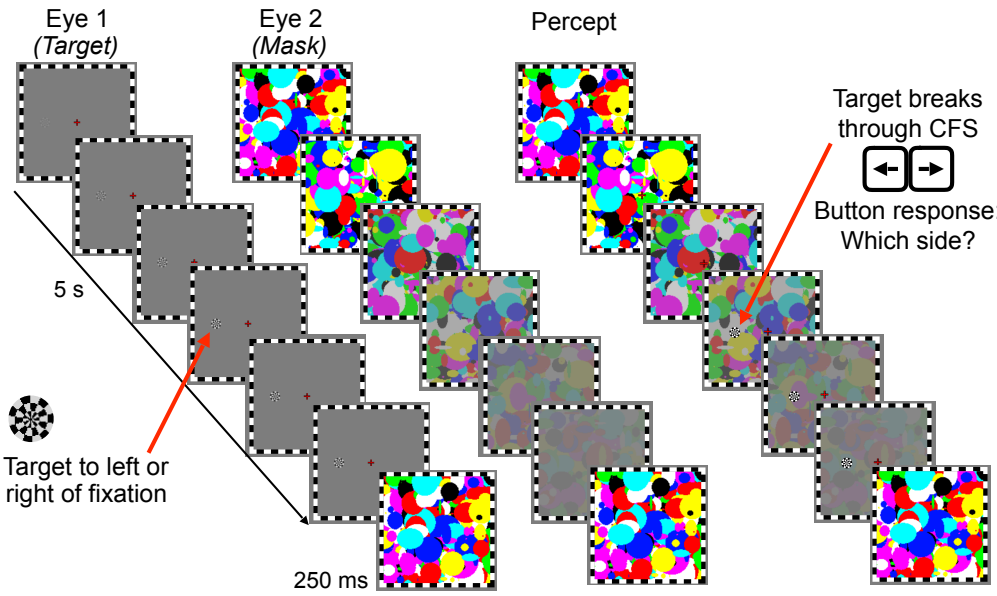

Figure 23 — tACS experiment 2: CFS & RT
The target canvas (here shown in Eye 1) consisted of a black and white flickering circular checkerboard that could be to the left or right of the fixation cross (left shown here). The CFS mask (here shown in Eye 2) was a series of images of colourful circles (200 different patterns). All stimuli were delimited by a square black and white fusion aid. In each trial, the stimuli were presented for 5 s during which the CFS mask gradually faded out and the checkerboard gradually faded in. At some point within these 5 s, participants were likely to see the target break through the mask. Following the task, the mask was presented to both eyes for 250 ms to avoid afterimages of the target.

The second tACS experiment utilised CFS. Participants were instructed to fixate on the red fixation cross. Following a button press, participants viewed the *CFS stimuli* for 12 blocks of 90 s each. Each block had 16 trials. In each trial, the stimuli were presented for 5 s, during which the circular checkerboard (target) gradually faded in and the CFS mask gradually faded out (*figure* 23). Since the target could be either to the left or right side of the fixation cross, participants were instructed to

press the left or right button as soon as they saw the target. We hence used a two-alternate-forced-choice (2AFC) design, measuring stimulus detection through accuracy and RT. The target flickering frequency was 7.2 Hz (slow frequency) while the CFS mask change rate was 9 Hz (fast frequency). After 5 s, identical CFS masks were presented to both eyes for 250 ms to avoid after-image effects (visual illusion in which retinal impressions persist after the removal of stimulus). Then the plain gray fixation screen was presented for 375 ms before the following trial began. Experimental conditions and tACS were identical to experiment 1 (*figure* 23 a & c; except eye 1 receives the slow target and eye 2 the fast mask).

1.3.4 tACS experiment 3: CFS & metacognition

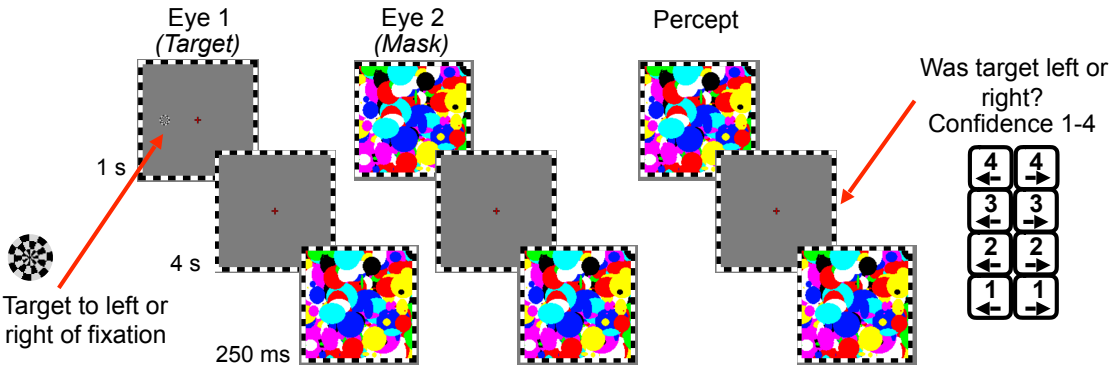

Figure 24 — tACS experiment 3: CFS & metacognition
The target canvas (here shown in Eye 1) consisted of a black and white flickering circular checkerboard, which could be to the left or right of the fixation cross. For illustration only, the target (shown on the left here) is displayed at a high contrast level of 100%. The CFS mask (here shown in Eye 2) was a series of images of colourful circles (200 different patterns). Both were delimited by a square black and white fusion aid. In each trial, the stimuli were presented for 1 s. Then participants had 4 s to make a 2AFC judgment paired with a confidence rating. Following the task, the mask was presented to both eyes for 250 ms to avoid afterimages of the target.

The third tACS experiment was identical to the second one, except for the following differences. In each trial, the stimuli were presented for 1 s only. This short duration did not allow for the target to become consciously perceptible. Following presentation of the mask for 250 ms to avoid after-image effects (*figure* 24). The target flickering frequency was 7.2 Hz while the change frame rate was 9 Hz. Afterwards, a grey screen with red fixation cross was displayed for 4 s. Participants were instructed to report which side the target had been on as well as how confident they are in this answer. To that end, participants had four right and four left buttons, to indicate side as well as how sure they are on a 1-4 scale by pressing one of the eight buttons. Then the grey fixation screen was presented for 375 ms before the following trial began. Experimental conditions and tACS were dentical to experiments 1 and 2 (*figure* 23 a & c; except eye 1 receives the slow target and eye 2 the fast mask).

1.4 EEG recording and SSR latency analysis

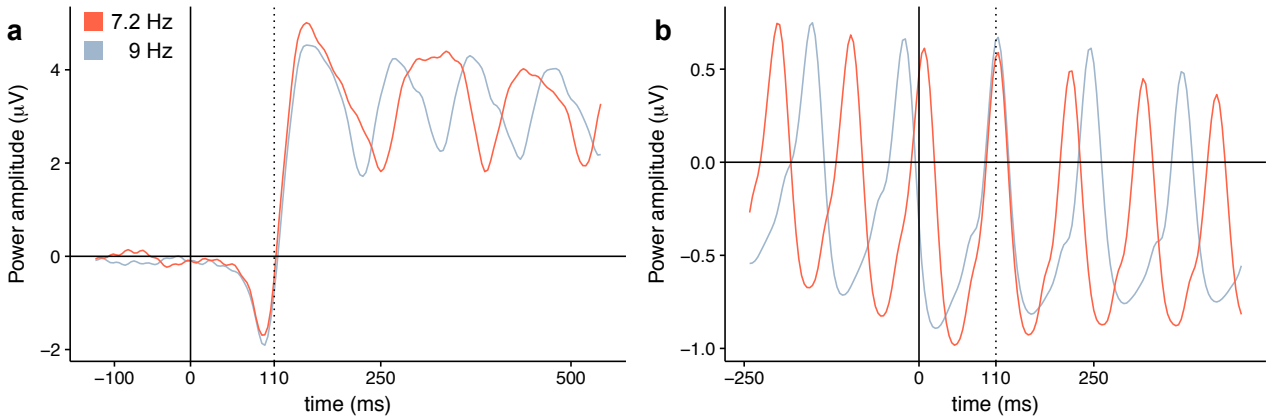

Figure 25 — EEG signal traces of the pre-experiment
(**a**) Baseline-corrected grand averaged onsets of SSRs for 10 participants, showing traces evoked by the fast stimulus (9 Hz flickering frequency) in red and by the slow stimulus (7.2 Hz flickering frequency) in blue for the P1 electrode. Stimulus onsets were at time 0. The EEG signal fell into the repeating SSR pattern beyond 110 ms. (**b**) Grand averaged EEG signal over the O2 electrode during the trial, where x = 0 represents for each stimulus separately the time that it flickered on the screen. At about x = 110 ms, the two signals were synchronised, meaning that the stimulus flicker evoked its neural response at this time. Before and after, the signal desynchronised due to the different flicker frequencies of the fast and slow stimulus.

EEG data were recorded at 2500 Hz acquisition rate using a BrainAmp MR Plus system (Brain Vision; bandpass 0.016–250 Hz) with 11 active actiCap Ag/AgCl electrodes placed over occipital and parietal areas (in the international 10-20 system: Pz, P1, P2, POz, PO3, PO4, PO7, PO8, Oz, O1, O2) as well as the ground (AFz) and reference (FCz) electrodes, at an impedance lower than 5 kΩ (*figure* 26). EEG data were processed offline with ERPLAB, a plugin for the EEGLAB toolbox in Matlab R2014a (Mathworks, USA). The signal was downsampled to 256 Hz, referenced to the average of all electrodes and a bandpass filter with the cutoff values of 0.05 Hz and 30 Hz was applied. Baseline-corrected epochs were extracted for time intervals of -500 ms to +1000 ms around either the 300 trial onsets or the roughly 4000 flicker reversals across all trials. Despite the trials being longer, this period proved sufficient for detecting the SSR. The epochs were averaged for each participant and later into a grand average.

SSRs offer good signal to noise ratios, as a large portion of signal power is contained within a few frequency bands. Since these are known to the experimenter, their isolation from the EEG signal is comparably easy, even by eye. Visual inspection of the SSRs for each participant individually, as well as on the grand average, revealed that the onset delay between the stimulus being drawn on the screen and the neural signal being detectable on the EEG was at about + 110 ms for each participant (*figure* 25). This is important, because in order to phase-lock the tACS to the SSRs, the tACS onset must be adjusted by this latency (see section 2.3.1).

1.5 tACS parameters

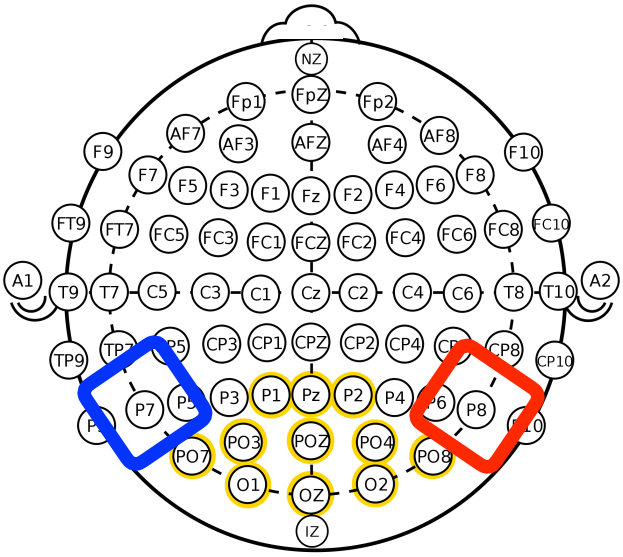

Figure 26 — tACS/EEG montage
Yellow: Electrodes that were used for recording EEG in the pre-experiment within the international 10-20 system. Blue/red: Cathode and Anode for the tACS placed over the P7/P8 electrode sites.

The stimulus computer controlled the battery-driven tACS device (DC-Stimulation Plus, NeuroConn GmbH, Ilmenau, Germany). tACS is mainly driven by the parameters of frequency, current amplitude/intensity and stimulation phase (Antal & Paulus, 2013). An alternating sinusoidal current at 1000 µA intensity was delivered through two conductive-rubber electrodes that were positioned on the scalp at P7 and P8 positions according to the International 10-20 system (*figure* 26). Prior studies have shown that perceptual and neural effects depend on tACS intensity: 500 µA or higher of 10 Hz tACS over visual cortex (electrodes 4 cm over inion and on vertex, corresponding to Cz/Oz) were sufficient to cause visual phosphenes in darkness (Kanai et al., 2008). 140 Hz tACS stimulation of M1 had an inhibitory effect on TMS induced MEP amplitude at 400 µA, had no effect at 200 µA, 600 µA and 800 µA, but had an excitatory effect at 1000 µA (Moliadze et al., 2012). We therefore chose 1000 µA to form part of an excitatory protocol. The electrode montage was chosen based on the work of Neuling et al. (2012b). By use of finite-element models to predict current flow through the brain during electrical neurostimulation dependent on electrode position, Neuling et al. (2012b) were able to show that the P7/P8 montage was particularly suited for occipital stimulation, reaching current densities of up to 0.089 A/m^2. Compared to the Cz/Oz montage, this approach is also less likely to elicit phosphenes (Zaehle et al., 2010).

The electrodes were placed into sponges (5.5 x 6 cm size) and soaked in 0.9% NaCl solution, resulting in impedances lower than 20 kΩ. In all experiments, tACS was applied for 90 s at a time (see session 2.3). Right before the beginning and right after the end of each trial, the current linearly faded-in (from zero to 1000 µA) and out (from 1000 µA to zero), respectively, during 10 sec.

1.6 Behavioural data analysis

1.6.1 Experiment 1: binocular rivalry

Our measure of interest was the modulation of predominance as a function of the different tACS conditions. To that end, I first extracted rivalry dominance durations from the button presses of participants. We excluded button presses that were interrupted by the end of the trial and treated double button presses and no button presses as mixed percepts. We next investigated if the data followed previously reported gamma distributions (Levelt, 1967) for each participant and each condition separately. Predominance was calculated as the sum of all slow (red target) dominance durations divided by the sum of both (green and red targets) dominance durations. We used this measure for the main analysis, since it indicates if an experimental manipulation biased participants to see the slow over the fast stimulus contingent on how tACS was applied. Then I checked if predominance was abnormal (< 0.3 or > 0.7). Finally I entered predominance as dependent variable into a repeated measures ANOVA, using tACS frequency and phase as factors.

Next to predominance, I decided to also test whether tACS had modulated dominance durations overall, as well as for only the fast stimulus, slow stimulus and mixes percepts. We therefore entered each of these as dependent variable into separate repeated measures ANOVAs, using tACS frequency and phase as factors.

1.6.2 Experiment 2: CFS & RT

We were interested in the tACS effect on RT and accuracy. For each participant and each condition separately, I first examined if accuracy was higher than 0.8 to ensure participants adequately performed in each condition. Then I looked at all RTs to see if they followed a gamma distribution. The median RT for all trials within a condition was then used for the main analysis. Here I entered RT and accuracy as dependent variables into two separate repeated measures ANOVAs, using tACS frequency and phase as factors.

1.6.3 Experiment 3: CFS & metacognition

We aimed to examine detection sensitivity and metacognitive sensitivity. There is no widespread consensus on a standard computation of metacognitive sensitivity. Here, I calculated type I and type II receiver operating characteristic (ROC) curves and then the area under this curve (AUC). To obtain type I ROC curves, the data was partitioned into hypothetical levels of decision thresholds. With a response scale of 8 (4 in favour of either percept *p1* or *p2*, with increasing degrees of confidence hence -4 to +4, see section 2.3.4), there were 8-1 partitions. Starting with a threshold where -4 indicates indicates *p1*, and all other buttons *p2*, I calculated a hit and false alarm rate. Next

this can be done assuming that -4 and -3 indicate *p1* and all others *p2*, and so forth. Hence, for each criterion, I obtain a set of numbers, that can be plotted against each other, yielding the ROC curve. The area under this curve now represents discrimination performance, where 0.5 is chance and higher curves entail more sensitivity (Sherman et al. 2015). To obtain type II ROC curves, the data was partitioned similarly into criteria along the levels of confidence (1 - 4). First, let 1 represent low confidence and 2-4 high, then 1-2 represent low and 3-4 high, and so forth. For each criterion, I calculated the type II false alarm rate, which is the proportion of high confidence trials, when the participant is incorrect, or p(confidence | incorrect); as well as the hit rate, which is the proportion of high confidence trials, when the participant is correct, or p(confidence | correct). Connecting these points yields the type II ROC curve. To this end, I used the method and code provided by Fleming & Lau (2014). The advantage of this non-parametric method is its robustness against violations of Gaussian equal variance. The area under this curve now represents metacognitive sensitivity.

Finally, I entered type I AUC and type II AUC as dependent variables into two separate repeated measures ANOVAs, using tACS frequency and phase as factors.

2. Results

2.1 Experiment 1: binocular Rivalry

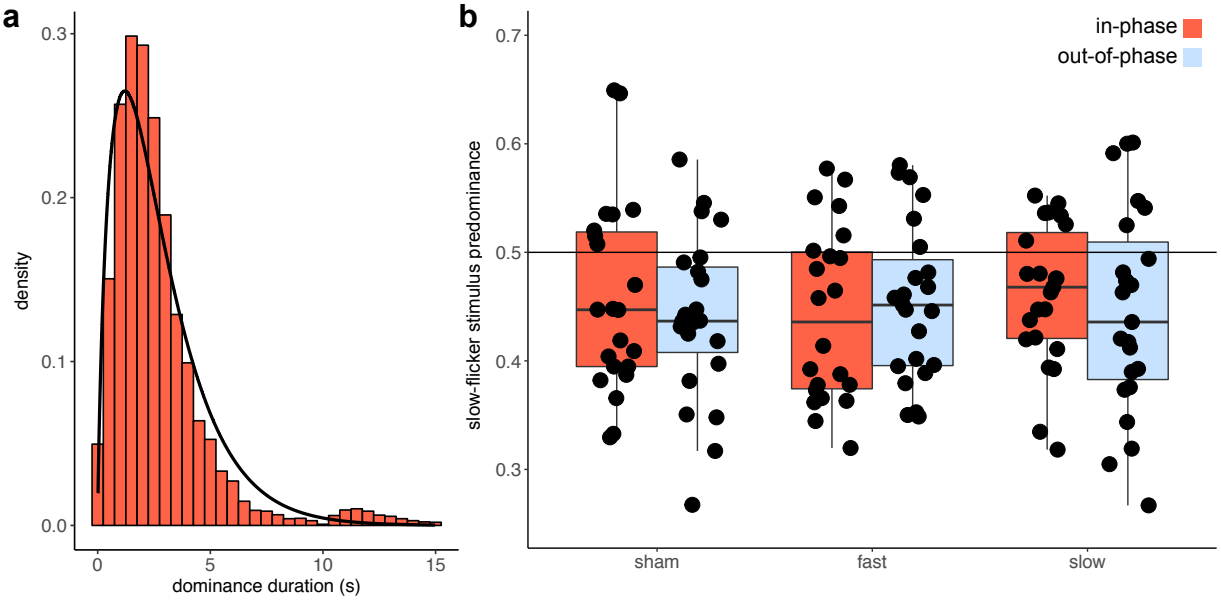

Figure 27 — tACS experiment 1: results
(a) Binocular rivalry dominance durations histogram pooled from all trials of all participants, with density distribution overlaid. The durations follow a gamma distribution (shape = 1.78, scale = 0.65, median dominance is 2.61 s). **(b)** Predominance across conditions: The slow predominance (y axis) represents the proportion of the sum of all slow (red target) dominance compared to the sum of all percetual dominances (slow and fast). If predominance is 0.5, then both percepts were perceived in equal parts. Each dot is a data point from one tACS frequency condition (sham, fast, slow) and tACS phase condition (in-phase, out-of-phase) of one participant. In-phase is red, out-of-phase is blue.

The dominance durations pooled from all participants together followed a gamma distribution (*figure* 27a). We therefore chose the median as measure of central tendency. One participant, whose data was corrupted, needed to be excluded from the analysis. The average of all participants' median dominance durations was 2.58 s ± 0.83 s.d. for the fast flickering stimulus (green target), 2.24 s ± 0.74 s.d. for the slow stimulus (red target) and 2.39 s ± 0.74 s.d. considering both together.

Entering the predominances into a repeated measures ANOVA, using as factors tACS frequency (sham, slow, fast) and tACS phase (in-phase, out-of-phase), I found that there was neither a significant main effect of tACS frequency ($F(2,44) < 1$, *ns*), tACS phase ($F(1,22) = 1.03$, *ns*), nor a significant interaction between the two factors ($F(2,44) < 1$, *ns*) (*figure* 27b). Since the absence of an effect is not evidence in favour of the null hypothesis (H0), I used Bayesian statistics to ascertain how strong the above null results were. Using the BayesFactor package (0.9.2) for R64, I modelled a Bayesian ANOVA with the mathematical underpinnings presented by Rouder et al. (2012), computing a Bayes Factor (BF) for each combination of factors and interaction, against the null that all effects are 0. The analysis resulted in a BF of 0.09 (strong evidence for H0) for the main effect of

tACS frequency, a BF of 0.2 (substantial evidence for H0) for main effect of tACS phase, and a BF of 0.002 (very strong evidence for H0) for the interaction term. This provides overall strong evidence that the tACS conditions did not affect predominance. ANOVAs using other dependent variables, such as dominance duration for fast, slow, mixed and all percepts, yielded similar null results.

2.2 Experiment 2: CFS & RT

The RT values pooled across all conditions and participants followed a gamma distribution (*figure* 28c). We therefore chose the median as measure of central tendency. One participant needed to be excluded from the analysis due to data corruption. The average of all participants' median RT was 2.01 s ± 0.47 s.d. Moreover, participants correctly identified the position of the target most of the time at an overall accuracy of 96%. For the subsequent RT analyses, incorrect trials were excluded.

The median RTs for each condition from each participant were entered into a repeated measures ANOVA with two factors: tACS frequency (sham, fast, slow) and tACS phase (in-phase, out-of-phase). Mauchly´s test indicated that the assumption of sphericity had been violated for the interaction term ($\chi^2(2) = 8.84$, $p = 0.01$), therefore degrees of freedom were corrected using Greenhouse-Geisser estimates of sphericity ($\varepsilon = 0.74$). The ANOVA showed that there was neither significant main effect of tACS frequency ($F(2,44) < 1$, *ns*) nor tACS phase ($F(1,22) < 1$, *ns*), nor a significant interaction between the two ($F(2,44) < 1$, *ns*) (*figure* 28d). The cumulative density plots corroborate these results since the density curves for tACS frequency conditions (*figure* 28a) and tACS phase conditions (*figure* 28b) overlap and show no clear difference pattern. A Bayesian ANOVA produced a BF of 0.08 (strong evidence for H0) for the main effect of tACS frequency, a BF of 0.2 (substantial evidence for H0) for the main effect of tACS phase, and a BF of 0.002 (very strong evidence for H0) for the interaction term. This provides overall strong evidence that the tACS conditions did not affect RT.

When accuracy was entered into the same ANOVA as dependent variable, it showed that there was neither a significant main effect of tACS frequency ($F(2,44) < 1$, *ns*), tACS phase ($F(1,22) < 1$, *ns*), nor an interaction between the two ($F(2,44) < 1$, *ns*) (*figure* 28e). This null effect was again supported by Bayesian statistics, which produced a BF of 0.09 (strong evidence for H0) for the main effect of tACS frequency, a BF of 0.2 (substantial evidence for H0) for the main effect of tACS phase, as well as a BF of 0.002 (very strong evidence for H0) for the interaction term. This provides overall strong evidence that the tACS conditions also did not affect accuracy.

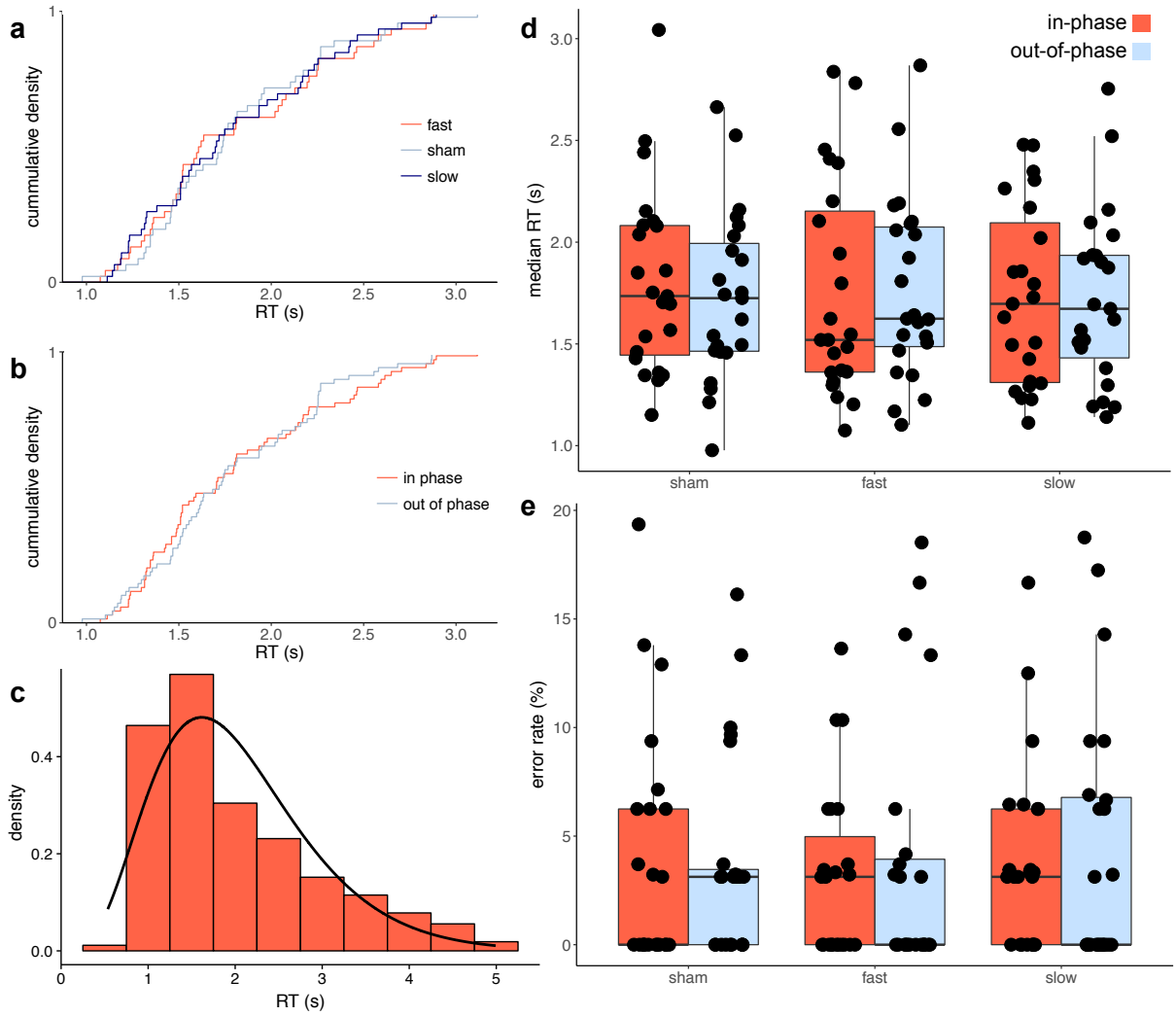

Figure 28 — tACS experiment 2: results
(a, b) Cumulative density curves for the median RTs for each condition in each participant separated by tACS frequency (sham, fast, slow) (a) and by tACS phase (in-phase, out-of-phase) (b). **(c)** RT histogram pooled from all trials of all participants. The durations follow a gamma distribution (shape = 4.96, scale = 2.45, median RT is 1.70 s). RT histogram. **(d)** Median RT and **(e)** error rate across experimental conditions. Error rate was calculated as 100% - accuracy. Each dot is a data point from one tACS frequency and phase condition. In-phase is red, out-of-phase is blue.

Despite the absence of a tACS effect, performance in the task could have improved over time due to perceptual learning or training. To test this, the three experimental blocks (comprised of four 90 s trials each) were sorted chronologically, regardless of the tACS frequency condition. To begin, I calculated a linear regression to test if time (in three bins) was a significant predictor of accuracy and found a positive relationship, such that training led to higher performance (Formula: Accuracy = 0.83 + 0.04 * time, $F(1, 70) = 9.22$, $p = 0.003$, $R^2 = 0.10$). This entails that accuracy increased by 4% each time bin (*figure* 29 top). Next, I asked if time was also a significant predictor or RT and found a negative relationship, such that training led to a lower RT (Formula: RT = 2.40 – 0.19 * time, $F(1, 70) = 8.80$, $p = 0.004$, $R^2 = 0.10$). This entails that RT decreased 0.19 s for each time bin (*figure* 29 bottom). Both these results together point out that more time elapsing led to better performance.

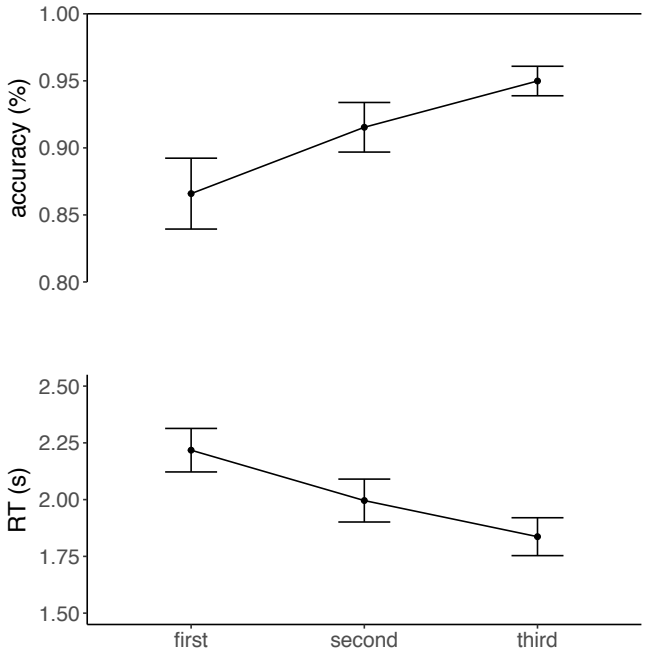

Figure 29 — tACS experiment 2: effect of time
Effect of time (block number) on accuracy **(a)** and median RT **(b):** On the x axis are the first, second and third experimental blocks according to temporal order and independent on what the tACS frequency condition was. Error bars indicate SEM.

2.3 Experiment 3: CFS & Metacognition

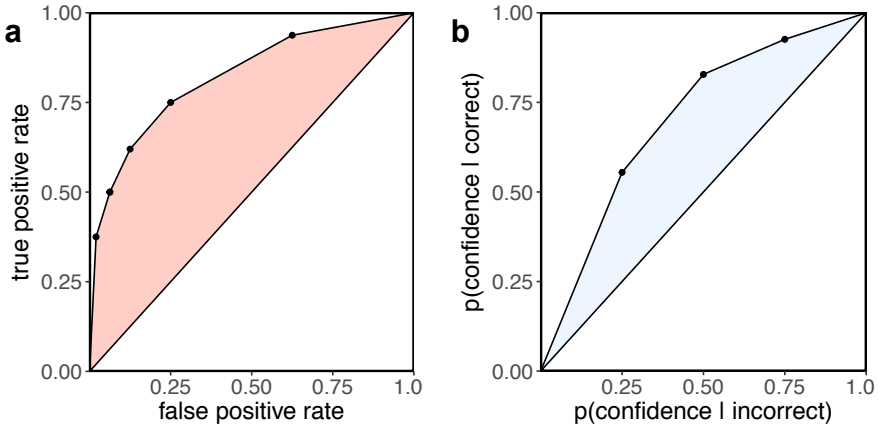

Figure 30 — ROC curves
(a) Type I ROC for a representative participant. For each confidence criterion, type I false alarm rate (x) is plotted against type I hit rate (y). AUC, representing detection sensitivity, is shaded in red. **(b)** Type II ROC curve for a representative participant. For each confidence criterion, type II false alarm rate (x) is plotted against type II hit rate (y). AUC, representing metacognitive sensitivity, is shaded in blue.

Type I and II AUC were computed for each participant individually. A representative set of curves is shown in *figure* 30. 5 participants needed to be excluded from the analysis for being at ceiling or floor in terms of confidence. The mean type I AUC for all participants was 0.83 ± 0.14 s.d., the mean type II AUC was 0.73 ± 0.06 s.d.

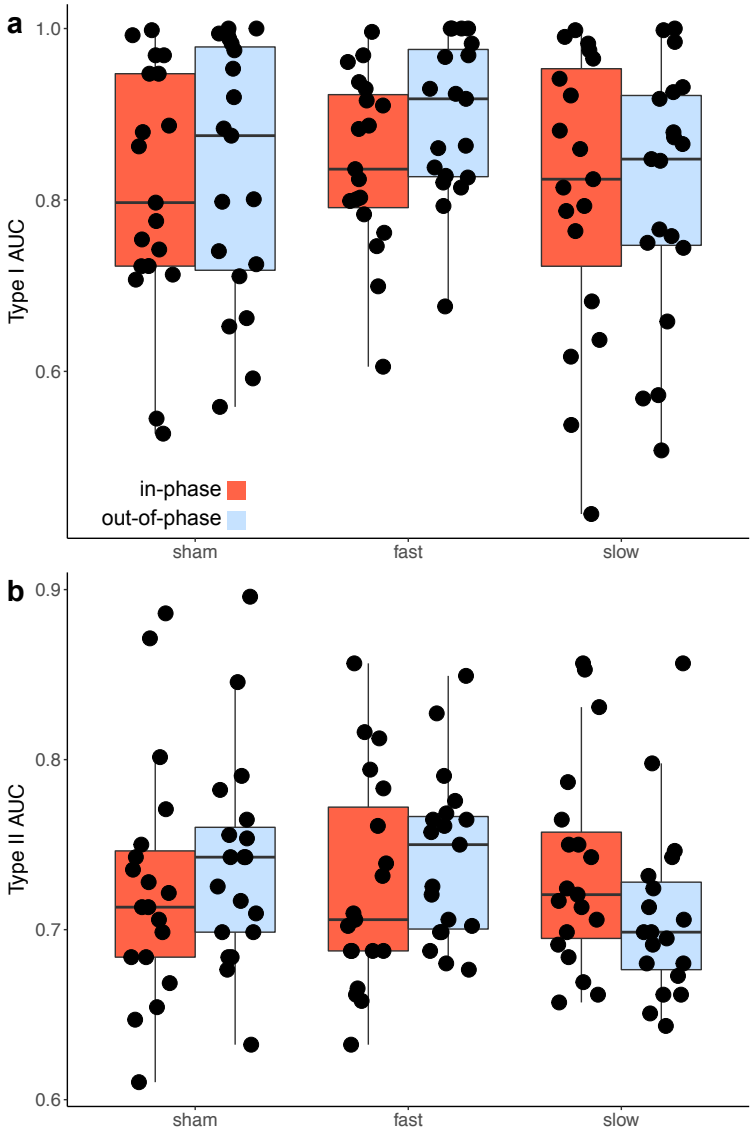

Figure 31 — tACS experiment 3: results
(**a**) Type I AUC and (**b**) type II AUC across experimental conditions. Each dot is a data point from one tACS frequency and phase condition tACS. In-phase is red, out-of-phase is blue.

First, type I AUC for each condition from each participant was entered into a repeated measures ANOVA with factors tACS frequency (sham, fast, slow) and tACS phase (in-phase, out-of-phase). We found that the main effect of tACS frequency approached significance ($F(2,36) = 2.87$, $p = 0.07$), whereas there was no main effect of tACS phase ($F(1,18) = 1.83$, *ns*) nor interaction ($F(2,36) < 1$, *ns*) (*figure* 31a). A Bayesian ANOVA showed that there was only anecdotal evidence in favour of the main effect of tACS frequency ($BF = 0.44$). Visual inspection of the data revealed that this was merely due to less spread of the data in the fast condition. The analysis furthermore produced a BF of 0.28 with regard to the main effect of tACS phase (substantial evidence for the H0) and a BF of 0.022 for the interaction (very strong evidence for the H0). In essence, the analysis showed that

tACS phase and its interaction with frequency had no modulating effect on type I AUC, while I cannot draw any conclusion about the main effect of tACS frequency.

Next, I constructed an identical ANOVA with type II AUC as dependent variable. We found no main effect of tACS frequency ($F(2,36) < 1$, *ns*), nor of tACS phase ($F(1,18) < 1$, *ns*). However, there was a significant interaction term ($F(2,36) = 6.39$, $p = 0.005$). This interaction indicates that tACS frequency modulated the effect of tACS phase, even in the absence of main effects. This can be visually seen in the data (*figure* 31b), where out-of-phase tACS produced a higher mean type I AUC in the fast and sham frequencies, while this effect was reversed for the slow frequency. However, already visual inspection cautions me to over-interpret this term, since it could easily be attributed to noise, given the spread of the data. Bayesian statistics confirm this suspicion, yielding a BF of 0.01 for the interaction, which is substantial evidence for the null. Similarly, for the main effects of tACS frequency and phase, BF of 0.12 and 0.2 respectively also point towards the H0.

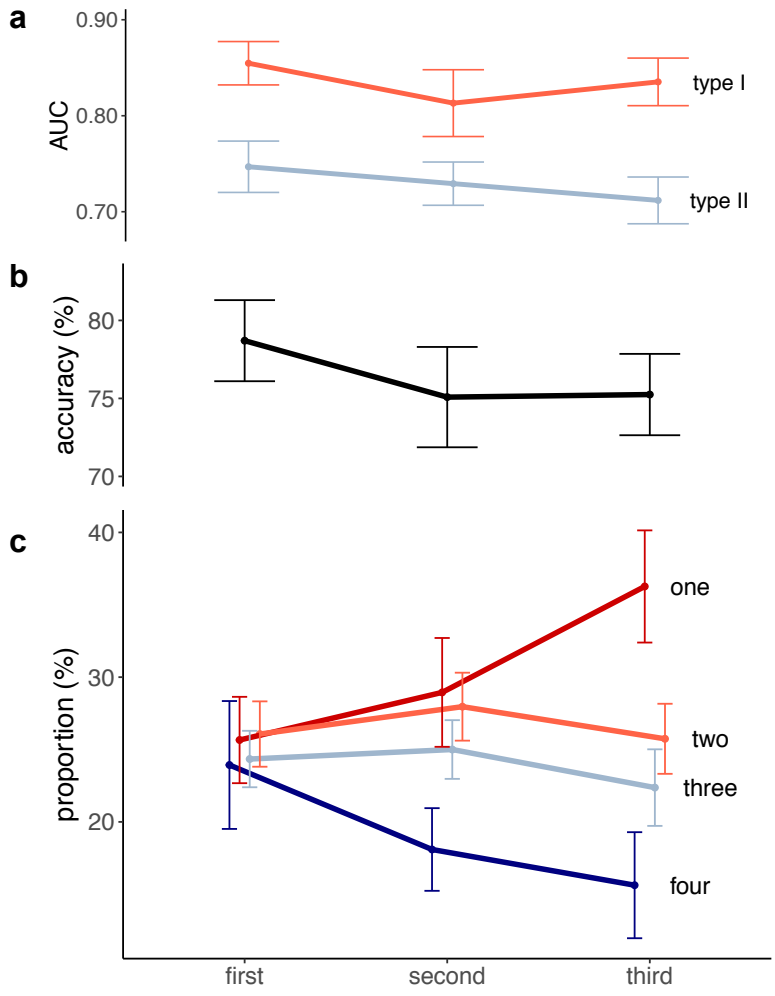

Figure 32 — tACS experiment 3: effect of time
Effect of time (block number) on AUC (**a**), accuracy (**b**), and the proportion of button presses corresponding to the different confidence levels from 1-4, where 4 is highest (**c**). On the x axis are the first, second and third experimental blocks according to temporal order and independent on what the tACS frequency condition was. Error bars indicate SEM.

As in experiment 2, despite the absence of a tACS effect, performance in the task could have improved over time due to perceptual learning or training. To test this, the three experimental blocks (comprised of four 90 s trials each) were sorted chronologically, regardless of the tACS frequency condition. First, linear regressions were calculated to test if time was a significant predictor of the proportion of the different confidence levels. We found that the lowest confidence level (button 1) was pressed more often as time went on (Formula: Proportion = 0.20 + 0.05 * time, $F(1,55) = 4.50$, $p = 0.04$, $R^2 = 0.06$). There was furthermore a trend for fewer presses of the highest confidence button as time progressed (Formula: Proportion = 0.27 - 0.04 * time, $F(1,55) = 2.56$, $p = 0.12$, $R^2 = 0.12$). There was no trend evident for the middle two confidence levels.

Hence, the lowest confidence button was pressed 5% more each block, while the highest confidence button was pressed 4% less (*figure* 32c). Despite training, this interestingly indicates less confidence over time. This is especially remarkable since accuracy did not change significantly ($F(1,55) > 1$, *ns*) (*figure* 32b). These results are captured also in the respective ROC curves: While there was no change in type I AUC ($F(1,55) > 1$, *ns*), metacognitive sensitivity decreased over time (Formula: AUC = 0.53 - 0.04 * time, $F(1,55) = 4.13$, $p < 0.05$, $R^2 = 0.05$) (*figure* 32a).

3. Discussion

In this study, I tested whether application of tACS at congruent or incongruent frequencies (or phases) with stimulus-induced SSRs influenced perception. In particular, I used two types of stimuli that I expected to be highly sensitive for detection of neural intervention effects - binocular rivalry and continuous flash suppression - as both allow for continuous shifts of perceptual balance towards one or the other percept. Effects on perception, in the form of binocular rivalry dominances as well as conscious awareness of targets under CFS, would entail that modulation of the SSR causally influences perception (Sejnowski & Paulsen, 2006). That would be relevant since it could elucidate whether SSRs only correlate with visual perception, or if their modulation influence it. Our results, however, showed that the different tACS conditions did not affect perceptual measures: predominance (in the binocular rivalry experiment), RT and accuracy (in the first CFS experiment) as well as detection and metacognitive sensitivity (in the second CFS experiment) were not significantly different across tACS conditions. tACS did not not differentially affect binocular rivalry dominance durations, improve or impair detection of targets masked by CFS, nor modify metacognitive sensitivity. Thus, one might tentatively conclude that modulation of SSRs does not alter the dynamics of perception of flickering stimuli, but instead only correlate with them. What I observed were training effects independent of tACS. In the first CFS experiment, RT and accuracy improved over time, as could be expected (Zizlsperger et al., 2016). In the second CFS experiment, contrary to the expectation, metacognitive sensitivity decreased with time, an effect driven by a decrease in confidence. Several explanations could account for this: participants could have become more tired and less concentrated, making it harder to detect the near threshold stimuli, or, the lack of perceptual feedback led to increasing insecurity for psychological reasons. Alternatively, it may be that tACS had a cumulative negative effect on cognitive performance, however, this is unlikely given the positive training effect observed in the first CFS experiment.

3.1 tACS modulation of SSRs

Concluding from the results that SSRs do not have any causal role in determining the dynamics of perception of flickering stimuli may be premature though: since I did not record EEG during the two main experiments, I cannot claim with certainty whether SSRs were effectively modulated by tACS in this study. Especially in the CFS experiments, where targets were not presented foveally, I cannot even say with certainty that the targets evoked an SSR. Moreover, Ruhnau et al. (2016) reported SSRs modulation only at the 3f and 4f harmonics rather than at fundamental frequency and only when tACS was applied at the same frequency as the SSR. Conversely, tACS reduced phase synchrony at fundamental frequency and 2nd harmonic. If SSRs

at the fundamental frequency are indeed not influenced by tACS, but only at its 3f or 4f harmonics, I should have chosen lower tACS frequencies in order to affect the fundamental SSR frequency. Specifically, 3 Hz (9/3, as 3f harmonic) or 2.25 Hz (9/4, as 4f harmonic) for the fast condition, and 2.4 Hz (7.2/3, for 3f harmonic) or 1.8 Hz (7.2/4, for 4f harmonic) for the slow condition. This lack of tACS effect on the fundamental SSR frequency may however be due to the phase lag between tACS and SSR, which Ruhnau et al. (2016) did not control for. Since in this experiment, the phase relationship between tACS and SSR was controlled, I believe it more likely that also fundamental SSR frequencies were modulated by tACS. However, I must concede that without EEG evidence, I cannot be certain, especially since it is possible that the phase lag did not remain constant during stimulation. Still, even if I were only modulating higher SSR harmonics, (9 x 3 = 27 Hz and 9 x 4 = 36 Hz SSRs elicited by fast flickering stimulation; 7.2 x 3 = 21.6 Hz and 7.2 x 4 = 28.8 Hz elicited by slow), I would still have modulated the SSR (albeit only in part), and a positive result would have allowed me to make inferences as to my hypotheses. In this case, I may cautiously conclude that these results cannot demonstrate the absence of any causal role of the SSR, but rather the absence of a causal role of higher order dynamics.

3.2 Montage

There are several other explanations for this null result though. To begin, it may be that the presently used electrode montage (positions P7 and P8 according to the International 10-20 system), which differed from the montage used by Ruhnau et al. (2016) (Cz and Oz), was ineffective in modulating the SSR. One reason for this could be the propensity of the Cz/Oz montage to reach more medial occipital areas (Neuling et al. 2012) and hence the calcerine sulcus, from whence I reason the SSRs to originate. Therefore, anterior/superior—posterior/inferior tACS stimulation could affect neural firing in occipital cortex differently from left—right stimulation employed here. However, I believe the orientation of the calcarine sulcus alone cannot account for differential effects of different tACS directions. One reason is that SSRs do not have exclusively occipital sources. In fact, functional magnetic resonance imaging results demonstrate the involvement of a variety of widespread cortical regions, including frontal and prefrontal cortices (Ding et al., 2006; Di Russo et al., 2007; Pastor et al., 2003; Srinivasan et al., 2007, Li et al., 2015). It was also theorised that the SSR eliciting stimulus activates primary visual cortex directly through thalamocortical inputs, while more distant regions are recruited through indirect connections, although it remains possible that thalamic inputs lead signals directly to more anterior regions (Tononi et al., 1998). We therefore are not aware of any theoretical reason to expect one montage to work and not the other. Next, a computational model of tACS suggested that during stimulation, the firing of neurons is

modulated according to where in the stimulation curve I am, while the average firing rate is left as is (Reato et al., 2010). This suggests that the montage and direction of current only play a subsidiary role in determining the modulation of cortical activity. Lastly, my choice of montage was not arbitrary, but based on modelling results by Neuling et al. (2012).

3.3 Limitations

Interestingly, tACS at alpha frequency not only affects neural oscillations during stimulation, but has after effects as well. While the mechanism behind these effects is disputed (Vossen et al., 2015), it is possible that they led to carry over effects as I proceeded from one condition to the next. Another possible confound are skin sensations induced by tACS. More sensitive participants may better feel the stimulation and hence be able to distinguish between the experimental conditions. However, I controlled for this in three ways: Firstly, I gradually faded stimulation in and out, leading to sensation mostly confined to time periods outside the main trials. Secondly, the stimulation frequencies were so close together that it participants were unable to discriminate between them, as indexed by subjective report. Lastly, I also faded in and out a weak tACS current at a frequency between the fast and slow, leading to the same skin sensations as are experienced during non-sham trials.

Yet another concession to make is the sample of $n = 20$. While this sample size is standard for tACS publications (average $n = 17$ in 50 studies reviewed in Table 1 of Schutter & Wischnewski, 2016), caution is indicated: Veniero et al. (2017) showed an effect of tACS on a perceptual estimation task in a sample of $n = 19$. However, trying to replicate the same effect in an independent sample in the very same study revealed only a null result at $n = 20$ as well as in the combined sample of $n = 49$. It is hence possible that there is actually a small effect, only that it is obscured by the spread of the data. However, I am reasonably confident in the validity of the null result, also because of the use of Bayesian statistics and because I could not even observe a trend. Still, given the large inter-subject variability in response to tACS (review in Krause & Cohen Kadosh, 2014), this is a possibility I cannot dismiss.

One issue to consider is that the alpha frequency band (7.5 – 12.5 Hz), into which the SSR fell, may not easily be susceptible to tACS modulation. In particular, there may a task and baseline power dependence, such that tACS can only modulate alpha when endogenous alpha is low: phase coherence between tACS at individual alpha frequency and endogenous brain oscillations over occipital pole have been reported to increase only when participants had their eyes open (Ruhnau et al., 2016b). Also, Neuling et al. (2013) tried to entrain alpha power while participants had their eyes either open or closed. Again, when eyes were closed and endogenous alpha power was high, tACS

was unable to modulate it, possibly due to ceiling effects in the current densities: Neuling et al. (2012b) demonstrated that 417 μV/mm electric field can be induced with tACS over occipital regions; occipital alpha in awake monkeys has been estimated at 400 μV/mm (Bollimunta et al., 2008). When eyes are closed, alpha is expected to far exceed this value, hence there may not be enough tACS current strength available to modulate it. SSRs are known to be high in alpha power (Herrmann, 2001), especially in participants with already high endogenous alpha (Pigeau & Frame, 1992).

CHAPTER 4

cTBS to the right superior parietal cortex does not modulate dominance of multistable perception

1. Materials and method

1.1. Participants

20 healthy volunteers with normal or corrected to normal vision took part in the TMS experiments (mean age = 24.9 yrs ± 4.89 s.d., 15 female, 2 left-handed). All participants were screened to meet health guidelines for neurostimulation and gave written consent. The study was approved by the local ethics committee.

1.2 Visual stimuli and apparatus

All stimuli were presented on a 27 inch monitor (width = 602 mm, ASUS, Taiwan) operating at 144 Hz, on a grey background (half of maximum illumination). There was no natural light contamination nor room lighting. Participants' head position was fixed by a head and chin-rest. Binocular rivalry between two stimuli was created with a mirror stereoscope: Two stimuli were presented on the two sides of the screen separated by a board. The stereoscope then projected the images into the same retinal space of the participant. The mirrors were carefully adjusted for each participant to achieve fusion of the fixation cross and lines. The distance between monitor and participant through the stereoscope was 700 mm. All stimuli were created and controlled by a stimulus computer (Ubuntu 17.10) running Psychtoolbox 3 for Matlab R2014a (Mathworks, USA). Participants´ button press responses were collected with an adapted numeric keypad with eight buttons (two columns, four rows).

There were three visual stimuli: A structure from motion rotating sphere (SFM), checkerboard BR (checker) and random dot motion cloud BR (cloud) (*figure* 33).

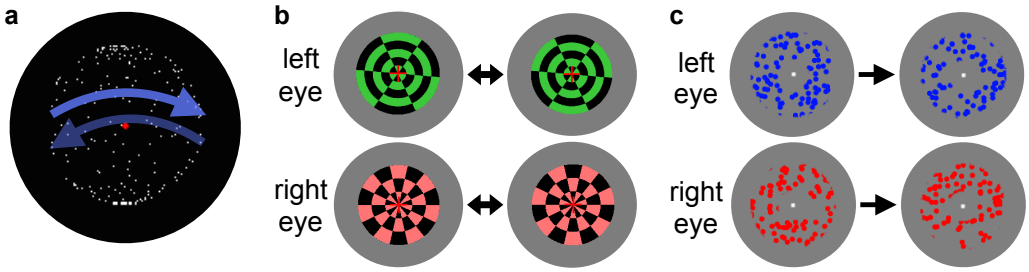

Figure 33 — Visual stimuli
(a) SFM Stimulus; 200 white dots on a black background moving coherently left and right to create the illusion of a rotating sphere, a red fixation dot at the centre. blue arrows indicate possible direction of movement. **(b)** Checker stimulus; two different circular checkerboards (green and red) presented separately to each eye in the the same retinal location, a red cross at their centre. Flickering emerges through alternating presentation of the circular checkerboard and its inverted image (left and right). **(c)** Cloud stimulus; 100 red or blue dots moving randomly within a circular patch with a white fixation dot at the centre (see change in dot location left to right).

1.2.1 SFM stimulus

The first stimulus was an ambiguous structure from motion rotating sphere. Dots moved horizontally back and forth within the boundary of a circle in a coherent fashion. All dots took the same amount of time to move from one end to the other, so that dots closer to the vertical midpoint of the stimulus moved faster. This created the illusion of a rotating sphere, which can be seen either rotating to the left or the right. The sphere moved at a pace where it took 3 seconds for dots to move once to either side and back to their starting position. The sphere had a central red fixation dot and was 1.25 dva in diameter. The dots were white on a black background. The sphere was surrounded by a grey (half of maximum illumination) and white frame to aid binocular fusion. The initial screen presented before the trial was comprised of the fusion aid in addition to a red fixation dot at its centre. Identical SFM spheres were presented to both eyes via the stereoscope, leading to a complete binocular match. The initial screen presented before the trial was comprised of the fusion aid in addition to a red fixation dot at its centre.

1.2.2 Checker stimulus

The second stimulus were two circular flickering checkerboards, one was black and green while the other was black and red. Each was presented to the same retinal space in each eye through the mirror stereoscope to create BR. The checkerboards were 1.25 dva in diameter in size and flickered at 7.2 Hz (red) and 9 Hz (green) respectively, where the flicker was created through alternating presentation of the circular checkerboard and its inverted image (Regan, 1966). Moreover, the checkerboards rotated clockwise (36 degrees per second). Around each checkerboard was a fusion aid, which was a black and white checkerboard frame with a width of 3 dva. The initial screen presented before the trial was comprised of the fusion aid in addition to a red fixation cross at its centre. The presentation eye of the checkerboards (i.e. which eye was presented with which checkerboard) was counterbalanced and determined randomly.

1.2.3 Cloud stimulus

The third stimulus were two apertures (inner radius = 0.15 dva, outer radius = 1.25 dva) of randomly moving dots (radius = 0.08 dva; density = 165 dva^2; speed = 5.7 dva /s). The stimulus was identical to the one used by Brascamp et al. (2016). The apertures were presented to to the same retinal space in each eye through the mirror stereoscope to create BR. Around each aperture was a fusion aid, which was a pattern of random white and black pixels within a square outline (3.5 dva across). At the centre of each aperture was a white fixation dot (radius = 0.025 dva, surrounded by a Gaussian radial falloff to background luminance, σ = 0.03 dva). Each aperture's dots had a

within-eye coherence of 0.4, i.e. 40% of dots moved in a single direction (signal dots), while the rest moved randomly (noise dots). Dot direction was reset in 300 ms intervals, where identity and movement direction all dots were randomly assigned, subject to signal dots in one eye moving at a direction ± 90° (randomly chosen) removed from the direction of the other eye's signal dots. All dots in a given eye were either red-tinted or blue-tinted. The luminance of both colour tints were approximately identical. The luminance of the maximum screen output of blue (1.393 cd/m2, through the mirror stereoscope) was used to obtain equivalent luminance levels for red and white by use of heterochromatic flicker photometry (HFC, Kaiser & Comerford, 1975). The colour tint was created by blending portions of either this red or blue with the equalised white. HFC yielded an average result of 112.5 ± 24.1 s.d., on a scale from 0 to 200, where 0 represents all blue and 200 all red.

1.3 Experimental design

Participants came to the lab on two separate occasions, at least 48 hours apart to prevent TMS carry over effects. During each occasion, the participant first completed an experimental session, followed by application of theta burst TMS to either ant-SPLr vertex (see section 2.5). The order of TMS sites was fully counterbalanced. Immediately after TMS application, participants completed another experimental session.

While cortical inhibition following Theta burst TMS has been observed in a window of time ranging up to 50 minutes post stimulation (Huang et al., 2005; Schindler et al., 2008), evidence also suggests that its effect might disperse much sooner (Nyffeler et al., 2006; Zafar et al., 2008; Zapallow et al., 2011), in the range of 16-30 minutes. To ensure that the entirety of the post-TMS experimental session lay within this window of opportunity, I chose a conservative session length of 24 minutes: Each experimental session consisted of 6 trials of 4 min of stimulus viewing. In each session, the three stimuli appeared twice: for the checker and cloud stimuli once with red in the left and right eye, respectively. The sequence was randomised.

In each trial, participants first initiated the trial at their own discretion with a button press. Then, they were instructed to fixate on the fixation aid the centre of the screen on press the left or right button depending on their percept. In case of the SFM stimulus, participants pressed right when the front face of the sphere appeared to be moving from left to right; in case of the checker and cloud stimuli, when the red coloured version was perceptually dominant. In case of perceptual mixtures, participants were asked to not press any button.

1.4 MRI Scan acquisition

MRI scans acquired using a 3T Siemens Prisma at the Max Planck Institute for Biological Cybernetics, Tübingen. For each participant, a T1-weighted ADNI sequence (TR = 2000 ms, TE = 3.06 ms, FOV = 232 x 256 x 192 mm, voxel size = 1 x 1 x 1 mm, matrix 232 x 256, Flip angle 9°, 192 sagittal plane slices, acquisition time 7 min 46 s) was used to obtain structural MR images.

1.5 TMS and neuronavigation

Participants were stimulated at an individual stimulation intensity, namely 90% of their resting motor threshold (RMT). To determine the RMT, participants were asked to relax their right hand with their lower arm resting on an armrest. At initially 25% maximal stimulation output, single pulses (frequency < 0.3 Hz) were delivered 2 cm anterior to left hemispheric central midline above the ear at a 45° coil angle relative to the ground while the coil shaft pointed directly downward. The coil was moved between pulses until a motor response in the contralateral hand was observable. Staying at that position with the coil, which marks the right hand representation of the primary motor cortex, stimulation intensity was adjusted until the pulses were just able to reliably evoke a motor response (6 out of 10 times). The mean RMT was 30.6 % ± 3.76 s.d. maximum stimulator output.

For the main experiment, TMS stimulation was a continuous theta burst protocol (Huang et al., 2005), consisting of bursts of three 50Hz TMS pulses, applied every 200 ms for 40 seconds (600 pulses in total). TMS pulses were delivered using a figure-of-eight coil (MC-B70) connected to a MagPro X100 stimulator (MagVenture). Participants did not consume alcohol in the 24 hrs prior to each experiment and were well rested (to avoid the risk of a lowered seizure threshold, Rossi et al., 2009).

On separate days, pulses were applied either to the anterior IPS (MNI: x = 36, y = -45, z = 51; see *figure* 34), or to the control site vertex. IPS was localised using standard MNI brain coordinates on the basis of each participant's anatomical MRI scan using the neuronavigation system LOCALITE with an tracking system using a Polaris infra-red camera (Northern Digital, Waterloo, Canada), by co-registering individual MR images with the participant's head to which surface markers were attached. The coil was held manually by the experimenter with its shaft pointing posterior/inferior at an angle of 45° to the floor. The distance between actual coil location and its optimal positioning was kept at less than 1.5 mm at all times during stimulation. The vertex was localised using externally visible anatomical landmarks. Using flexible measuring tape, the midpoint of the medial line on the scalp between nasion and inion was marked on the swim cap, which is directly superior to the vertex. For vertex stimulation the coil was held against the participant's scalp with its handle

pointing straight behind the participant, with the experimenter standing behind the participant and holding the coil parallel to the floor.

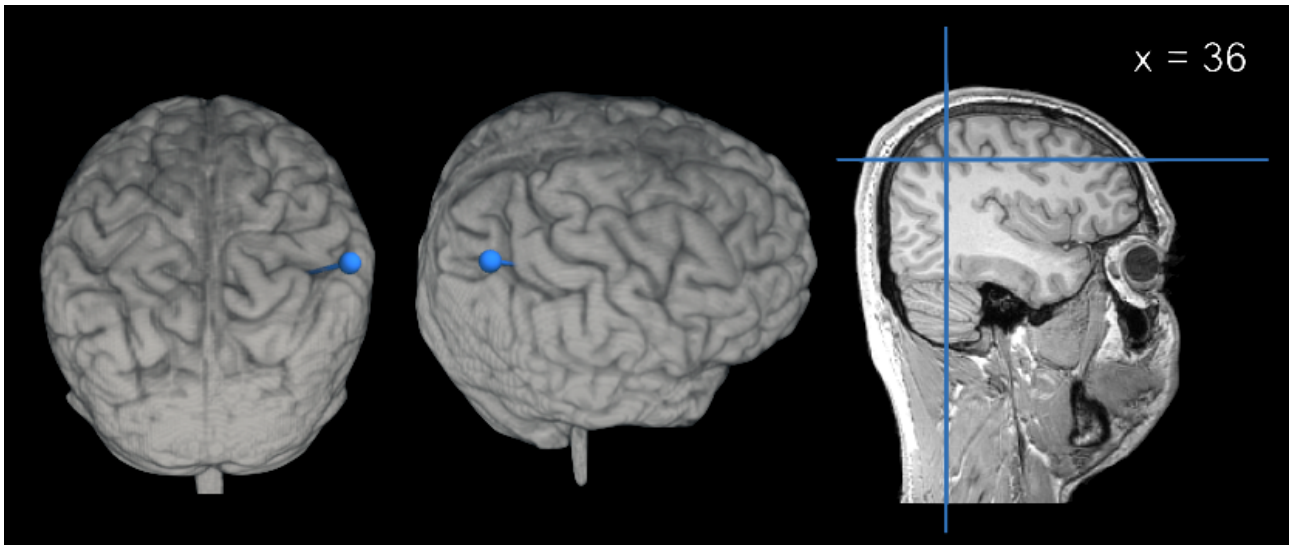

Figure 34 — TMS stimulation site IPS
The anterior intraparietal sulcus as shown on the T1-weighted brain scan of a representative participant at MNI coordinates x = 36, y = -45, z = 51. Blue dots and line in the left two images represent entry points for where the TMS coil was placed on the head.

1.6 Voxel-based morphometry

Based on the previous finding of a significant correlation between percept dominance durations and grey matter density using small volume correction over the anterior IPS (Kanai et al., 2011), I conducted an identical voxel-based morphometry analysis (VBM) over this sites using the T1-weighted structural MRI images of this study's participants. First, grey and white matter were segmented using the automated segmentation algorithms of the Matlab package SPM8 (http://www.fil.ion.ucl.ac.uk/spm), which was followed by inter-subject registration of only the gray matter images using the diffeomorphic anatomical registration through exponentiated lie algebra (DARTEL) function. The resulting images were smoothed with a Gaussian kernel of FWHM = 8 mm and then mapped onto the Montreal Neurological Institute (MNI) template. In a regression analysis over the whole brain, participants' gender and sex were included in the design matrix as covariates of no interest, and a family-wise error corrected alpha level of 0.05 was used to identify voxels which showed a significant correlation between percept durations and grey matter density. Next, given the strong theoretical support for a correlation at the specific region of interest IPS, another regression analysis was carried out predicting dominance durations from grey matter density over IPS using small volume correction with a sphere radius of 15 mm.

1.7 Behavioural data analysis

Our main measure of interest was the change BR dominance durations following TMS, found by comparing the behavioural results post-TMS to pre-TMS for each experimental day. The reason that I recorded a new baseline of performance each experimental day is to control for day to day variations in, for instance, arousal and attention, that may give rise to between-day performance differences. Any pre-post difference in behavioural performance for TMS to the vertex was assumed to reflect TMS site-unspecific effects on the brain and was subtracted from the difference in performance found for the other TMS sites to find the site-specific effect of parietal TMS on behavioural performance.

To obtain this measure, I first extracted rivalry dominance durations from the button presses of participants. We excluded button presses that were interrupted by the end of the trial and treated double button presses and no button presses as mixed percepts. We next visually investigated if the data followed previously reported gamma distributions (Levelt, 1967) for each participant and each condition separately. We used the median dominance in seconds as measure of central tendency for each participant in each condition calculated from the pooled dominance durations of the two trials that belonged to each condition. Then I checked if median dominance was abnormal (< 1 or > 10). Finally I entered median dominance as dependent variable into a repeated measures ANOVA, using TMS site and whether the session was pre or post TMS as well as stimulus type as factors.

Finally, I investigated how coherent the results were across the three stimuli. To that end, I correlated the baseline median dominance durations (obtained from a pool of all pre TMS rivalry recordings for each participant and stimulus separately) between the three stimuli. Last, I did the same with the percentage difference in dominance pre and post IPS stimulation.

2. Results

2.1 Behavioural data analysis

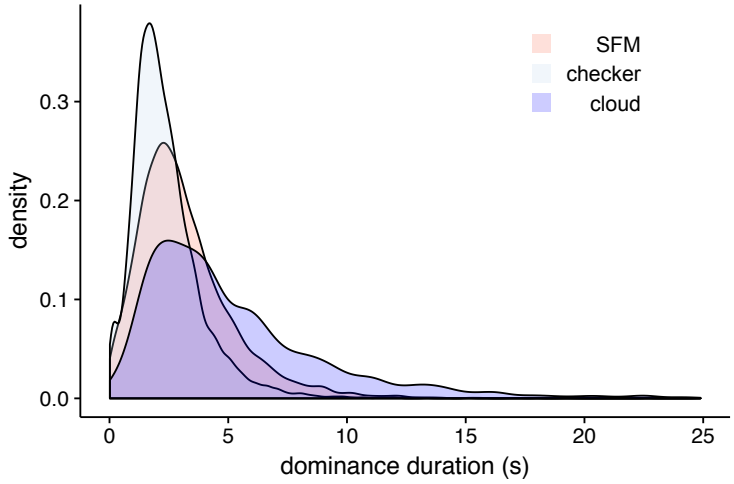

Figure 35 — Distributions of dominance durations
Binocular rivalry dominance durations density distribution pooled from all trials of all participants. Orange: SFM (shape = 2.28, scale = 0.72, pooled median dominance 2.76 s); grey: Checker (shape = 2.54, scale = 1.07, pooled median dominance 2.09 s); blue: Cloud (shape = 2.01, scale = 0.39, pooled median dominance 4.12 s).

The dominance durations pooled from all participants together followed a gamma distribution (*figure* 35). One participant, whose data was corrupted, needed to be excluded from the analysis. The average of the remaining participants' median dominance durations can be found in *table* 5.

Descriptive Statistics

Stimulus	Site	TMS	Dominance (s)	s.e.m.	% difference	s.e.m.
SFM	IPS	pre	3.11	0.21	7.02	4.60
SFM	IPS	post	3.36	0.29		
SFM	vertex	pre	2.88	0.17	7.85	2.98
SFM	vertex	post	3.08	0.17		
checker	IPS	pre	2.40	0.12	3.14	2.43
checker	IPS	post	2.50	0.15		
checker	vertex	pre	2.33	0.16	0.71	3.38
checker	vertex	post	2.34	0.13		
cloud	IPS	pre	5.21	0.44	-1.18	6.63
cloud	IPS	post	5.67	1.02		
cloud	vertex	pre	5.06	0.40	-2.25	4.32
cloud	vertex	post	4.97	0.51		

Table 5 — Descriptive statistics
For each stimulus, TMS site and TMS timing, the median dominance duration (s) ± 1 s.e.m. For each stimulus and TMS site, percent difference in median dominance post vs pre TMS ± 1 s.e.m, displayed in *figure* 37.

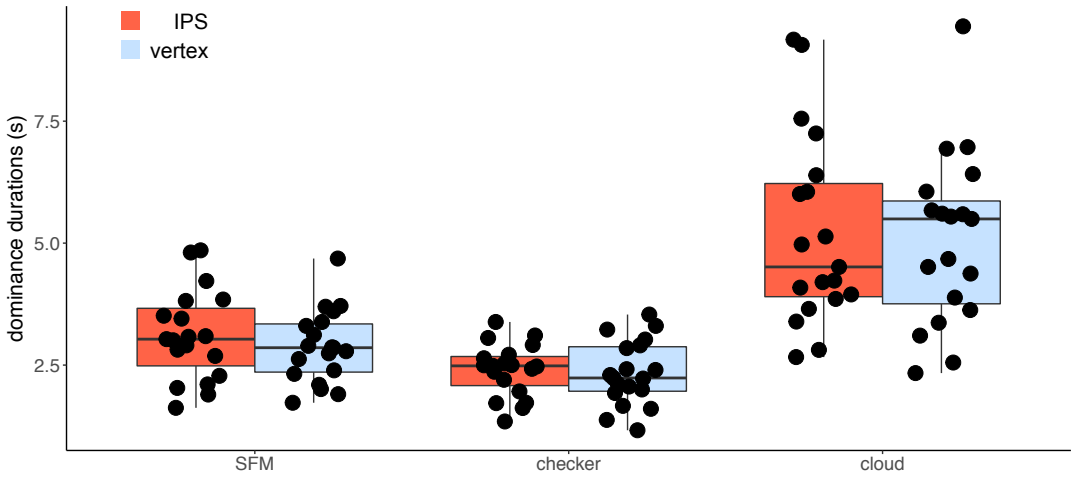

Figure 36 — Pre-TMS rivalry dominance across conditions
Each dot is a data point from one baseline recordings ordered by stimulus condition (SFM, checker, cloud) and TMS site (IPS, vertex) of one participant. IPS is red, vertex is blue.

Baseline rivalry durations across stimuli and days. As a first step I aimed to rule out differences in the baseline rivalry recordings that could later account for differences between the experimental conditions. To this end, I entered baseline rivalry median dominance as dependent variable into a repeated-measures ANOVA using TMS site and stimulus type as factors. Mauchly´s test indicated that the assumption of sphericity had been violated for the main effect of stimulus type ($\chi^2(2) = 16.22$, $p < 0.01$), therefore degrees of freedom were corrected using Greenhouse-Geisser estimates of sphericity ($\varepsilon = 0.65$). This was driven by the much larger variance of dominance durations in the cloud stimulus (*figure* 36). The ANOVA revealed a significant main effect of stimulus type ($F(2,36) = 49.38$, $p < 0.0001$), but not of TMS site ($F(1,18) = 2.12$, $p = 0.16$), nor an interaction term ($F(2,44) < 1$, *ns*). In essence, baseline recordings across the two days when participants came to the lab, were not significantly different, indicating similar baseline levels of arousal as well as stability in how participants view the stimuli over time. The different stimuli bing forward different dominance durations, which is however not surprising, since dominance is in large determined by low-level stimulus properties, such as contrast (Hollins, 1980), movement (Fox & Check, 1968), or colour (Levelt, 1965), all of which differed between the stimuli (see also Blake, 1989; Logothetis et al., 1996; Tong et al., 2006).

Correlation of individual dominance durations across stimuli. Next, I tested if the dominance durations of the three stimuli correlated with one another, i.e. if a participant with longer dominance in one stimulus was expected to have longer dominance in the other stimuli as well. To this end, I performed three correlation analyses and found positive significant correlations between baseline dominance durations of checker and cloud ($r = 0.69$, $p = 0.001$), checker and SFM ($r = 0.61$, $p = 0.006$), as well as SFM and cloud ($r = 0.53$, $p = 0.019$) (*figure* 38 bottom). These

results show that there is a strong contribution of individual idiosyncrasies, in that if one individual has long dominance durations in one stimulus this is predictive also for the other two stimuli.

Effect of TMS. Next, I performed the main analysis, which consisted in testing if there are differences between TMS site and stimulus type in the percentage difference between pre and post TMS recordings, or, if the effect of TMS is different for IPS compared to vertex, as well as consistent across stimulus types. To that end, I entered the percentage difference between pre and post TMS recordings for each stimulus as dependent variable into a repeated-measures ANOVA using TMS site and stimulus type as factors. We found that there was neither a significant main effect of TMS site ($F(1,18) < 1$, *ns*), stimulus type ($F(2,36) = 1.99$, $p = 0.15$), nor a significant interaction between the two factors ($F(2,36) < 1$, *ns*) (*figure* 37).

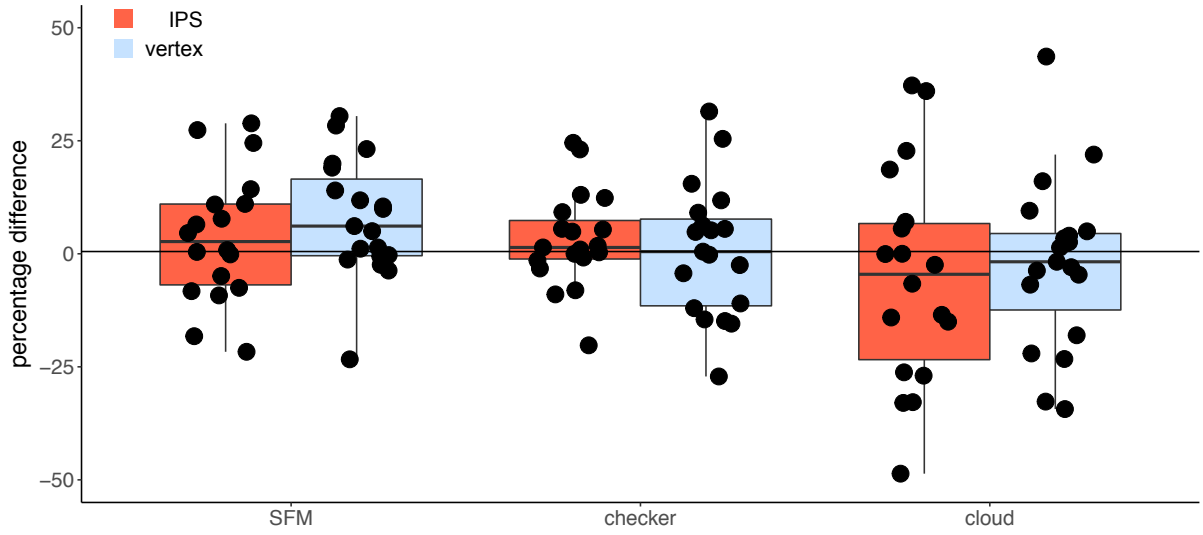

Figure 37 — Percentage difference in rivalry dominance pre vs post TMS across conditions
Each dot is a data point from one difference pre vs post TMS ordered by stimulus condition (SFM, checker, cloud) and TMS site (IPS, vertex) of one participant. IPS is red, vertex is blue.

Bayesian evidence for the null hypothesis. Since the absence of an effect is not evidence in favour of the null hypothesis (H0), I used Bayesian statistics to ascertain how strong the above null results are. Using the BayesFactor package (0.9.2) for R64, I modelled a Bayesian ANOVA using the theoretical background put forward by Rouder et al. (2012). We computed a Bayes Factor (BF) for each main effect factors and the interaction against the null hypothesis that all effects are 0. The analysis resulted in a BF of 0.57 (inconclusive evidence for H0) for the main effect of stimulus type, a BF of 0.2 (substantial evidence for H0) for main effect of TMS site, and a BF of 0.02 (strong evidence for H0) for the interaction term (Kass & Raftery, 1995). This provides overall strong evidence that TMS to the IPS did not affect rivalry compared to the control site vertex, nor that TMS differentially affected rivalry dependent on the stimulus. While the BF for this hypothesis

is inconclusive, I believe that is was driven entirely by the larger variance in the dominance durations of the cloud stimulus rather than a TMS effect.

Correlation of individual TMS effects across stimuli. Finally, I attempted to correlate the percentage difference in dominance after TMS vertex compared to IPS between the stimuli. If there were correlations, it would entail that although TMS did not produce an overall effect, its effect would still be consistent across stimuli. However, I were unable to find such relationships between the stimuli. Specifically, there was no significant correlation between the percentage difference of checker and cloud (r = 0.15, p = 0.54), checker and SFM (r = -0.15, p = 0.55), as well as SFM and cloud (r = -0.29, p = 0.23) (*figure* 38 top).

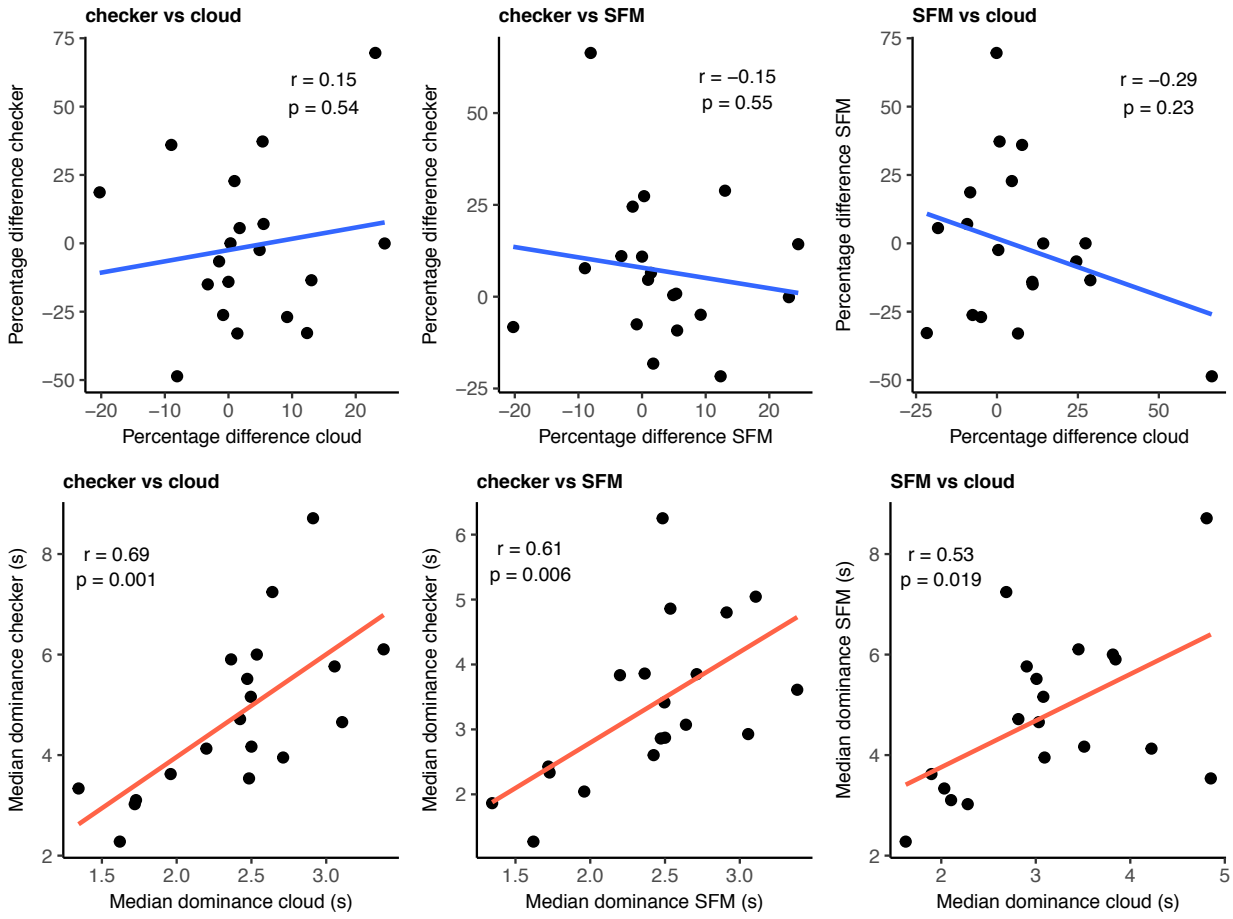

Figure 38 — Correlations between stimuli
top) Correlation between the percentage difference in dominance pre vs post TMS in one stimulus compared to another. Each data point is the difference in one participant. **bottom)** Correlation between the baseline dominance in one stimulus compared to another. Each data point is the median dominance of one participant.

2.2 Voxel-based morphometry

No positive or negative correlation between percept dominance durations and grey matter density reached statistical significance following correction for multiple comparisons across the whole brain. Even without correction and using a liberal significance threshold of $p < 0.05$ the IPS showed no significant correlation. Alas, also analysis of the IPS as ROIs using small volume correction revealed no significant correlation. Hence, the VBM findings in Kanai (et al., 2010, 2011) could not be replicated. However, at a sample size of 19, this is not surprising since VBM studies usually require substantial larger sample sizes to yield significant results. Also, a null result in orthodox statistics does not lend support to the hypothesis that no correlation exists. Instead, the absence os a statistically significant result is likely due to a lack of power.

3. Discussion

In this study, I attempted to resolve the conflicting results previously observed in the TMS literature on the causal causal role of the IPS in bistable perception and BR. In the past, cTBS to the IPS has led shortenings or lengthenings of bistable dominance durations depending on stimulus properties (Kanai et al., 2011; Zaretskaya et al., 2013; also chapters 1 & 2). We aimed to see if this stimulus dependence of cTBS could be replicated, or alternatively if the cTBS effect would be consistent across stimuli reflecting inter-subject variability in response to TMS.

Neither hypothesis could be confirmed. We observed no stimulus dependence in the cTBS effect nor did parietal stimulation significantly affect SFM or BR dominance compared to vertex control. This null effect was consistent across stimuli and was supported by Bayes factors. As could be expected, the baseline dominance durations of each stimulus correlated with one another, showing perceptual consistency within subjects, such that participants with more stable perception in one stimulus will demonstrate more perceptual stability in the others. Whether this stability is driven by IPS activity or hindered by it remains unclear as I observed no cTBS effect in either direction. We are confident in the validity of this null effect since not only did I observe neither a shortening nor lengthening of dominance, but the direction of the cTBS effect also did correlate across stimuli within participants. This means that the null was not due to a parcellation in this sample, where some participants reacted to cTBS with a shortening while others with the opposite effect, leading to an overall null. In essence, cTBS did neither consistently affect stimuli nor participants. Finally, I failed to replicate the VBM results reported by Kanai et al. (2011), which however is unsurprising given my sample size, which falls short of the requirements for VBM.

3.1 Lack of cTBS effect

Several explanations could account for these null results. First, it may just be that the behavioural tasks were not sensitive enough to pick up changes in cTBS induced cognitive function. Also, it may be that cTBS led to mere site-unspecific changes in arousal (Carter et al., 2007), obscuring the parietal effect. However, this I controlled for by utilising vertex as control site. Perhaps TMS only induced a response bias, leading to a more conservative criterion for what constitutes dominance. In this case though I would have expected to see an changes in the mixed percept durations, which I did not.

What I believe to be most likely is alas that I failed to replicate previous results due to a lack of an actual effect. Previous studies suffered from small samples and weak effect sizes (Carmel et al., 2010: N = 6; Kanai et al., 2010: N = 12; Zaretskaya et al., 2010: N = 15; Zaretskaya et al., 2013: N = 18; Kanai et al., 2011: N = 8; Wood et al., in preparation: N(experiment 1) = 17, N(experiment 2)

= 19). Given the knowledge that's some cTBS results remained unpublished due to their lack of significant effects, I am forced to wonder if previously published results merely represent two tails of a distribution around zero. In the future, a meta analysis could elucidate this. The confusion in the literature as to whether rivalry dominance is prolonged or shortened by TMS may therefore be absolved by the hypothesis that it is in fact neither. Tentative evidence in favour of this assertion comes from my previous work (*chapter* 1). Here I were able to show a significant lengthening of SFM dominance durations following IPS cTBS compared to vertex. However, the behavioural effect was not accompanied by any significant change in BOLD activation or brain network connectivity. Hence, the behavioural effect may have been a fluke without any brain substrate. Moreover, when I previously observed a behavioural null effect of IPS cTBS on perception of the clouds stimulus (*chapter* 2), I tried to verify if cTBS has had the expected inhibitory effect by stimulating primary motor cortex (M1) and measuring motor evoked potentials (MEPs). While cTBS was able to modulate MBP amplitude, this cTBS effect on MEPs did not correlate with the cTBS effect on bistable perception. Already then, this raised the question of how reliable inhibitory parietal cTBS is, where contrary to the motor cortex I have no experimental way of verifying that cortical inhibition took place. Overall, this casts a dark shadow over the cTBS literature on bistable perception.

We must concede, that this does not entail that cTBS does not have an inhibitory effect. For instance, it may be possible that individual differences in parietal anatomy may obscure any effect. Depending on how deeply the specific subsection of the IPS involved in perceptual ambiguity lies within the sulcus, the cortical tissue may have different properties that affect how TMS is able to modulate it. However, I do not believe this likely, since I would still have expected to see correlations between the direction of the cTBS effect between stimuli. We therefore must tentatively conclude that IPS cTBS does not effect parietal cortex in an inhibitory fashion and hence does not systematically modulate bistable perception. Therefore, parietal cTBS cannot demonstrate a causal role of the parietal cortex in resolving perceptual ambiguity.

3.2 Differences in TMS protocol

We must forcefully point out that this conclusion only applies to cTBS. Other inhibitory TMS protocols, such as on-rTMS as was used by Zaretskaya et al. (2010), maybe more apt to elucidate the causal role of the IPS by directly injecting noise into the system while it operates. Also fruitful is the combination of TMS with other neuroimaging techniques. For instance, Schauer et al. (2016a) recorded EEG while applying single pulse TMS to IPS as well as posterior parietal cortex , all while participants viewed SFM or replay. However, also they were not able to show any

behavioural effect of TMS nor systematic difference in the EEG response to TMS depending on the brain's state. Since their study was constrained by some methodological issues, their results should not be viewed as conclusive. One further alternative would be to combine fMRI with online TMS (see for instance Ruff et al., 2006). This setup might elucidate how TMS affects parietal function at specific moments during the processes that govern perceptual reversals.

CONCLUSION

1. Accounts for parietal involvement in multistability

The question remains what the causal role of the parietal cortex in multistability is. Zaretskaya et al. (2010) suggested that IPS is involved in destabilising the percept, since interfering with its function led to greater perceptual stability. Evidence for this assertion also comes from neglect patients, who display longer dominance durations following lesions to the posterior parietal cortex, further indicating that parietal areas are involved in bringing about perceptual reversals. (Bonneh et al., 2004). A larger theoretical framework, within which the parietal involvement in multistability is often interpreted is predictive processing (Kanai et al., 2010, 2011; Megumi et al., 2015; Zaretskaya et al., 2010; Wood et al., in prep; Watanabe et al., 2014; Schauer et al. 2016a, 2016b; Brascamp et al., 2018). According to this theory, different layers of the visual architecture form part of a hierarchical Bayesian network that computes the likelihood of sensory signals by comparing perceptual predictions to error signals. Higher cortical regions are meant to be involved in generating these perceptual predictions that are constantly checked against error signals coming from lower perceptual regions (Friston, 2005; Hohwy et al. 2008). The parietal cortex could now serve as a gateway where feedforward and feedback signals are compared to one another. A shortening or lengthening of dominance following inhibitory stimulation of parietal cortex would then speak in favour of having disrupted predictions or error signals.

An alternate account lends itself from the anatomical overlap of IPS to regions closely associated with attention, as well as the functional similarity of perceptual selection and spatially shifting attention, making a shared mechanism for both likely (Slotnick et al. 2005; Corbetta, et al., 1995; Yantis et al., 2002; Serences et al., 2004). Parietal lesions are associated with impaired attentional function (Hilgetag et al., 2001; Hodsoll et al., 2009; Malhotra et al., 2009; Rueckert & Grafman, 1998; Rushworth & Taylor, 2006; Thut et al., 2005). Parietal TMS has similarly led to modulations in stimulus change detection (Beck et al., 2005), feature-based attention (Schenkluhn et al., 2008), spatial attention (Bressler et al., 2008) and pseudoneglect (Bjoertomt et al., 2002; Fierro et al., 2000; Hilgetag et al., 2001). Moreover, rivalry dominance durations are largely influenced by the allocation of attention to the stimulus (Alais et al., 2010; Paffen et al., 2006; Pastukhov & Braun, 2007). For instance, Bahrami et al. (2007) could modulate the activity in V1 pertaining to the suppressed BR stimulus depending on the intensity of a peripheral attention task. Behaviourally, diverting attention from a BR stimulus also lengthens its dominance (Paffen & Alais, 2011), an effect that linearly increases with the difficulty of the attention task (Paffen et al., 2006), to the extent that completely diverting attention from a rivalry stimulus leads to the seizure of BR (Brascamp & Blake, 2012). Hence, TMS interference with sustained attention could lead to a shortening, whereas interference with attentional shifting a lengthening of bistable dominance. Schauer et al. (2016b)

tested this hypothesis by applying cTBS to the IPS and probing attentional tasks, but were not able to find any effect, and were hence unable to endorse this account.

One assumption inherent to both frameworks is that IPS has a singular function. This critically precludes the possibility of differential parietal function contingent on the observer's perceptual state. It may be that just prior or after a multistable perceptual reversal, the computations taking place in parietal cortex take different form. A paradigm like cTBS, which is meant to globally inhibit cortical function of a certain area, will be unable to successfully distinguish these. More fine-grained online stimulation techniques such as single pulse TMS, that can be used to probe parietal cortex at specific times during perception, may prove to be able to overcome this constraint.

2. Chapter-wise conclusions

Taken together, the results presented in *chapter 1* demonstrate the importance of brain networks involving the IPS in the resolution of perceptual bistability. In the past, the literature had been split between two viewpoints: According to one view, the resolution of bistability was believed to occur in V1, then carried feed-forward to higher brain regions, whose activation is a mere consequence of early activity (Knapen et al., 2011), especially since bistability occurs in the absence of consciousness and parietal activity (Brascamp et al., 2015; Zou et al., 2016). Another view posits that IPS is involved in (de)stabilisation of bistability though feedback connections (Carmel et al., 2010; Zaretskaya et al., 2010; Kanai et al., 2010, 2011), since TMS stimulation leads to changes in perception. The results of *chapter 1* instead point to the IPS acting as gateway between higher-level brain areas coding predictions and low-level error-coding regions.

Chapter 2 turned to the role of parietal cortex in unreported and unreportable BR. This was motivated by the previous use of multistable perception as paradigm to uncover the NCC. This venture is subject to a number of pitfalls (Blake et al., 2014). Most prominently, it is conceptually uncertain if the assertion is true, that BR consists of an unchanging stimulus giving rise to a change in consciousness. Whether the stimulus is actually invariant is disputable. For instance, specific microsaccades arise alongside BR (Sabrin & Kertesz, 1980), as do pupil dilations prior (Einhäuser et al., 2008) and during perceptual reversals (Naber et al., 2011). Moreover, consequences of consciousness, such as motor-report could lead to an overestimation of the NCC by including the neural correlates of motor-planning and execution. To overcome this, *chapter 2* employed a no-report paradigm. The criticism aside that no-report paradigms are still not free of introspection (Overgaard & Fazekas, 2016), the presented null results were alas not able to elucidate further the role of IPS and SPL activity as candidates for the NCC.

More drastically still, cTBS could turn out to be altogether ineffectual over parietal cortex. The lack of correlation between the cTBS effect over M1 and IPS or SPL observed in *chapter 2*, together with the lack of any cTBS effect over parietal cortex in *chapter 4*, is indicative hereof.

Another candidate for the NCC are SSRs, which were investigated in *chapter 3*, where again only null effects were observed. One account for the absence of perceptual effects of tACS in *chapter 3* could be that the SSR amplitude was too large to be effectively modulated by tACS. Without this modulation, there naturally would not be a behavioural effect. Since my results did not demonstrate a causal role of the SSR in conscious perception, the question of its efficacy remains elusive. Also neural oscillations in the gamma band, that have been associated to BR (Engel et al., 2001), have been modulated by tACS to also affect perception by disturbing inter-hemispheric phase coherence by use of two tACS montages, one on each hemisphere (Strüber et al., 2013). This leads to another issue that must be addressed: if endogenous alpha has already some causal role, then modulating an alpha based SSR through tACS will by necessity also modulate endogenous alpha. Hence, with any effect, I cannot be sure if what I observe is due to a modulation of endogenous alpha or the SSR, since brain oscillations are not independent of the signal designed to probe them (Keitel et al., 2014). In the worst case, both might have opposing effects that cancel each other out. In summary, it is hence still doubtful if SSRs have a causal role in visual perception. Future studies should record EEG data concurrently with tACS in order to test whether SSRs are actually modulated while perceptual measures are taken. Given the large inter-subject variability observed with tACS, this would also allow investigating if EEG parameters predict the direction and strength of the tACS effect. For now, I tentatively conclude that the SSR merely correlates with the content of visual consciousness, however, its modulation does not affect it.

3. Closing remarks

In conclusion, the role of parietal cortex in multistable perception remains unclear. cTBS has not successfully been used to elucidate this role. This is due to it likely not having any effect at all. I provocatively suggest that previous publications using cTBS in bistable perception and BR only reported chance effects due to small samples and effect sizes.

Further research should decisively address criticisms that have been part of the recent plea against the replicability crisis (Cumming, 2014) to ensure the validity of neurostimulation results. Since the unpredictable fluctuation of perception during BR necessitates dynamic neural processes (Blake et al., 2014), further research should moreover concentrate on online TMS methods that can directly probe parietal activity at the time it is most relevant (for instance Vernet et al., 2016) as well as combinations of TMS with neuroimaging techniques (Ruff et al., 2006).

Moreover, the neural substrate of multistable perception is likely timing dependent with rapid modulations in parietal cortex during perceptual reversals paired with gradual changes during stability (Brascamp et al., 2018). Hence, it is fallacious to assume that the neural processes that initiate perpetual reversals must also immediately precede them, as modelling approaches have indicated the importance of both rapid neural processes around the time of switches combined with gradual changes during dominance periods (Brascamp et al., 2018). cTBS cannot address this critique adequately since it is meant to affect a cortical area for the entire duration of a trial. Since cTBS affects cortical function for minutes following stimulation rather than during specific points of parietal activity, its use could turn out to be a *tour-de-force*, where multiple distinct cognitive processes that occur in temporal succession in SPL, IPS, MT, V1 and thalamus are affected all at once, hence yielding a compounded view of their respective activity. For instance, if parietal cortex is involved both in percept maintenance and destabilisation at different points in time, then cTBS inhibition would affect both and my fMRI results would be indicative of a composite of these processes. In the future, it would be more advantageous to use single pulse TMS instead of cTBS to approach this question and disentangle the various cognitive processes subserved by parietal cortex in multistable perception.

REFERENCES

Alais, D., van Boxtel, J. J., Parker, A., & van Ee, R. (2010). Attending to auditory signals slows visual alternations in binocular rivalry. *Vision Research, 50*(10), 929–935.

Amedi, A., Malach, R., & Pascual-Leone, A. (2005). Negative BOLD differentiates visual imagery and perception. *Neuron*, *48*(5), 859-872.

Andersen, S. K., & Müller, M. M. (2015). Driving steady-state visual evoked potentials at arbitrary frequencies using temporal interpolation of stimulus presentation. *BMC Neuroscience, 16*(1), 95.

Andersen, S. K., Hillyard, S. A., & Müller, M. M. (2013). Global facilitation of attended features is obligatory and restricts divided attention. *Journal of Neuroscience, 33*(46), 18200-18207.

Andersen, S. K., Müller, M. M., & Hillyard, S. A. (2011). Tracking the allocation of attention in visual scenes with steady-state evoked potentials. *Cognitive Neuroscience of Attention, 2*, 197-216.

Andersen, S. K., Müller, M. M., & Hillyard, S. A. (2015). Attentional selection of feature conjunctions is accomplished by parallel and independent selection of single features. *Journal of Neuroscience, 35*(27), 9912-9919.

Antal, A., & Paulus, W. (2013). Transcranial alternating current stimulation (tACS). *Frontiers in Human Neuroscience, 7*.

Aru, J., Bachmann, T., Singer, W., & Melloni, L. (2012). Distilling the neural correlates of consciousness. *Neuroscience & Biobehavioral Reviews, 36*(2), 737-746.

Bahrami, B., Lavie, N., & Rees, G. (2007). Attentional load modulates responses of human primary visual cortex to invisible stimuli. *Current Biology*, *17*(6), 509-513.

Baker, D. H., Karapanagiotidis, T., Coggan, D. D., Wailes-Newson, K., & Smallwood, J. (2015). Brain networks underlying bistable perception. *NeuroImage, 119*, 229-234.

Bartels, A., & Logothetis, N. K. (2010). Binocular rivalry: a time dependence of eye and stimulus contributions. *Journal of Vision, 10*(12), 3-3.

Battleday, R. M., Muller, T., Clayton, M. S., & Kadosh, R. C. (2014). Mapping the mechanisms of transcranial alternating current stimulation: a pathway from network effects to cognition. *Frontiers in Psychiatry, 5*.

Beck, D. M., Muggleton, N., Walsh, V., & Lavie, N. (2005). Right parietal cortex plays a critical role in change blindness. *Cerebral Cortex, 16*(5), 712-717.

Beer A. L. Watanabe T. Ni R. Sasaki Y. Andersen G. J . (2009). 3D surface perception from motion involves a temporal-parietal network. *European Journal of Neuroscience, 30*, 703–713

Bjoertomt, O., Cowey, A., & Walsh, V. (2002). Spatial neglect in near and far space investigated by repetitive transcranial magnetic stimulation. *Brain, 125*(9), 2012–2022.

Blake, R. (1989). A neural theory of binocular rivalry. *Psychological review, 96*(1), 145.

Blake, R., & Logothetis, N. K. (2002). Visual competition. *Nature Reviews Neuroscience, 3*(1), 13-21.

Blake, R., Brascamp, J., & Heeger, D. J. (2014). Can binocular rivalry reveal neural correlates of consciousness?. *Philosophical Transactions of the Royal Society B: Biological Sciences, 369*(1641), 20130211.

Blankenburg, F., Ruff, C. C., Bestmann, S., Bjoertomt, O., Eshel, N., Josephs, O., ... & Driver, J. (2008). Interhemispheric effect of parietal TMS on somatosensory response confirmed directly with concurrent TMS–fMRI. *Journal of Neuroscience, 28*(49), 13202-13208.

Blankenburg, F., Ruff, C. C., Bestmann, S., Bjoertomt, O., Josephs, O., Deichmann, R., & Driver, J. (2010). Studying the role of human parietal cortex in visuospatial attention with concurrent TMS–fMRI. *Cerebral Cortex, 20*(11), 2702-2711.

Bollimunta, A., Chen, Y., Schroeder, C. E., & Ding, M. (2008). Neuronal mechanisms of cortical alpha oscillations in awake-behaving macaques. *Journal of Neuroscience, 28*(40), 9976-9988.

Bonneh, Y. S., Pavlovskaya, M., Ring, H., & Soroker, N. (2004). Abnormal binocular rivalry in unilateral neglect: evidence for a non-spatial mechanism of extinction. *Neuroreport, 15*(3), 473-477.

Bor, D., & Seth, A. K. (2012). Consciousness and the prefrontal parietal network: insights from attention, working memory, and chunking. *Frontiers in Psychology, 3*, 63.

Bradley, D. C., Chang, G. C., & Andersen, R. A. (1998). Encoding of three-dimensional structure-from-motion by primate area MT neurons. *Nature, 392*(6677), 714.

Brascamp, J. W., & Blake, R. (2012). Inattention abolishes binocular rivalry: perceptual evidence. *Psychological Science, 23*(10), 1159-1167.

Brascamp, J., Blake, R., & Knapen, T. (2015). Negligible fronto-parietal BOLD activity accompanying unreportable switches in bistable perception. *Nature Neuroscience, 18*, 1672–1678.

Brascamp, J., Sterzer, P., Blake, R., & Knapen, T. (2018). Multistable Perception and the Role of the Frontoparietal Cortex in Perceptual Inference. *Annual Review of Psychology, 69*, 77-103.

Bressler, S. L., Tang, W., Sylvester, C. M., Shulman, G. L., & Corbetta, M. (2008). Top-down control of human visual cortex by frontal and parietal cortex in anticipatory visual spatial attention. *Journal of Neuroscience, 28*(40), 10056-10061.

Brignani, D., Ruzzoli, M., Mauri, P., & Miniussi, C. (2013). Is transcranial alternating current stimulation effective in modulating brain oscillations?. *PloS one, 8*(2), e56589.

Brodt, S., Pöhlchen, D., Flanagin, V. L., Glasauer, S., Gais, S., & Schönauer, M. (2016). Rapid and independent memory formation in the parietal cortex. *Proceedings of the National Academy of Sciences, 113*(46), 13251-13256.

Brouwer, G. J., & van Ee, R. (2007). Visual cortex allows prediction of perceptual states during ambiguous structure-from-motion. *Journal of Neuroscience, 27*(5), 1015-1023.

Brown, R. J., & Norcia, A. M. (1997). A method for investigating binocular rivalry in real-time with the steady-state VEP. *Vision research, 37*(17), 2401-2408.

Buckthought, A., Fesi, J. D., Kirsch, L. E., & Mendola, J. D. (2015). Comparison of stimulus rivalry to binocular rivalry with functional magnetic resonance imaging. *Journal of Vision, 15*(14), 2-2.

Busch, N. A., Dubois, J., & VanRullen, R. (2009). The phase of ongoing EEG oscillations predicts visual perception. *Journal of Neuroscience, 29*(24), 7869-7876.

Capilla, A., Pazo-Alvarez, P., Darriba, A., Campo, P., & Gross, J. (2011). Steady-state visual evoked potentials can be explained by temporal superposition of transient event-related responses. *PloS one, 6*(1), e14543.

Carmel, D., Walsh, V., Lavie, N., & Rees, G. (2010). Right parietal TMS shortens dominance durations in binocular rivalry. *Current Biology, 20*(18), R799-R800.

Carter, O. L., Hasler, F., Pettigrew, J. D., Wallis, G. M., Liu, G. B., & Vollenweider, F. X. (2007). Psilocybin links binocular rivalry switch rate to attention and subjective arousal levels in humans. *Psychopharmacology, 195*(3), 415-424.

Casagrande, V. A., Sary, G., Royal, D., & Ruiz, O. (2005). On the impact of attention and motor planning on the lateral geniculate nucleus. *Progress in Brain Research, 149*, 11-29.

Casula, E. P., Tarantino, V., Basso, D., Arcara, G., Marino, G., Toffolo, G. M., ... & Bisiacchi, P. S. (2014). Low-frequency rTMS inhibitory effects in the primary motor cortex: Insights from TMS-evoked potentials. *Neuroimage, 98*, 225-232.

Clark, A. (2013). Whatever next? Predictive brains, situated agents, and the future of cognitive science. *Behavioral and Brain sciences, 36*(03), 181-204.

Contini, M., Baccarini, M., Borra, E., Gerbella, M., Rozzi, S., & Luppino, G. (2010). Thalamic projections to the macaque caudal ventrolateral prefrontal areas 45A and 45B. *European Journal of Neuroscience, 32*(8), 1337-1353.

Corbetta, M., & Shulman, G. L. (2002). Control of goal-directed and stimulus-driven attention in the brain. *Nature Reviews Neuroscience, 3*(3), 201.

Corbetta, M., Shulman, G. L., Miezin, F. M., & Petersen, S. E. (1995). Superior parietal cortex activation during spatial attention shifts and visual feature conjunction. *Science, 270*(5237), 802-805.

Cumming, G. (2014). The new statistics: Why and how. *Psychological Science, 25*(1), 7-29.

Crick, F., & Koch, C. (1995). Are we aware of neural activity in primary visual cortex?. *Nature*, *375*(6527), 121-123.

Day, B. L., Dressler, D., Maertens de Noordhout, A., Marsden, C. D., Nakashima, K., Rothwell, J. C., & Thompson, P. D. (1989). Electric and magnetic stimulation of human motor cortex: surface EMG and single motor unit responses. *The Journal of Physiology, 412*(1), 449-473.

De Graaf, T. A., Hsieh, P. J., & Sack, A. T. (2012). The 'correlates' in neural correlates of consciousness. *Neuroscience & Biobehavioral Reviews, 36*(1), 191-197.

Di Russo, F., Pitzalis, S., Aprile, T., Spitoni, G., Patria, F., Stella, A., & Hillyard, S. A. (2007). Spatiotemporal analysis of the cortical sources of the steady-state visual evoked potential. *Human Brain Mapping, 28*(4), 323-334.

Ding, J., Sperling, G., & Srinivasan, R. (2005). Attentional modulation of SSVEP power depends on the network tagged by the flicker frequency. *Cerebral Cortex, 16*(7), 1016-1029.

Dodd, J. V., Krug, K., Cumming, B. G., & Parker, A. J. (2001). Perceptually bistable three-dimensional figures evoke high choice probabilities in cortical area MT. *Journal of Neuroscience, 21*(13), 4809-4821.

Dogge, M., Gayet, S., Custers, R., & Aarts, H. (2018). The influence of action-effect anticipation on bistable perception: differences between onset rivalry and ambiguous motion. *Neuroscience of Consciousness, 2018*(1), niy004.

Driver, J., Vuilleumier, P., & Husain, M. (2004). Spatial neglect and extinction. In M. J. Gazzaniga (Ed.) *The new cognitive neurosciences* (pp. 589 - 606). Cambridge MA, MIT Press.

Dumoulin, S. O., Bittar, R. G., Kabani, N. J., Baker Jr, C. L., Le Goualher, G., Pike, G. B., & Evans, A. C. (2000). A new anatomical landmark for reliable identification of human area V5/MT: a quantitative analysis of sulcal patterning. *Cerebral Cortex, 10*(5), 454-463.

Eickhoff, S. B., Stephan, K. E., Mohlberg, H., Grefkes, C., Fink, G. R., Amunts, K., & Zilles, K. (2005). A new SPM toolbox for combining probabilistic cytoarchitectonic maps and functional imaging data. *Neuroimage, 25*(4), 1325-1335.

Einhäuser, W., Stout, J., Koch, C., & Carter, O. (2008). Pupil dilation reflects perceptual selection and predicts subsequent stability in perceptual rivalry. *Proceedings of the National Academy of Sciences*, *105*(5), 1704-1709.

Engel, A. K., Fries, P., & Singer, W. (2001). Dynamic predictions: oscillations and synchrony in top–down processing. *Nature Reviews Neuroscience, 2*(10), 704-716.

Fang, F., Kersten, D., & Murray, S. O. (2008). Perceptual grouping and inverse fMRI activity patterns in human visual cortex. *Journal of Vision, 8*(7), 2-2.

Fierro, B., Brighina, F., Oliveri, M., Piazza, A., La Bua, V., Buffa, D., & Bisiach, E. (2000). Contralateral neglect induced by right posterior parietal rTMS in healthy subjects. *Neuroreport, 11*(7), 1519–1521.

Fitzgerald, P. B., Fountain, S., & Daskalakis, Z. J. (2006). A comprehensive review of the effects of rTMS on motor cortical excitability and inhibition. *Clinical Neurophysiology, 117*(12), 2584-2596.

Fleming, S. M., & Lau, H. C. (2014). How to measure metacognition. *Frontiers in Human Neuroscience, 8*.

Fox, R., & Check, R. (1968). Detection of motion during binocular rivalry suppression. *Journal of Experimental Psychology, 78*(3p1), 388.

Friston, K. (2005). A theory of cortical responses. *Philosophical Transactions of the Royal Society of London B: Biological Sciences, 360*(1456), 815-836.

Frässle, S., Sommer, J., Jansen, A., Naber, M., & Einhäuser, W. (2014). Binocular rivalry: frontal activity relates to introspection and action but not to perception. *Journal of Neuroscience, 34*(5), 1738-1747.

Giles, N., Lau, H., & Odegaard, B. (2016). What type of awareness does binocular rivalry assess?. *Trends in Cognitive Sciences, 20*(10), 719-720.

Grassi, P. R., Zaretskaya, N., & Bartels, A. (2017). Scene segmentation in early visual cortex during suppression of ventral stream regions. *NeuroImage, 146*, 71-80.

Grassi, P. R., Zaretskaya, N., & Bartels, A. (2018). A generic mechanism for perceptual organization in the parietal cortex. *Journal of Neuroscience, 0436-18*.

Groppa, S., Oliviero, A., Eisen, A., Quartarone, A., Cohen, L. G., Mall, V., et al. (2012). A practical guide to diagnostic transcranial magnetic stimulation: Report of an IFCN committee. *Clinical Neurophysiology, 123*, 858–882.

Grunewald, A., Bradley, D. C., & Andersen, R. A. (2002). Neural correlates of structure-from-motion perception in macaque V1 and MT. *Journal of Neuroscience*, *22*(14), 6195-6207.

Gutierrez, C., Cola, M. G., Seltzer, B., & Cusick, C. (2000). Neurochemical and connectional organization of the dorsal pulvinar complex in monkeys. *Journal of Comparative Neurology, 419*(1), 61-86.

Hamada, M., Murase, N., Hasan, A., Balaratnam, M., & Rothwell, J. C. (2012). The role of interneuron networks in driving human motor cortical plasticity. *Cerebral Cortex, 23*(7), 1593-1605.

Haynes, J. D., & Rees, G. (2005b). Predicting the stream of consciousness from activity in human visual cortex. *Current Biology, 15*(14), 1301-1307.

Haynes, J. D., Deichmann, R., & Rees, G. (2005a). Eye-specific effects of binocular rivalry in the human lateral geniculate nucleus. *Nature, 438*(7067), 496.

Herrmann, C. S. (2001). Human EEG responses to 1–100 Hz flicker: resonance phenomena in visual cortex and their potential correlation to cognitive phenomena. *Experimental Brain Research, 137*(3-4), 346-353.

Herrmann, C. S., Rach, S., Neuling, T., & Strüber, D. (2013). Transcranial alternating current stimulation: a review of the underlying mechanisms and modulation of cognitive processes. *Frontiers in Human Neuroscience, 7*, 279.

Hilgetag, C. C., Théoret, H., & Pascual-Leone, A. (2001). Enhanced visual spatial attention ipsilateral to rTMS-induced 'virtual lesions' of human parietal cortex. *Nature Neuroscience, 4*(9), 953–957.

Hodsoll, J., Mevorach, C., & Humphreys, G. W. (2009). Driven to less distraction: rTMS of the right parietal cortex reduces attentional capture in visual search. *Cerebral Cortex, 19*(1), 106–114.

Hohwy, J., Roepstorff, A., & Friston, K. (2008). Predictive coding explains binocular rivalry: an epistemological review. *Cognition, 108*(3), 687-701.

Hollins, M. (1980). The effect of contrast on the completeness of binocular rivalry suppression. *Attention, Perception, & Psychophysics, 27*(6), 550-556.

Horton, J. C., & Hoyt, W. F. (1991). Quadrantic visual field defects: a hallmark of lesions in extrastriate (V2/V3) cortex. *Brain*, *114*(4), 1703-1718.

Huang, Y. Z., Edwards, M. J., Rounis, E., Bhatia, K. P., & Rothwell, J. C. (2005). Theta burst stimulation of the human motor cortex. *Neuron, 45*(2), 201-206.

Huk, A. C., & Shadlen, M. N. (2005). Neural activity in macaque parietal cortex reflects temporal integration of visual motion signals during perceptual decision making. *Journal of Neuroscience, 25*(45), 10420-10436.

Intaitė, M., Duarte, J. V., & Castelo-Branco, M. (2016). Working memory load influences perceptual ambiguity by competing for fronto-parietal attentional resources. *Brain Research, 1650*, 142-151.

Itthipuripat, S., Garcia, J. O., & Serences, J. T. (2013). Temporal dynamics of divided spatial attention. *Journal of Neurophysiology, 109*(9), 2364-2373.

Kaas, J. H., & Lyon, D. C. (2007). Pulvinar contributions to the dorsal and ventral streams of visual processing in primates. *Brain Research Reviews, 55*(2), 285-296.

Kaiser P. K., Comerford J. P. (1975). Flicker photometry of equally bright lights. *Vision Research, 15*, 1399–1402.

Kanai, R., Bahrami, B., & Rees, G. (2010a). Human parietal cortex structure predicts individual differences in perceptual rivalry. *Current Biology, 20*(18), 1626-1630.

Kanai, R., Carmel, D., Bahrami, B., & Rees, G. (2011). Structural and functional fractionation of right superior parietal cortex in bistable perception. *Current Biology, 21*(3), R106-R107.

Kanai, R., Chaieb, L., Antal, A., Walsh, V., & Paulus, W. (2008). Frequency-dependent electrical stimulation of the visual cortex. *Current Biology, 18*(23), 1839-1843.

Kanai, R., Komura, Y., Shipp, S., & Friston, K. (2015). Cerebral hierarchies: predictive processing, precision and the pulvinar. *Philosophical Transactions of the Royal Society B: Biological Sciences, 370*(1668), 20140169.

Kanai, R., Paulus, W., & Walsh, V. (2010b). Transcranial alternating current stimulation (tACS) modulates cortical excitability as assessed by TMS-induced phosphene thresholds. *Clinical Neurophysiology, 121*(9), 1551-1554.

Karnath, H. O., Himmelbach, M., & Rorden, C. (2002). The subcortical anatomy of human spatial neglect: putamen, caudate nucleus and pulvinar. *Brain, 125*(2), 350-360.

Kass, R. E., & Raftery, A. E. (1995). Bayes factors. *Journal of the American Statistical Association, 90*(430), 773-795.

Kastner, S., O'Connor, D. H., Fukui, M. M., Fehd, H. M., Herwig, U., & Pinsk, M. A. (2004). Functional imaging of the human lateral geniculate nucleus and pulvinar. *Journal of Neurophysiology, 91*(1), 438-448.

Kastner, S., Ungerleider, L. G. (2000). Mechanisms of visual attention in the human cortex. *Annual Review of Neuroscience, 23*(1), 315-341.

Keitel, C., Quigley, C., & Ruhnau, P. (2014). Stimulus-driven brain oscillations in the alpha range: entrainment of intrinsic rhythms or frequency-following response?. *Journal of Neuroscience, 34*(31), 10137-10140.

Kim, Y. J., Grabowecky, M., Paller, K. A., Muthu, K., & Suzuki, S. (2007). Attention induces synchronization-based response gain in steady-state visual evoked potentials. *Nature Neuroscience, 10*(1), 117-125.

Kleinschmidt, A., Büchel, C., Zeki, S., & Frackowiak, R. S. (1998). Human brain activity during spontaneously reversing perception of ambiguous figures. *Proceedings of the Royal Society of London B: Biological Sciences, 265*(1413), 2427-2433.

Klink, P. C., & Roelfsema, P. R. (2016). Binocular rivalry outside the scope of awareness. *Proceedings of the National Academy of Sciences, 113*(30), 8352-8354.

Knapen, T., Brascamp, J., Pearson, J., van Ee, R., & Blake, R. (2011). The role of frontal and parietal brain areas in bistable perception. *The Journal of Neuroscience, 31*(28), 10293-10301.

Koch, C., Massimini, M., Boly, M., & Tononi, G. (2016). Neural correlates of consciousness: progress and problems. *Nature Reviews Neuroscience*, *17*(5), 307.

Koch, C., & Tsuchiya, N. (2007). Attention and consciousness: two distinct brain processes. *Trends in Cognitive Sciences, 11*(1), 16-22.

Krause, B., & Kadosh, R. C. (2014). Not all brains are created equal: the relevance of individual differences in responsiveness to transcranial electrical stimulation. *Frontiers in Systems Neuroscience, 8*(25), 1-12.

Kähkönen, S., Komssi, S., Wilenius, J., & Ilmoniemi, R. J. (2005). Prefrontal TMS produces smaller EEG responses than motor-cortex TMS: implications for rTMS treatment in depression. *Psychopharmacology, 181*(1), 16-20.

Laczó, B., Antal, A., Niebergall, R., Treue, S., & Paulus, W. (2012). Transcranial alternating stimulation in a high gamma frequency range applied over V1 improves contrast perception but does not modulate spatial attention. *Brain Stimulation, 5*(4), 484-491.

Lawwill, T., & Biersdorf, W. R. (1968). Binocular rivalry and visual evoked responses. *Investigative Ophthalmology & Visual Science, 7*(4), 378-385.

Lee, S. H., Blake, R., & Heeger, D. J. (2005). Traveling waves of activity in primary visual cortex during binocular rivalry. *Nature Neuroscience, 8*(1), 22.

Leopold, D. A., & Logothetis, N. K. (1999). Multistable phenomena: changing views in perception. *Trends in Cognitive Sciences, 3*(7), 254-264.

Levelt, W. J. (1965). On binocular rivalry (Doctoral dissertation, Van Gorcum Assen).

Levelt, W. J. (1967). Note on the distribution of dominance times in binocular rivalry. *British Journal of Psychology, 58*(1-2), 143-145.

Li, F., Tian, Y., Zhang, Y., Qiu, K., Tian, C., Jing, W., & Xu, P. (2015). The enhanced information flow from visual cortex to frontal area facilitates SSVEP response: evidence from model-driven and data-driven causality analysis. *Scientific Reports, 5*.

Li, H. H., Rankin, J., Rinzel, J., Carrasco, M., & Heeger, D. J. (2017). Attention model of binocular rivalry. *Proceedings of the National Academy of Sciences, 114*(30), E6192-E6201.

Logothetis, N. K. (1999). Vision: a window on consciousness. *Scientific American, 281*(5), 68-75.

Logothetis, N. K., Leopold, D. A., & Sheinberg, D. L. (1996). What is rivalling during binocular rivalry?. *Nature, 380*(6575), 621.

Luck, S. J., Vogel, E. K., & Shapiro, K. L. (1996). Word meanings can be accessed but not reported during the attentional blink. *Nature*, *383*(6601), 616.

Lumer, E. D., & Rees, G. (1999). Covariation of activity in visual and prefrontal cortex associated with subjective visual perception. *Proceedings of the National Academy of Sciences, 96*(4), 1669-1673.

Lumer, E. D., Friston, K. J., & Rees, G. (1998). Neural correlates of perceptual rivalry in the human brain. *Science, 280*(5371), 1930-1934.

Mack, A., & Rock, I. (1998). *Inattentional blindness* (Vol. 33). Cambridge, MA: MIT press.

Maier, A., Logothetis, N. K., & Leopold, D. A. (2007). Context-dependent perceptual modulation of single neurons in primate visual cortex. *Proceedings of the National Academy of Sciences*, *104*(13), 5620-5625.

Malhotra, P., Coulthard, E. J., & Husain, M. (2009). Role of right posterior parietal cortex in maintaining attention to spatial locations over time. *Brain, 132*(3), 645-660.

Mars, R. B., Jbabdi, S., Sallet, J., O'Reilly, J. X., Croxson, P. L., Olivier, E., ... & Behrens, T. E. (2011). Diffusion-weighted imaging tractography-based parcellation of the human parietal cortex and comparison with human and macaque resting-state functional connectivity. *Journal of Neuroscience, 31*(11), 4087-4100.

Mathewson, K. E., Prudhomme, C., Fabiani, M., Beck, D. M., Lleras, A., & Gratton, G. (2012). Making waves in the stream of consciousness: entraining oscillations in EEG alpha and fluctuations in visual awareness with rhythmic visual stimulation. *Journal of Cognitive Neuroscience, 24*(12), 2321-2333.

Mazzi, C., Mancini, F., & Savazzi, S. (2014). Can IPS reach visual awareness without V1? Evidence from TMS in healthy subjects and hemianopic patients. *Neuropsychologia*, *64*, 134-144.

McAlonan, K., Cavanaugh, J., & Wurtz, R. H. (2008). Guarding the gateway to cortex with attention in visual thalamus. *Nature, 456*(7220), 391.

Megumi, F., Bahrami, B., Kanai, R., & Rees, G. (2015). Brain activity dynamics in human parietal regions during spontaneous switches in bistable perception. *NeuroImage, 107*, 190-197.

Miles, W. R. (1931). Movement interpretations of the silhouette of a revolving fan. *The American Journal of Psychology, 43*(3), 392-405.

Mitchell, J. F., Stoner, G. R., & Reynolds, J. H. (2004). Object-based attention determines dominance in binocular rivalry. *Nature, 429*(6990), 410.

Moliadze, V., Atalay, D., Antal, A., & Paulus, W. (2012). Close to threshold transcranial electrical stimulation preferentially activates inhibitory networks before switching to excitation with higher intensities. *Brain Stimulation, 5*(4), 505-511.

Montemurro, M. A., Rasch, M. J., Murayama, Y., Logothetis, N. K., & Panzeri, S. (2008). Phase-of-firing coding of natural visual stimuli in primary visual cortex. *Current Biology, 18*(5), 375-380.

Morgan, S. T., Hansen, J. C., & Hillyard, S. A. (1996). Selective attention to stimulus location modulates the steady-state visual evoked potential. *Proceedings of the National Academy of Sciences, 93*(10), 4770-4774.

Naber, M., Frässle, S., & Einhäuser, W. (2011). Perceptual rivalry: reflexes reveal the gradual nature of visual awareness. *PLoS One*, *6*(6), e20910.

Nakamura, R. K., & Mishkin, M. (1980). Blindness in monkeys following non-visual cortical lesions. *Brain Research, 188*(2), 572-577.

Neuling, T., Rach, S., & Herrmann, C. S. (2013). Orchestrating neuronal networks: sustained after-effects of transcranial alternating current stimulation depend upon brain states. *Frontiers in Human Neuroscience, 7*.

Neuling, T., Rach, S., Wagner, S., Wolters, C. H., & Herrmann, C. S. (2012a). Good vibrations: oscillatory phase shapes perception. *Neuroimage, 63*(2), 771-778.

Neuling, T., Wagner, S., Wolters, C. H., Zaehle, T., & Herrmann, C. S. (2012b). Finite-element model predicts current density distribution for clinical applications of tDCS and tACS. *Frontiers in Psychiatry, 3*.

Norcia, A. M., Appelbaum, L. G., Ales, J. M., Cottereau, B. R., & Rossion, B. (2015). The steady-state visual evoked potential in vision research: a review. *Journal of Vision, 15*(6), 4-4.

Nyffeler, T., Wurtz, P., Lüscher, H. R., Hess, C. W., Senn, W., Pflugshaupt, T., ... & Müri, R. M. (2006). Repetitive TMS over the human oculomotor cortex: comparison of 1-Hz and theta burst stimulation. *Neuroscience Letters, 409*(1), 57-60.

O'Connor, D. H., Fukui, M. M., Pinsk, M. A., & Kastner, S. (2002). Attention modulates responses in the human lateral geniculate nucleus. *Nature Neuroscience, 5*(11), 1203.

Overgaard, M., & Fazekas, P. (2016). Can no-report paradigms extract true correlates of consciousness?. *Proceedings of the National Academy of Sciences USA, 105,* 1704-1709.

Paffen, C., & Alais, D. (2011). Attentional modulation of binocular rivalry. *Frontiers in Human Neuroscience*, *5*, 105.

Paffen, C. L., Alais, D., & Verstraten, F. A. (2006). Attention speeds binocular rivalry. *Psychological Science, 17*(9), 752-756.

Paffen, C. L., & Van der Stigchel, S. (2010). Shifting spatial attention makes you flip: exogenous visual attention triggers perceptual alternations during binocular rivalry. *Attention, Perception, & Psychophysics, 72*(5), 1237-1243.

Panagiotaropoulos, T. I., Kapoor, V., & Logothetis, N. K. (2014). Subjective visual perception: from local processing to emergent phenomena of brain activity. *Philosophical Transactions of the Royal Society of London B: Biological Sciences, 369*(1641), 20130534.

Pastor, M. A., Artieda, J., Arbizu, J., Valencia, M., & Masdeu, J. C. (2003). Human cerebral activation during steady-state visual-evoked responses. *Journal of Neuroscience, 23*(37), 11621-11627.

Pastukhov, A., & Braun, J. (2007). Perceptual reversals need no prompting by attention. *Journal of Vision, 7*(10), 5.

Pearson, J., Tadin, D., & Blake, R. (2007). The effects of transcranial magnetic stimulation on visual rivalry. *Journal of Vision, 7*(7), 2.

Persaud, N., McLeod, P., & Cowey, A. (2007). Post-decision wagering objectively measures awareness. *Nature Neuroscience, 10*(2), 257-261.

Petersen, S. E., Robinson, D. L., & Morris, J. D. (1987). Contributions of the pulvinar to visual spatial attention. *Neuropsychologia, 25*(1), 97-105.

Petruk, V., He, B., Engel, S., & He, S. (2018). Stimulus rivalry and binocular rivalry share a common neural substrate. *Journal of Vision, 18*(9), 18-18.

Pigeau, R. A., & Frame, A. M. (1992). Steady-state visual evoked responses in high and low alpha subjects. *Electroencephalography and Clinical Neurophysiology/Evoked Potentials Section, 84*(2), 101-109.

Pogosyan A., Gaynor L. D., Eusebio A., Brown P. (2009) Boosting cortical activity at Beta-band frequencies slows movement in humans. *Current Biology 19*, 1637–1641.

Polanía, R., Nitsche, M. A., Korman, C., Batsikadze, G., & Paulus, W. (2012). The importance of timing in segregated theta phase-coupling for cognitive performance. *Current Biology, 22*(14), 1314-1318.

Polonsky, A., Blake, R., Braun, J., & Heeger, D. J. (2000). Neuronal activity in human primary visual cortex correlates with perception during binocular rivalry. *Nature Neuroscience, 3*(11), 1153-1159.

Rabovsky, M., Stein, T., & Rahman, R. A. (2016). Access to awareness for faces during continuous flash suppression is not modulated by affective knowledge. *PloS one, 11*(4), e0150931.

Rao, R. P., & Ballard, D. H. (1999). Predictive coding in the visual cortex: a functional interpretation of some extra-classical receptive-field effects. *Nature Neuroscience, 2*(1), 79.

Reato, D., Rahman, A., Bikson, M., & Parra, L. C. (2010). Low-intensity electrical stimulation affects network dynamics by modulating population rate and spike timing. *Journal of Neuroscience, 30*(45), 15067-15079.

Rees, G., Kreiman, G., & Koch, C. (2002). Neural correlates of consciousness in humans. *Nature Reviews Neuroscience, 3*(4), 261-270.

Regan D. (1989). Human brain electrophysiology: evoked potentials and evoked magnetic fields in science and medicine. New York: Elsevier.

Regan, D. (1966). An effect of stimulus colour on average steady-state potentials evoked in man. *Nature, 210*, 1056–1057.

Ridding, M. C., & Ziemann, U. (2010). Determinants of the induction of cortical plasticity by non-invasive brain stimulation in healthy subjects. *The Journal of Physiology, 588*(13), 2291-2304.

Rossi, S., Hallett, M., Rossini, P. M., & Pascual-Leone, A. (2009). Safety, ethical considerations, and application guidelines for the use of transcranial magnetic stimulation in clinical practice and research. *Clinical Neurophysiology, 120*(12), 2008-2039.

Rouder, J. N., Morey, R. D., Speckman, P. L., & Province, J. M. (2012). Default Bayes factors for ANOVA designs. *Journal of Mathematical Psychology, 56*(5), 356-374.

Rounis, E., Maniscalco, B., Rothwell, J. C., Passingham, R. E., & Lau, H. (2010). Theta-burst transcranial magnetic stimulation to the prefrontal cortex impairs metacognitive visual awareness. *Cognitive Neuroscience, 1*(3), 165-175.

Rueckert, L., & Grafman, J. (1998). Sustained attention deficits in patients with lesions of posterior cortex. *Neuropsychologia, 36*(7), 653–660.

Ruff, C. C., & Driver, J. (2006). Attentional preparation for a lateralized visual distractor: Behavioral and fMRI evidence. *Journal of Cognitive Neuroscience, 18*(4), 522-538.

Ruff, C. C., Bestmann, S., Blankenburg, F., Bjoertomt, O., Josephs, O., Weiskopf, N., ... & Driver, J. (2008a). Distinct causal influences of parietal and frontal brain regions on activity in human retinotopic visual cortex. *Cerebral Cortex, 18*(4), 817-827.

Ruff, C. C., Blankenburg, F., Bjoertomt, O., Bestmann, S., Freeman, E., Haynes, J. D., ... & Driver, J. (2006). Concurrent TMS-fMRI and psychophysics reveal frontal influences on human retinotopic visual cortex. *Current Biology, 16*(15), 1479-1488.

Ruff, C. C., Blankenburg, F., Bjoertomt, O., Bestmann, S., Weiskopf, N., & Driver, J. (2008b). Hemispheric differences in frontal and parietal influences on human occipital cortex: direct confirmation with concurrent TMS–fMRI. *Journal of Cognitive Neuroscience, 21*(6), 1146-1161.

Ruhnau, P., Keitel, C., Lithari, C., Weisz, N., & Neuling, T. (2016a). Flicker-driven responses in visual cortex change during matched-frequency transcranial alternating current stimulation. *Frontiers in Human Neuroscience, 10*.

Ruhnau, P., Neuling, T., Fuscá, M., Herrmann, C. S., Demarchi, G., & Weisz, N. (2016b). Eyes wide shut: transcranial alternating current stimulation drives alpha rhythm in a state dependent manner. *Scientific Reports, 6*, 27138.

Rushworth, M. F. S., & Taylor, P. C. J. (2006). TMS in the parietal cortex: Updating representations for attention and action. *Neuropsychologia, 44*(13), 2700–2716.

Sabrin, H. W., & Kertesz, A. E. (1980). Microsaccadic eye movements and binocular rivalry. *Perception & Psychophysics*, *28*(2), 150-154.

Sakai, K., Ugawa, Y., Terao, Y., Hanajima, R., Furubayashi, T., & Kanazawa, I. (1997). Preferential activation of different I waves by transcranial magnetic stimulation with a figure-of-eight-shaped coil. *Experimental Brain Research, 113*(1), 24-32.

Sandberg, K., Blicher, J. U., Del Pin, S. H., Andersen, L. M., Rees, G., & Kanai, R. (2016). Improved estimates for the role of grey matter volume and GABA in bistable perception. *Cortex, 83*, 292-305.

Schauer, G., Chang, A., Schwartzman, D., Rae, C. L., Iriye, H., Seth, A. K., & Kanai, R. (2016a). Fractionation of parietal function in bistable perception probed with concurrent TMS-EEG. *Scientific data, 3*, 160065.

Schauer, G., Kanai, R., & Brascamp, J. W. (2016b). Parietal theta burst TMS: Functional fractionation observed during bistable perception not evident in attention tasks. *Consciousness and Cognition, 40*, 105-115.

Schenkluhn, B., Ruff, C. C., Heinen, K., & Chambers, C. D. (2008). Parietal stimulation decouples spatial and feature-based attention. *Journal of Neuroscience, 28*(44), 11106-11110.

Schindler, K., Nyffeler, T., Wiest, R., Hauf, M., Mathis, J., Hess, C. W., & Müri, R. (2008). Theta burst transcranial magnetic stimulation is associated with increased EEG synchronization in the stimulated relative to unstimulated cerebral hemisphere. *Neuroscience Letters, 436*(1), 31-34.

Schutter, D. J., & Wischnewski, M. (2016). A meta-analytic study of exogenous oscillatory electric potentials in neuroenhancement. *Neuropsychologia, 86*, 110-118.

Schutter, D. J., Van Honk, J., & Panksepp, J. (2004). Introducing transcranial magnetic stimulation (TMS) and its property of causal inference in investigating brain-function relationships. *Synthese, 141*(2), 155-173.

Sejnowski, T. J., & Paulsen, O. (2006). Network oscillations: emerging computational principles. *Journal of Neuroscience, 26*(6), 1673-1676.

Serences, J. T., & Yantis, S. (2006). Selective visual attention and perceptual coherence. *Trends in Cognitive Sciences, 10*(1), 38-45.

Serences, J. T., Schwarzbach, J., Courtney, S. M., Golay, X., & Yantis, S. (2004). Control of object-based attention in human cortex. *Cerebral Cortex, 14*(12), 1346-1357.

Shah, A. S., Bressler, S. L., Knuth, K. H., Ding, M., Mehta, A. D., Ulbert, I., & Schroeder, C. E. (2004). Neural dynamics and the fundamental mechanisms of event-related brain potentials. *Cerebral Cortex, 14*(5), 476-483.

Sheinberg, D. L., & Logothetis, N. K. (1997). The role of temporal cortical areas in perceptual organization. *Proceedings of the National Academy of Sciences*, *94*(7), 3408-3413.

Sherman, M. T., Barrett, A. B., & Kanai, R. (2015). Inferences about consciousness using subjective reports of confidence. In: Overgaard, Morten (ed.) Behavioral Methods in Consciousness Research. Oxford University Press, Oxford, UK.

Sherman, M. T., Kanai, R., Seth, A. K., & VanRullen, R. (2016). Rhythmic influence of top–down perceptual priors in the phase of prestimulus occipital alpha oscillations. *Journal of Cognitive Neuroscience 28*(9), 1318-1330.

Sherman, S. M., & Guillery, R. W. (2002). The role of the thalamus in the flow of information to the cortex. *Philosophical Transactions of the Royal Society of London B: Biological Sciences, 357*(1428), 1695-1708.

Shipp, S. (2003). The functional logic of cortico–pulvinar connections. *Philosophical Transactions of the Royal Society of London B: Biological Sciences, 358*(1438), 1605-1624.

Shipp, S. (2004). The brain circuitry of attention. *Trends in Cognitive Sciences, 8*(5), 223-230.

Sillito, A. M., Cudeiro, J., & Jones, H. E. (2006). Always returning: feedback and sensory processing in visual cortex and thalamus. *Trends in Neurosciences, 29*(6), 307-316.

Slotnick, S. D., & Yantis, S. (2005). Common neural substrates for the control and effects of visual attention and perceptual bistability. *Cognitive Brain Research, 24*(1), 97-108.

Spaak, E., de Lange, F. P., & Jensen, O. (2014). Local entrainment of alpha oscillations by visual stimuli causes cyclic modulation of perception. *Journal of Neuroscience, 34*(10), 3536-3544.

Srinivasan, R., & Petrovic, S. (2005). MEG phase follows conscious perception during binocular rivalry induced by visual stream segregation. *Cerebral Cortex, 16*(5), 597-608.

Srinivasan, R., Fornari, E., Knyazeva, M. G., Meuli, R., & Maeder, P. (2007). fMRI responses in medial frontal cortex that depend on the temporal frequency of visual input. *Experimental Brain Research, 180*(4), 677-691.

Srinivasan, R., Russell, D. P., Edelman, G. M., & Tononi, G. (1999). Increased synchronization of neuromagnetic responses during conscious perception. *Journal of Neuroscience, 19*(13), 5435-5448.

Sterzer P. Eger E. Kleinschmidt A . (2003). Responses of extrastriate cortex to switching perception of ambiguous visual motion stimuli. *Neuroreport, 14*, 2337–2341.

Sterzer P. Kleinschmidt A . (2005). A neural signature of colour and luminance correspondence in bistable apparent motion. *European Journal of Neuroscience, 21*, 3097–3106.

Sterzer P. Kleinschmidt A . (2007). A neural basis for inference in perceptual ambiguity. *Proceedings of the National Academy of Sciences USA, 104*, 323–328.

Sterzer P. Russ M. O. Preibisch C. Kleinschmidt A . (2002). Neural correlates of spontaneous direction reversals in ambiguous apparent visual motion. *Neuroimage, 15*, 908–916.

Sterzer, P., & Kleinschmidt, A. (2007). A neural basis for inference in perceptual ambiguity. *Proceedings of the National Academy of Sciences, 104*(1), 323-328.

Sterzer, P., Kleinschmidt, A., & Rees, G. (2009). The neural bases of multistable perception. *Trends in Cognitive Sciences, 13*(7), 310-318.

Sterzer, P., Russ, M. O., Preibisch, C., & Kleinschmidt, A. (2002). Neural correlates of spontaneous direction reversals in ambiguous apparent visual motion. *Neuroimage, 15*(4), 908-916.

Stewart, L. M., Walsh, V., & Rothwell, J. C. (2001). Motor and phosphene thresholds: a transcranial magnetic stimulation correlation study. *Neuropsychologia, 39*(4), 415-419.

Strüber, D., Rach, S., Trautmann-Lengsfeld, S. A., Engel, A. K., & Herrmann, C. S. (2014). Antiphasic 40 Hz oscillatory current stimulation affects bistable motion perception. *Brain Topography, 27*(1), 158-171.

Thut, G., Nietzel, A., & Pascual-Leone, A. (2005). Dorsal posterior parietal rTMS affects voluntary orienting of visuospatial attention. *Cerebral Cortex, 15*(5), 628–638.

Thut, G., Schyns, P. G., & Gross, J. (2011). Entrainment of perceptually relevant brain oscillations by non-invasive rhythmic stimulation of the human brain. *Frontiers in psychology, 2*.

Toffanin, P., de Jong, R., Johnson, A., & Martens, S. (2009). Using frequency tagging to quantify attentional deployment in a visual divided attention task. *International Journal of Psychophysiology, 72*(3), 289-298.

Tong, F., & Engel, S. A. (2001). Interocular rivalry revealed in the human cortical blind-spot representation. *Nature, 411*(6834), 195-199.

Tong, F., Meng, M., & Blake, R. (2006). Neural bases of binocular rivalry. *Trends in Cognitive Sciences, 10*(11), 502-511.

Tong, F., Nakayama, K., Vaughan, J. T., & Kanwisher, N. (1998). Binocular rivalry and visual awareness in human extrastriate cortex. *Neuron, 21*(4), 753-759.

Tononi, G., & Koch, C. (2008). The neural correlates of consciousness. *Annals of the New York Academy of Sciences*, *1124*(1), 239-261.

Tononi, G., & Koch, C. (2015). Consciousness: here, there and everywhere?. *Philosophical Transactions of the Royal Society B: Biological Sciences*, *370*(1668), 20140167.

Tononi, G., Srinivasan, R., Russell, D. P., & Edelman, G. M. (1998). Investigating neural correlates of conscious perception by frequency-tagged neuromagnetic responses. *Proceedings of the National Academy of Sciences, 95*(6), 3198-3203.

Treue, S., Husain, M., & Andersen, R. A. (1991). Human perception of structure from motion. *Vision Research, 31*(1), 59-75.

Tsuchiya, N., & Koch, C. (2005). Continuous flash suppression reduces negative afterimages. *Nature Neuroscience, 8*(8), 1096-1101.

Tsuchiya, N., Wilke, M., Frässle, S., & Lamme, V. A. (2015). No-report paradigms: extracting the true neural correlates of consciousness. *Trends in Cognitive Sciences, 19*(12), 757-770.

van Ee, R., Van Dam, L. C. J., & Brouwer, G. J. (2005). Voluntary control and the dynamics of perceptual bi-stability. *Vision Research, 45*(1), 41-55.

VanRullen, R., Busch, N. A., Drewes, J., & Dubois, J. (2011). Ongoing EEG phase as a trial-by-trial predictor of perceptual and attentional variability. *Frontiers in Psychology, 2*(60), 1-9.

Vernet, M., Brem, A. K., Farzan, F., & Pascual-Leone, A. (2015). Synchronous and opposite roles of the parietal and prefrontal cortices in bistable perception: A double-coil TMS–EEG study. *Cortex, 64*, 78-88.

Vialatte, F. B., Maurice, M., Dauwels, J., & Cichocki, A. (2010). Steady-state visually evoked potentials: focus on essential paradigms and future perspectives. *Progress in Neurobiology, 90*(4), 418-438.

Vossen, A., Gross, J., & Thut, G. (2015). Alpha power increase after transcranial alternating current stimulation at alpha frequency (α-tACS) reflects plastic changes rather than entrainment. *Brain Stimulation, 8*(3), 499-508.

Wallach, H. and O'Connell, D.N. (1953) The kinetic depth effect. *Journal of Experimental Psychology, 45*(4), 205.

Wang, M., Arteaga, D., & He, B. J. (2013). Brain mechanisms for simple perception and bistable perception. *Proceedings of the National Academy of Sciences, 110*(35), E3350-E3359.

Watanabe, T., Masuda, N., Megumi, F., Kanai, R., & Rees, G. (2014). Energy landscape and dynamics of brain activity during human bistable perception. *Nature Communications, 5*.

Weilnhammer, V. A., Ludwig, K., Hesselmann, G., & Sterzer, P. (2013). Frontoparietal cortex mediates perceptual transitions in bistable perception. *Journal of Neuroscience, 33*(40), 16009-16015.

Wilcke, J. C., O'Shea, R. P., & Watts, R. (2009). Frontoparietal activity and its structural connectivity in binocular rivalry. *Brain Research, 1305*, 96-107.

Wilke, M., Mueller, K. M., & Leopold, D. A. (2009). Neural activity in the visual thalamus reflects perceptual suppression. *Proceedings of the National Academy of Sciences, 106*(23), 9465-9470.

Witkowski, M., Garcia-Cossio, E., Chander, B. S., Braun, C., Birbaumer, N., Robinson, S. E., & Soekadar, S. R. (2016). Mapping entrained brain oscillations during transcranial alternating current stimulation (tACS). *Neuroimage, 140*, 89-98.

Wood, D., Schauer, G., Bak, T., Carmel, D. (in prep). Parietal TMS and binocular rivalry: stimulus and timing dependence resolve contradictory findings.

Wunderlich, K., Schneider, K. A., & Kastner, S. (2005). Neural correlates of binocular rivalry in the human lateral geniculate nucleus. *Nature Neuroscience, 8*(11), 1595.

Xu, H., Han, C., Chen, M., Li, P., Zhu, S., Fang, Y., ... & Lu, H. D. (2016). Rivalry-like neural activity in primary visual cortex in anesthetized monkeys. *The Journal of Neuroscience, 36*(11), 3231-3242.

Yang, E., Brascamp, J., Kang, M. S., & Blake, R. (2014). On the use of continuous flash suppression for the study of visual processing outside of awareness. *Frontiers in Psychology, 5*.

Yantis, S., Schwarzbach, J., Serences, J. T., Carlson, R. L., Steinmetz, M. A., Pekar, J. J., & Courtney, S. M. (2002). Transient neural activity in human parietal cortex during spatial attention shifts. *Nature Neuroscience, 5*(10), 995-1002.

Zaehle, T., Rach, S., & Herrmann, C. S. (2010). Transcranial alternating current stimulation enhances individual alpha activity in human EEG. *PloS one, 5*(11), e13766.

Zafar, N., Paulus, W., & Sommer, M. (2008). Comparative assessment of best conventional with best theta burst repetitive transcranial magnetic stimulation protocols on human motor cortex excitability. *Clinical Neurophysiology, 119*(6), 1393-1399.

Zapallow, C. M., Asmussen, M. J., Bolton, D. A., Lee, K. G., Jacobs, M. F., & Nelson, A. J. (2012). Theta burst repetitive transcranial magnetic stimulation attenuates somatosensory evoked potentials from the lower limb. *BMC Neuroscience, 13*(1), 133.

Zaretskaya, N., Anstis, S., & Bartels, A. (2013). Parietal cortex mediates conscious perception of illusory gestalt. *Journal of Neuroscience, 33*(2), 523-531.

Zaretskaya, N., Thielscher, A., Logothetis, N. K., & Bartels, A. (2010). Disrupting parietal function prolongs dominance durations in binocular rivalry. *Current Biology, 20*(23), 2106-2111.

Zizlsperger, L., Kümmel, F., & Haarmeier, T. (2016). Metacognitive confidence increases with, but does not determine, visual perceptual learning. *PloS one, 11*(3), e0151218.

Zou, J., He, S., & Zhang, P. (2016). Binocular rivalry from invisible patterns. *Proceedings of the National Academy of Sciences, 113*(30), 8408-8413.